UNIVERSIDADE ESTADUAL PAULISTA
"JÚLIO DE MESQUITA FILHO"
Campus de São José do Rio Preto

Daiane Bertholin Anselmo

Potencial Antitumoral e Antimetastático de Híbridos Moleculares Curcumina-Cinamaldeído: Estudos Celulares e Moleculares

São José do Rio Preto
2020

Daiane Bertholin Anselmo

Potencial Antitumoral e Antimetastático de Híbridos Moleculares Curcumina-Cinamaldeído: Estudos Celulares e Moleculares

Tese apresentada como parte dos requisitos para obtenção do título de Doutor em Microbiologia, junto ao Programa de Pós-Graduação em Microbiologia, do Instituto de Biociências, Letras e Ciências Exatas da Universidade Estadual Paulista "Júlio de Mesquita Filho", Campus de São José do Rio Preto.

Financiadora: CAPES

Orientador: Prof. Dr. Luis Octávio Regasini
Coorientador: Prof. Dr. Mozart de Azevedo Marins
Coorientadora: Profª. Drª. Marília de Freitas Calmon

São José do Rio Preto
2020

A618p

Anselmo, Daiane Bertholin

Potencial antitumoral e antimetastático de híbridos moleculares curcumina-cinamaldeído: Estudos celulares e moleculares / Daiane Bertholin Anselmo. -- São José do Rio Preto, 2020

136 f. : il., tabs., fotos

Tese (doutorado) - Universidade Estadual Paulista (Unesp), Instituto de Biociências Letras e Ciências Exatas, São José do Rio Preto

Orientadora: Luis Octávio Regasini

Coorientadora: Mozart de Azevedo Marins e Marília de Freitas Calmon

1. Câncer. 2. Metástase. 3. Apoptose. 4. Curcumina. 5. Chalcona. I. Título.

Sistema de geração automática de fichas catalográficas da Unesp. Biblioteca do Instituto de Biociências Letras e Ciências Exatas, São José do Rio Preto. Dados fornecidos pelo autor(a).

Essa ficha não pode ser modificada.

Daiane Bertholin Anselmo

Potencial Antitumoral e Antimetastático de Híbridos Moleculares Curcumina-Cinamaldeído: Estudos Celulares e Moleculares

Tese apresentada como parte dos requisitos para obtenção do título de Doutor em Microbiologia, junto ao Programa de Pós-Graduação em Microbiologia, do Instituto de Biociências, Letras e Ciências Exatas da Universidade Estadual Paulista "Júlio de Mesquita Filho", Campus de São José do Rio Preto.

Financiadora: CAPES

Comissão Examinadora

Prof. Dr. Luis Octávio Regasini
UNESP – Câmpus de São José do Rio Preto
Orientador

Profª. Drª. Denise Crispim Tavares
UNIFRAN – Universidade de Franca

Profª. Drª. Rejane Maira Góes
UNESP - Câmpus de São José do Rio Preto

Profª. Drª. Ana Lúcia Fachin Saltoratto
UNAERP – Universidade de Ribeirão Preto

Profª. Drª. Christiane Pienna Soares
UNESP - Câmpus de Araraquara

São José do Rio Preto
20 de fevereiro de 2020

Dedico este trabalho
ao meu marido Emerson,
meus pais Valter e Leonise,
e ao meu irmão Daniel, com carinho.
E por fim, dedico a minha cunhada Elisângela, saudades eternas.

AGRADECIMENTOS

À Deus pela vida, saúde, força, conquistas e todos os ensinamentos e experiência de vida durante esta jornada.

À minha família, especialmente ao meu marido Emerson, por sempre estar comigo nesta caminhada, tanto em São José do Rio Preto, Ribeirão Preto e até no Canadá. Em especial também aos meus pais e meu irmão, por sempre me incentivarem, me darem força, suporte e mostrarem o quanto a educação é importante. Obrigada família pelo amor, apoio, ajuda e paciência. Amo vocês!

Ao meu orientador Prof. Dr. Luis Octávio Regasini, por toda a orientação, ajuda, paciência, amizade, conselhos e ensinamentos durante esses quatro anos. Obrigada por ter me mostrado os melhores caminhos e por confiar em mim e no meu trabalho mesmo eu estando longe, principalmente no fim do doutorado, agradeço pela ajuda e por ter me apoiado com minha ida ao Canadá! Ao meu coorientador Prof. Dr. Mozart Marins, por ter me recebido tão bem no Laboratório GMB da UNAERP de Ribeirão Preto, me ajudou em tudo o que foi necessário com os experimentos e também com minha ida ao Canadá. Obrigada por confiar em mim esta grande oportunidade de experiência internacional, por todo conhecimento, paciência e amizade! À minha coorientadora Profa. Dra. Marília de Freitas Calmon, por todo conhecimento transmitido e paciência em me ensinar a trabalhar com cultivo celular e ter disponibilizado junto à Profa. Dra. Paula Rahal, o laboratório de estudos genômicos (GENOMA) para que eu realizasse meus primeiros experimentos.

À Dra. Tairine Zara, por sua grande amizade, ajuda e união em nossos primeiros passos no trabalho com cultivo celular no Genoma. Agradeço também a todo o pessoal do Genoma pela ajuda, ensinamentos e amizade, em especial Me. Tamara Carvalho, Me. Francielly Cristina, Me. Maria Letícia, Me. Carina Machado, Me. Lucas Carvalho, Dayla Geraldini, Me. Guilherme Campos, Dra. Cintia Bittar, Me. Ana Emília, Bianca Godoy, Rafael Beltrão, Me. Rafael Rahal e Dra. Ana Braga.

Ao Dr. Gabriel por toda ajuda nos experimentos e ensinamentos com biologia celular e molecular no Grupo de Genética Molecular e Bioinformática (GMB), além de sua amizade e paciência. Agradeço a todo o pessoal do laboratório GMB por toda a ajuda, paciência e amizade. Por todos os momentos que passamos juntos, em especial a Me. Viviane Seba, Dra. Tatiana Takahasi, Me. Mariana Romani, Me. Gabriela Segura, Me. Bruna Baruco, Tayná Bernardes, Felipe Nishimura, Me. Monise Petrucelli, Carol, Vanessa Borges, Sthefanie,

Alessandra, Gabriela e Dra. Tamires Bitencourt. Agradeço também a Profa. Dra. Ana Lúcia Fachin, por me acolher também ao grupo GMB, por toda amizade, ensinamentos e auxílio com os experimentos.

Ao Me. Carlos Polaquini do Laboratório de Antibióticos e Quimioterápicos (LAQ) por toda amizade, ajuda, paciência e ensinamentos com minhas primeiras reações químicas.

À Dra. Mariana Bastos do LAQ que também sempre esteve disposta a me ajudar com minhas dúvidas de química e estatística. Obrigada por toda sua amizade e companherismo durante esses anos.

À Dra. Ana Nazaré, Dra. Mariana Bastos, Me. Carlos Polaquini e Caroline Sprengel (LAQ) por poder participar e me aventurar junto a vocês nos concursos de inovação e empreendedorismo.

À todos do LAQ em especial a Me. Beatriz Carvalho, Me. Gabriela Ayusso, Me. Guilherme Torrezan, Me. Leticia Ribeiro, Me. Thaíse Borges, Ricardo Bertani e Me. Mayara Garcia. Obrigada pessoal do LAQ por todo trabalho em equipe, ajuda, ensinamentos, conversas e amizade.

Ao Prof. Dr. Jonathan Dimmock por ter me recebido em seu laboratório de química na Universidade de Saskatchewan (U of S) no Canadá. Agradeço por toda sua paciência e seus grandes ensinamentos durante os quatro meses do qual aprendi muito, foi uma experiência incrível tanto profissional como pessoal. Agradeço também a todos do laboratório de química da U of S, Dr. Alireza Doroudi, Dr. Umashankar Das, Dra. Swagatika Das, Dra. Aruna Chhikara e Sukanya Pati.

À todos os professores e funcionários da UNESP/IBILCE – São José do Rio Preto, agradeço também ao programa de pós-graduação em Microbiologia do instituto.

À banca examinadora pelo tempo, disponibilidade e grande contribuição com meu trabalho.

Aos meus amigos de Potirendaba Me. Aline Coimbra, Anderson Méllo, Wesley Marques, Juliane Pavezi, Diego Pereira, Marta Tavares, e aos do IBILCE, Dra. Natália Righetti, Me. Diego Monteiro que me apoiaram e ajudaram a tornar esta fase mais leve.

À todos aqueles que direta ou indiretamente contribuíram com meu trabalho e/ou minha formação profissional e pessoal.

À PROPG (Pró-Reitoria de Pós-Graduação) pelos auxílios financeiros.

À bolsa prêmio ELAP (Emerging Leaders in the Americas Program) que foi essencial para meu intercâmbio na U of S - Canadá.

À FAPESP (Fundação de Amparo à Pesquisa do Estado de São Paulo) e CNPQ (Conselho Nacional de Desenvolvimento Científico e Tecnológico) pelos auxílios concedidos ao laboratório.

O presente trabalho foi realizado com apoio da Coordenação de Aperfeiçoamento de Pessoal de Nível Superior - Brasil (CAPES) - Código de Financiamento 001. Agradeço a CAPES pela bolsa, que foi essencial para a realização deste trabalho.

“A mente que se abre a uma nova ideia, jamais voltará ao seu tamanho original.”

(Albert Einstein)

RESUMO

O câncer é caracterizado por uma proliferação celular descontrolada, desencadeada por diversas mutações genéticas, fatores epigenéticos e ambientais. Apesar dos avanços terapêuticos, esta doença continua a ser responsável por índices de mortalidade elevados em todo o mundo, que é agravado pela grande resistência aos fármacos. Desta forma, se faz necessária a busca por novas substâncias potentes, seletivas e capazes de agir sobre células tumorais resistentes. Os produtos naturais têm despertado interesse científico devido suas inúmeras bioatividades. Dentre estes, a curcumina, isolada dos rizomas de *Curcuma longa* (popularmente conhecida como açafrão), o cinamaldeído, responsável pelo odor e sabor da canela (*Cinnamomum* sp.) e as chalconas, flavonoides abundantes em frutas, legumes e plantas, possuem potentes atividades antitumorais contra diversos tipos de câncer. O objetivo deste trabalho foi: a) avaliar a capacidade de inibição da proliferação celular de doze híbridos moleculares de curcumina-cinamaldeído contra células de câncer de mama MCF-7 e MDA-MB-231, câncer de colo do útero C33, HeLa, SiHa e CaSki e câncer de vulva A431; b) selecionar o híbrido mais ativo e investigar os possíveis mecanismos celulares e moleculares em linhagens de osteossarcoma U2OS (p53 selvagem) e SAOS (p53 ausente). Pelo ensaio de MTT foi observado que os híbridos foram mais potentes que o cinamaldeído, sendo que híbridos hidroxilados foram mais ativos do que os híbridos metoxilados. O híbrido **5a** apresentou maior potência antiproliferativa contra as células avaliadas de câncer feminino exceto para MCF-7, com valores de CI_{50} variando de 2,7 a 36,5 µM. O híbrido **5a** demonstrou maior potência que a curcumina contra as células CaSki, SiHa, C33 e A431, exibiu uma maior seletividade que a curcumina, quando ambas foram testadas contra queratinócitos (HaCaT), além de ter demonstrado mais estável do que curcumina e cinamaldeído sob condições fisiológicas. Ensaios clonogênicos indicaram que **5a** foi capaz de inibir a formação de colônias da linhagem A431, após 15 dias de tratamento. O híbrido **5a** foi mais ativo contra células de osteossarcoma U2OS (CI_{50} = 22,4 µM) quando comparado às células SAOS (CI_{50} = 45,0 µM), sugerindo que a proteína p53 pode ser o seu alvo molecular. O híbrido **5a** demonstrou boa atividade na inibição da migração e invasão de células U2OS por meio dos ensaios de *wound-healing* e *transwell*, respectivamente. Pela técnica de zimografia, o híbrido **5a** indicou que efeitos sobre a migração e invasão pode estar relacionada com a diminuição da atividade da metaloproteinase de matriz 2 (MMP-2). A análise de *Western Blot* evidenciou a

capacidade de **5a** em induzir a expressão das proteínas p53 e DNAJB1 (Heat shock protein 40). Essa indução pode contribuir na atividade de p53, visto que Hsp40 estabiliza a conformação da proteína p53. As análises de citometria de fluxo indicaram que a inibição da viabilidade celular por **5a** está relacionada com a indução de morte por apoptose, na qual p53 também pode estar envolvida. O estudo do potencial antitumoral e antimetastático de híbridos moleculares curcumina-cinamaldeídos é inédito na literatura, sendo o primeiro que avaliou a atividade de **5a** em níveis celulares e moleculares.

Palavras-chave: câncer, p53, apoptose, curcumina, cinamaldeído, chalcona

ABSTRACT

Cancer is characterized by uncontrolled cell proliferation, triggered by several genetic mutations. Despite the therapeutic advances, this disease continues to be responsible for high mortality rates worldwide. This fact is aggravated by high drug resistance and combination therapy. Thus, it is necessary to search for new substances potent, selective and able to act on tumor cells resistant. Natural products have aroused scientific interest due to their innumerable bioavailabilities. Among these, curcumin, isolated from *Curcuma longa* rhizomes (popularly known as saffron) and cinnamaldehyde, responsible for the cinnamon odor and flavor (*Cinnamomum* sp.) and chalcones, flavonoids abundant in fruits, vegetables and plants, have potent anti-tumor activities against various cancers. The objective of this study was: a) evaluate the ability of inhibit cell proliferation of twelve curcumin-cinnamaldehyde molecular hybrids against MCF-7 and MDA-MB-231 breast cancer cells, C33, HeLa, SiHa and CaSki cervical cancer and A431 vulvar cancer; b) select the most active hybrid and investigate possible cellular and molecular mechanisms in osteosarcoma cell lines U2OS (p53 wild) and SAOS (p53 null). By the MTT assay it was observed that the hybrids were more potent than the cinnamaldehyde, with hydroxyl hybrids being more active than the methoxylated hybrids. Hybrid **5a** presented higher antiproliferative potency against the cells evaluated for women cancer except for MCF-7, with IC_{50} values ranging from 2,7 to 36,5 μM. Hybrid **5a** demonstrated higher potency than curcumin against CaSki, SiHa, C33 and A431 cells, and exhibited higher selectivity than curcumin when both were tested against keratinocytes (HaCaT), besides has show more stable than curcumin and cinnamaldehyde under physiological conditions. Clonogenic assays indicated that **5a** was able to inhibit the colonies formation of A431 line after 15 days of treatment. Hybrid **5a** was more active against U2OS osteosarcoma cells (IC_{50} = 22,4 μM) when compared to SAOS cells (IC_{50} = 45,0 μM), suggesting that the p53 protein may be its molecular target. Hybrid **5a** demonstrated good activity in inhibiting the migration and invasion of U2OS cells by the *wound-healing* and *transwell assays*, respectively. By the zymography technique, hybrid **5a** indicated that effects on migration and invasion may be related to decreased matrix metalloproteinase 2 (MMP-2) activity. *Western Blot* analysis demonstrated the ability of **5a** to induce the expression of p53 and DNAJB1 (Heat shock protein 40). This induction may contribute to p53 activity, since Hsp40 stabilizes the conformation of the p53 protein. Flow cytometric analysis indicated that

inhibition of cell viability by **5a** is related to the induction of apoptosis death, in which p53 may also be involved. The study of the antitumor and antimetastatic potential of curcumin-cinnamaldehyde molecular hybrids is unprecedented in the literature, being the first to evaluate the activity of **5a** at cellular and molecular levels.

Keywords: cancer, p53, apoptosis, curcumin, cinnamaldehyde, chalcone

LISTA DE ILUSTRAÇÕES

Capítulo I

Capítulo II

Capítulo III

LISTA DE TABELAS

Capítulo II

Capítulo III

LISTA DE ABREVIATURAS E SÍMBOLOS

ºC: graus Celsius

μL: microlitros

μM: micromolar

A431: carcinoma escamoso de vulva

ABC: do inglês *ATP-Binding Cassette*

AIF: do inglês *Apoptosis-Inducing Factor*

ANOVA: do inglês *Analysis of Variance*

Apaf-1: do inglês *Apoptotic protease activating fator 1*

ARE: do inglês *Antioxidant Response Element*

ATCC: do inglês *American Type Culture Collection*

ATP: do inglês *Adenosine-5'-triphosphate*

BAD: do inglês *Bcl-2-associated death promoter*

BAK: do inglês *Bcl-2 homologous antagonist/killer*

BAX: do inglês *BCL2-associated X*

Bcl-2: do inglês *B-cell lymphoma protein-2*

Bcl-xl: do inglês *B-cell lymphoma-extra large*

BH3: ou BID, do inglês *Interacting Domain Death Agonist*

BID: do inglês *BH3 Interacting Domain Death Agonist*

BRCA1: do inglês *Breast Cancer 1*

BRCA2: do inglês *Breast Cancer 2*

C33: células de carcinoma cervical humano

CaSki: células de carcinoma cervical humano

Caspases: do inglês *Cysteine-dependent aspartate-specific proteases*

CCHs: do inglês *curcumin-cinnamaldehyde hybrids*

CMC: do inglês *Comprehensive Medicinal Chemistry*

DMEM: do inglês *Dulbecco's modified Eagle's medium*

DMSO: dimetilsulfóxido

DNA: do inglês *Deoxyribonucleic acid*

DNAJ: member of the heat shock protein 40 family (Hsp40)

E6: HPV early oncogene

E7: HPV early oncogene

EGFR: do inglês *Receptor Epidermal Growth Factor*

EMT: do inglês *epithelial-mesenchymal transition*

EROs: espécies reativas de oxigênio

FADD: do inglês *Fas Associated Via Death Domain*

FAS: do inglês *Apoptosis-Mediating Surface Antigen*

FBS: do inglês *fetal bovine serum*

FDA: do inglês *Food and Drug Administration*

FITC: do inglês *Fluorescein isothiocyanate*

G1: fase pós-mitótica do ciclo celular

G2: fase pré-mitótica do ciclo celular

GRAS: do inglês *Generally Recognized as Safe*

HaCaT: queratinócito humano imortalizada (não-tumorigênica)

HBA: do inglês *hydrogen bond acceptors*

HBD: do inglês *hydrogen bond donors*

HeLa: células de adenocarcinoma cervical

HER2: do inglês *Human Epidermal growth factor Receptor 2*

HIF: do inglês *Hypoxia Inducible Factor*

HPV: do inglês *Human Papillomavirus*

Hsp: do inglês *heat shock proteins*

IC_{50}: Inhibitory concentration 50%

INCA: Instituto Nacional do Câncer

IS: índice de seletividade

IUPAC: do inglês *International Union of Pure and Applied Chemistry*

Keap1: do inglês *Kelch-like ECH – associated protein 1*

log $P_{o/w}$: do inglês *logarithm partition coefficient octanol/water*

M: fase mitose do ciclo celular

MCF-7: células de adenocarcinoma de mama humano

Mcl-1: do inglês *Induced myeloid leukemia cell differentiation protein*

MDA-MB-231: células de adenocarcinoma de mama humano

MDM2: do inglês *Murine double minute type 2*

mg: miligrama

mIC_{50}: média da concentração inibitória 50%

mL: mililitro

mM: milimolar

MMPs: do inglês *matrix metalloproteínases*

MTT: 3- [4,5-dimethyl-thiazol-2-yl] -2,5-diphenyltetrazolium bromide

MW: do inglês *molecular weight*

nm: nanomolar

NMR: do inglês *Nuclear Magnetic Resonance*

NOXA: ou PMAIP1, do inglês Phorbol-*12-Myristate-13-Acetate-Induced Protein 1*

Nrf2: do inglês *Nuclear factor erythroid 2-related factor 2*

NROBT: do inglês *number of rotable bonds*

OS: Osteossarcoma

p53: proteína 53

p53AIP1: do inglês *Protein p53 Regulated Apoptosis Inducing Protein 1*

PAGE: do inglês *polyacrylamide gel electrophoresis*

PBS: tampão fosfato salina

P-gp: do inglês *P-glycoprotein*

PUMA: do inglês *p53 Up-Regulated Modulator Of Apoptosis*

RB: Retinoblastoma

RE: Receptor de Estrogênio

RIPA: do inglês *radioimmunoprecipitation*

RP: Receptor de Progesterona

rpm: rotação por minuto

S: fase de síntese do ciclo celular

SAOS-2: células de osteossarcoma humano (p53 ausente)

SD: do inglês *standard deviation*

SDS: do inglês *sodium dodecyl sulphate*

SDS-PAGE: do inglês *Sodium dodecyl sulfate polyacrylamide gel electrophoresis*

SiHa: célula de carcinoma cervical humano

SMAC: do inglês *Second Mitochondria-Derived Activator Of Caspase*

STAT3: do inglês *Signal Transducer and Activator of Transcription 3*

TBST: do inglês *Tris-buffered saline, 0.1% Tween 20*

TNBC: do inglês *Triple-Negative Breast Cancer*

TNF: do inglês *Tumor Necrosis Factor*

TP53: do inglês *Tumor Protein P53*

TRADD: do inglês *Tumor Necrosis Factor Receptor Type 1-Associated DEATH Domain Protein*

TRAIL-R: do inglês *TNF-related apoptosis-inducing ligand receptor*

TRIS/HCl: do inglês *Tris-Hydrochloride*

U2OS: células de osteossarcoma humano (p53 selvagem)

SUMÁRIO

Capítulo I – Considerações gerais e literatura

1. INTRODUÇÃO

1.1 Câncer

O câncer é definido como uma proliferação celular anormal, com elevado desenvolvimento e que não responde aos sinais de controle de divisão e morte celular. Esta proliferação descontrolada resulta de várias mutações no DNA das células, acarretando alterações de genes, que são responsáveis por codificarem mecanismos de bloqueio da divisão celular. Desta forma, estas células mutadas podem invadir os tecidos próximos ou distantes e até se dispersar para outros órgãos, desenvolvendo tumores secundários (ALBERTS et al., 2017; OPAS, 2019; TEWARI et al., 2019).

Esta doença é a segunda principal causa de morte no mundo, sendo considerada como um grande problema de saúde pública, gerando um alto e significativo impacto econômico (OPAS, 2019). De acordo com as últimas estimativas de incidência e mortalidade divulgadas pela GLOBOCAN, o câncer aumentou para 18,1 milhões de novos casos e 9,6 milhões de mortes em 2018, respectivamente. Os tipos mais comuns são o câncer de pulmão, mama, colorretal, próstata, câncer de pele não-melanoma e estômago. Os tipos que causam mais mortes são o câncer de pulmão, colorretal, estômago, fígado e mama (IARC, 2019; OPAS, 2019).

Aproximadamente um terço das mortes por câncer é devido ao estilo de vida, incluindo ausência de atividade física, dieta não saudável com baixa ingestão de frutas e vegetais e uso contínuo de álcool e tabaco (OPAS, 2019). Em torno de 70% das mortes por câncer são referentes à população de países de baixo e médio desenvolvimento. Deste total, 22% dos óbitos por câncer são devido a infecções virais, como hepatite e papilomavírus humano (HPV), principalmente devido ao diagnóstico e tratamento tardio e/ou inacessíveis (OPAS, 2019; INCA, 2019a).

No Brasil, em 2018, foram estimados 559.371 mil novos casos de câncer e 243.588 mil casos de morte (GLOBOCAN, 2019). Sendo os mais frequentes com exceção do câncer de pele não-melanoma: próstata, mama, colorretal, pulmão, estômago e colo uterino. Para 2019, estimaram-se 600 mil novos casos, com uma maior incidência no estado de São Paulo (INCA, 2019a). Estes dados nos mostram que ainda há muito a ser realizado para lidar com o aumento do número de casos e morte por câncer, incluindo ações profiláticas, melhorias em vários setores da saúde pública, detecção precoce e tratamentos inovadores e eficientes.

1.2 Câncer feminino

O câncer prejudica a qualidade de vida em variadas formas, principalmente em mulheres. Em todo o mundo, mais de dois milhões de mulheres são diagnosticadas com câncer de mama ou de colo uterino anualmente. Contudo, o seu estilo de vida pode influenciar no desenvolvimento desses cânceres (GINSBURG et al., 2017; HANSON et al., 2019). A ocorrência e mortalidade de câncer são maiores no sexo feminino (TEWARI et al., 2019), no mundo, em 2018, a estimativa de incidência foi de cerca de 8,6 milhões, mortalidade: 4,1 milhões e número de casos prevalentes em cinco anos são de 22,8 milhões. Sendo que os tipos mais incidentes são o câncer de mama, colorretal, pulmão, cervical e tireoide (GLOBOCAN, 2020). No Brasil, a estimativa realizada pelo INCA ilustrada abaixo (Figura 1), mostra os dez tipos de câncer mais incidentes nas mulheres no ano de 2018, exceto pele não-melanoma (INCA, 2019a).

Figura 1. Tipos de câncer mais comuns em mulheres previstos no ano de 2018, exceto pele não-melanoma (INCA, 2019a).

	Localização Primária	Casos	%
Mulheres 	Mama Feminina	59.700	29,5%
	Cólon e Reto	18.980	9,4%
	Colo do Útero	16.370	8,1%
	Traqueia, Brônquio e Pulmão	12.530	6,2%
	Glândula Tireoide	8.040	4,0%
	Estômago	7.750	3,8%
	Corpo do Útero	6.600	3,3%
	Ovário	6.150	3,0%
	Sistema Nervoso Central	5.510	2,7%
	Leucemias	4.860	2,4%

Fonte: http://www1.inca.gov.br/estimativa/2018/estimativa-2018.pdf

Além do desafio do combate de uma doença tão grave e com altos índices de mortalidade prematura, a mulher é afetada pela baixa autoestima durante e após o tratamento, acarretando problemas psicosociais (GINSBURG et al., 2017; INCA, 2019b; INCA, 2019e). No início do tratamento, há a alopecia devido aos efeitos adversos da quimioterapia ou radioterapia (TEWARI et al., 2019). Em muitos casos de câncer de mama, a cirurgia para retirada do tumor ou mastectomia são necessárias. Em alguns casos de câncer cervical ou

uterino é premente uma histerectomia, que é a remoção do útero e até ovários dependendo da severidade do câncer, resultando na infertilidade feminina (CARR, 2018; INCA, 2019d).

Todos estes fatores acometem as mulheres, não apenas sua saúde física como também mental. Neste contexto, a reconstrução mamária é relevante para minimizar os danos físicos e emocionais do tratamento (INCA, 2019e).

1.2.1 Câncer de mama

O câncer de mama é o maior causador de mortes por câncer na população feminina (15%), bem como o mais incidente (24,2%) (IARC, 2019). No Brasil, foram estimados 59.700 (29,5%) novos casos de câncer de mama, para cada ano do biênio 2018-2019. Com exceção do câncer de pele não-melanoma, o câncer de mama é o mais incidente em quase todas as regiões do Brasil (INCA, 2019a).

Este câncer compreende vários perfis moleculares, sendo classificado por suas características histológicas como, receptor de estrogênio (ER), receptor de progesterona (PR), receptor tipo 2 do fator de crescimento epidérmico humano (HER2) e o triplo negativo (TNBC), o qual é caracterizado pela ausência ou baixa expressão dos receptores ER, PR e HER2, sendo este, o tipo mais grave, pois não há terapia direcionada (HOUSSAMI et al., 2012; PROVENZANO et al., 2018).

O risco do câncer de mama possui várias causas, tais como: início da menstruação antes dos 12 anos de idade, menopausa após os 55 anos, mulheres que não tiveram filhos, primeira gravidez depois dos 30 anos, uso de alguns anticoncepcionais orais, reposição hormonal na menopausa por mais de 5 anos, exposição frequente à radiação ionizante, consumo de bebidas alcoólicas, dietas hipercalóricas, sedentarismo, histórico familiar de câncer de mama e ovário, fatores genéticos e hereditários, bem como mutações em genes de alto risco (BRCA1 e BRCA2) (INCA, 2019e).

A identificação da doença pode ser realizada nos estágios iniciais por meio de sinais e sintomas como caroço no local, pele da mama avermelhada ou retraída, pequenos nódulos nas axilas ou no pescoço e alterações e/ou saída de líquido pelos mamilos. Para melhor diagnóstico é necessário realizar exames de imagem como mamografia, ultrassonografia e ressonância magnética. No entanto, quando há indícios de malignidade é necessária a confirmação por meio da biópsia (INCA, 2019b; INCA, 2019e).

O tratamento atual consiste em cirurgia, radioterapia e quimioterapia conduzida individualmente ou de maneira conjunta, mas o resultado positivo não é garantido, havendo

efeitos adversos severos. Hormonioterápicos como tamoxifeno e anastrozol são empregados, da mesma forma que o anticorpo monoclonal trastuzumabe, que atinge antígenos da célula tumoral (INCA, 2019b).

Na quimioterapia, a doxorrubicina é comumente utilizada, havendo restrições por seus efeitos cardiotóxicos e resistência, dificultam a eficiência do tratamento (PUGAZHENDHI et al., 2018). Antraciclina e/ou taxanos são administrados no tratamento adjuvante em casos de câncer operável (INCA, 2019b).

1.2.2 HPV e Carcinogênese

O papiloma é uma doença silenciosa provocada pelo HPV (Human Papiloma Virus), sendo transmitida sexualmente. O HPV infecta células epiteliais por meio de lesões microscópicas no epitélio e seu genoma viral integra-se ao genoma do hospedeiro. A inserção do genoma viral aumenta a expressão dos oncogenes E6 e E7 responsáveis pelo estado imortalizado das células cervicais e sua malignidade. Esta doença é a mais comum dos últimos tempos, sendo o principal agente causador do câncer de colo uterino (TEYMOURI et al., 2017; OYERVIDES-MUÑOZ et al., 2018; INCA, 2019a).

Este câncer ocupa o quarto lugar tanto na incidência (6,6%) quanto na mortalidade (7,5%) em todo o mundo (IARC, 2019). No Brasil, foram estimados 16.370 casos novos de câncer cervical para cada ano do biênio 2018-2019, sendo o terceiro mais incidente sem considerar os tumores de pele não-melanoma, com maior predominância na região Norte, onde é a quarta causa de morte de mulheres por câncer (INCA, 2019a; INCA, 2019c).

A infecção das células pelo HPV produz partículas virais a quais iniciam o desenvolvimento de lesões de baixo e alto grau. Assim, o HPV é classificado em subtipos, onde o HPV 6 e 11 são considerados de baixo risco, causando proliferação epitelial benigna e o aparecimento de verrugas genitais. Os subtipos de alto risco como HPV 16 e 18 possuem potencial maligno associados diretamente ao desenvolvimento do tumor e são responsáveis por cerca de 70% dos casos de câncer cervical (OYERVIDES-MUÑOZ et al., 2018; INCA, 2019c). Os riscos para este tipo de câncer são mais elevados quando há um início precoce da atividade sexual e principalmente com vários parceiros, sendo diretamente relacionada ao tabagismo e uso prolongado de anticoncepcionais orais (INCA, 2019c).

O câncer cervical também está correlacionado com o câncer de vulva. O câncer vulvar é uma neoplasia ginecológica incomun que surge das vias mediadas pelo HPV e independentes de HPV (ARALDI et al., 2018; WEINBERG; GOMEZ-MARTINEZ, 2019).

Estimativas realizadas pela GLOBOCAN em 2018 mostraram 44.235 novos casos de câncer de vulva e 15.222 mortes no mundo. No Brasil, as estimativas mostraram 1.748 casos e 578 mortes (GLOBOCAN, 2019).

O carcinoma de células escamosas é o tipo histológico mais comum de câncer vulvar sendo responsável por quase 90% dos casos. O câncer de vulva associada ao HPV tem morfologia basaloide e verrucosa, sendo encontrado em mulheres mais jovens. Os subtipos HPV 6, 7, 8 e 16 estão relacionados com mais de 77% dos casos de lesão intraepitelial escamosa de alto grau, enquanto que os subtipos HPV 18 e 33 estão associados a 2,6% e 11% destes casos, respectivamente. O câncer vulvar não relacionado ao HPV acontece com maior frequência em mulheres mais velhas e vem sendo associado ao líquen escleroso, uma lesão mucocutânea crônico-inflamatória, normalmente encontrada na pele genital, na qual as pacientes desenvolvem um prurido, podem sentir dor, disfunção miccional, sexual e sangramento. A sobrevida global das pacientes com câncer vulvar em 5 anos é de 71% (ARALDI et al., 2018; WEINBERG; GOMEZ-MARTINEZ, 2019).

A prevenção pode ser realizada com o uso de preservativos, contudo esta ação protege parcialmente da transmissão pelo HPV, pois também podem decorrer do contato com a pele da vulva, região perineal, perianal e bolsa escrotal (INCA, 2019c). Atualmente, há três vacinas disponíveis contra o HPV, a Cervarix® produzida pela GlaxoSmithKline®, que é uma vacina bivalente capaz de proteger contra os subtipos do HPV 16 e 18; a Gardasil® fabricada pela Merck®, é uma vacina quadrivalente que confere imunidade contra os dois tipos de HPV de alto risco (HPV 16 e 18) e dois de baixo risco (HPV 6 e 11), associados a verrugas genitais e por último a vacina nonavalente da Merck® Gardasil 9® e tem como alvo os subtipos HPV 6, 11, 16, 18, 31, 33, 45, 52 e 58. A quadrivalente e nonavalente se mostraram eficientes na prevenção da lesão intraepitelial escamosa de alto grau. As vacinas bivalente e quadrivalente foram aprovadas em 2009 e 2006, respectivamente, para mulheres entre 9 e 26 anos (ARALDI et al., 2018; LAURENT et al, 2018; WEINBERG; GOMEZ-MARTINEZ, 2019). No entanto, de acordo com o Ministério da Saúde o grupo etário alvo da vacina é de 9 a 14 anos para meninas e de 11 a 14 anos para meninos, pois a vacina é mais eficaz se usada antes do início da vida sexual (INCA, 2019c).

A vacinação e a realização de exames preventivos como Papanicolau e ultrassom são as principais ações contra o câncer de colo do útero. As mulheres acima de 25 anos devem realizar anualmente o exame de Papanicolau mesmo vacinadas, pois há mais de 200 subtipos de HPV descritos, e os tipos de vacina não protegem contra todos os tipos oncogênicos. Caso

forem detectadas células anormais no exame de Papanicolau, é necessário realizar uma biópsia para confirmação do diagnóstico (ARALDI et al., 2018; INCA, 2019c).

Os sintomas do câncer cervical, podem não aparecer na fase inicial, porém nos casos mais avançados, pode apresentar sangramento vaginal irregular ou após a relação sexual, secreção vaginal anormal e dor abdominal associada a infecções urinárias ou intestinais, dores nas costas e nas pernas, fadiga, perda de peso e apetite. Quando diagnosticado na fase inicial, as chances de cura são de 100% (INCA, 2019c; WHO, 2019)

Os tratamentos utilizados contra este câncer são a histerectomia radical, exenterações, radioterapia e quimioterapia. Além do elevado custo econômico, os tratamentos causam sofrimento e afetam significativamente a qualidade de vida das mulheres (GAFFNEY et al., 2018). Nos serviços de saúde são empregados o ácido tricloroacético, podofilina, eletrocauterização, exérese cirúrgica e crioterapia, de acordo com a prescrição médica para cada caso de câncer cervical (MINISTÉRIO DA SAÚDE, 2019).

Para pacientes com verrugas genitais externas ou câncer vulvar, é muito utilizado o fármaco imiquimode de uso tópico, e sua ação melhorara a resposta imune contra o vírus, mostrando uma redução da carga de HPV com taxas de resposta parcial e completa de 80% e 50% respectivamente. Cidofovir é outro fármaco tópico comumente usado que demonstrou eficácia semelhante ao imiquimod. O 5-Fluourouracila tem demonstrado ação eficaz, no entanto, seu uso tem sido limitado devido aos efeitos adversos maiores do que imiquimod e cidofovir (WEINBERG; GOMEZ-MARTINEZ, 2019)

Uma revisão sobre a terapia para o câncer cervical indicou que o tratamento com radioterapia e quimioterapia à base de cisplatina mostrou um grande aumento na sobrevida de mulheres com câncer em estágio avançado. No entanto devido a sua toxicidade, a cisplatina foi substituída pela carboplatina, com efeitos antineoplásicos semelhantes, porém menos tóxica ao paciente. A adição de bevacizumab em combinação com cisplatina e paclitaxel ou topotecan e paclitaxel, ocasiona no aumento de sobrevida global de 3 a 7 meses quando comparado a quimioterapia isolada. Apesar da melhora na sobrevida dos pacientes, este tratamento ainda possui baixa eficácia e alta toxicidade, por isso há uma busca urgente de novos fármacos mais seletivos com o objetivo de aumentar ainda mais o tempo e a qualidade de vida das pacientes (GAFFNEY et al., 2018).

1.3 Osteossarcoma

O osteossarcoma (OS) é uma neoplasia óssea rara, mais comum entre crianças, adolescentes e jovens adultos, sendo que 60% dos casos ocorrem principalmente entre 10 e 20 anos de idade, e com maior incidência no sexo masculino (KANSARA et al., 2014; INCA, 2019f).

Pelo fato do OS ser uma doença esporádica e não ter demonstrado anormalidades genéticas específicas para auxiliar como um marcador no diagnóstico, uma maior predisposição a esta doença é ocasionada quando há mutações nos genes supressores de tumor Retinoblastoma (Rb) e Proteína de Tumor p53 (TP53) (WANG, 2005; KANSARA et al., 2014; INCA, 2019f). De modo geral, p53 é inativado no OS por mutações pontuais, perda alélica ou rearranjos gênicos (WANG, 2005). As mutações no gene RB são descritas em 70% dos OS, a perda deste gene é desfavorável devido ao seu papel importante no controle do ciclo celular. Casos de retinoblastoma bilateral pela associação com anomalias no gene RB, estão associados a uma maior predisposição ao OS (WANG, 2005; INCA, 2019f).

A doença de OS possui um mau prognóstico devido ao seu alto grau de malignidade, acomete principalmente os ossos longos na região da metáfise, como fêmur, tíbia e região proximal do úmero. Seus sintomas mais prevalentes são as dores que podem interromper as atividades diárias nos estágios mais avançados (KANSARA et al., 2014; INCA, 2019f).

Para o diagnóstico do OS, primeiramente é realizada uma radiografia que deve ser confirmado com ressonância magnética nuclear e biópsia, realizada por meio de cirurgia ou por punção com agulha, para assim determinar o tratamento, na qual a terapia adjuvante e neoadjuvante são utilizadas, que inclui ressecção cirúrgica associada à quimioterapia com cisplatina, doxorrubicina, metotrexato e ifosfamida, isoladamente ou em combinação. Alguns métodos cirúrgicos podem levar a preservação do membro, com utilização de endopróteses ou de enxerto ósseo, contudo em alguns casos pode ser necessária a amputação ou mesmo desarticulação (JAFFE; PURI; GELDERBLOM, 2013; INCA, 2019f).

Apesar da eficácia da quimioterapia atual utilizada, este tipo de tumor apresenta uma alta predisposição para invasão local e metástase. A inibição da metástase é uma das principais estratégias de terapia do OS, uma vez que o desenvolvimento de doença metastática devido à resistência aos fármacos mostra menores chances de sucesso no tratamento, diminui a taxa de sobrevida em longo prazo destes pacientes para aproximadamente 20% a 30% e continua a ser a causa mais importante de morte por esse tipo de câncer, principalmente porque o pulmão é o local mais comum de metástase de OS e geralmente levam à morte em um ano (LI et al., 2015a; ANDERSON, 2016; INCA, 2019f).

Além disso, também há os efeitos colaterais consideráveis que limitam as concentrações de tais fármacos utilizadas na quimioterapia, que incluem cardiotoxicidade, nefrotoxicidade, neurotoxicidade e indução de neoplasia secundária, sendo que estes fatores também afetam os efeitos anticâncer desejáveis (ANDERSON, 2016).

Desta forma, mesmo com os avanços no tratamento devido à árdua pesquisa no setor de oncologia, ainda há uma grande busca pela identificação de novos medicamentos com toxicidade reduzida, efeitos anti-metastáticos e mais eficazes de forma que atinja o alvo necessário contra esta doença, pois o OS permanece como uma das principais causas de morte entre as patologias associadas aos ossos (SILVA et al., 2016; LIMA et al., 2018; SEBA et al., 2018).

1.4 Metástase

A metástase é um processo complexo, sendo caracterizado pela capacidade invasiva das células tumorais. Este processo envolve várias etapas, na qual as células se separam do tumor primário, aderem e invadem a membrana basal, migram para locais adjacentes ou distantes por meio da circulação linfática e sanguínea, deixam o sistema vascular, aderem e proliferam em outro órgão e por fim desenvolvem um tumor secundário (SEYFRIED; HUYSENTRUYT, 2013; ANDERSON, 2016; OPAS, 2019).

O potencial metastático tem sido relacionado ao processo de transição epitélio-mesenquimal, na qual, em carcinomas de origem epitelial, as células tumorais sofrem alterações em seu transcriptoma, que controlam modificações bioquímicas e morfológicas e tem sido visto como um processo binário com duas populações celulares distintas, onde as células perdem suas características epiteliais pela perda das proteínas $\mathcal{E}$-caderina e adquirem a características mesenquimais pelo ganho da expressão das proteínas vimentina e *N*-caderina. (PASTUSHENKO; BLANPAIN, 2018). Já em tumores originados de tecidos mesenquimais, como sarcomas ósseos e de tecidos moles, este processo ainda é pouco claro e podem estar relacionados a um comportamento clínico desfavorável. Dependendo do seu histiótipo, podem transferir o seu fenótipo através de processos relacionados à transição epitélio-mesenquimal e transição mesenquimal-epitelial, o que pode contribuir para sua progressão e agressividade (SANNINO et al., 2017).

O aumento da capacidade da célula desencadear metástase está diretamente relacionado a estes processos por meio da regulação dessas proteínas citadas acima. Essas

alterações aumentam a capacidade das células tumorais em migrar, invadir, causar metástase e adquirir resistência à terapia (PASTUSHENKO; BLANPAIN, 2018).

No entanto, a transição epitélio-mesenquimal não tem sido elucidada completamente, mas sabe-se que uma alta expressão gênica de vimentina, *N*-caderina, Slug e β-catenina estão relacionados a este processo (ECCLES; WELCH, 2007; SEBA et al., 2018). Com base nisso, alguns grupos de pesquisas têm trabalhado para identificar substâncias de baixa massa molecular como agentes anti-metastáticos por meio da ativação da proteína p53, que pode reverter a transição epitélio-mesenquimal, reduzindo a migração e a invasão celular (ZAWACKA-PANKAU; SELIVANOVA, 2015; SILVA et al., 2016; LIMA et al., 2018; SEBA et al., 2018). Desta forma, a busca por fármacos que possam atuar na p53 são de grande interesse no objetivo de diminuir a metástase (SEYFRIED; HUYSENTRUYT, 2013; LIMA et al., 2018; SEBA et al., 2018).

1.4.1 Metaloproteinases de matriz

As metaloproteinases de matriz (MMPs) são endopeptidases dependentes de zinco que contribuem para a capacidade das células tumorais degradarem todos os componentes da matriz extracelular devido a atividade proteolítica. Fisiologicamente, este mecanismo é importante para a manutenção e renovação dos tecidos, no entanto, com a desregulação desse processo e superexpressão das MMPs há o desenvolvimento de células cancerígenas que migram e invadem o sistema linfático e vascular e se espalham para locais distantes do tumor primário (PITTAYAPRUEK et al., 2016).

Várias proteínas são responsáveis pela degradação da matriz extracelular, até agora, mais de 20 MMPs foram descritas. Segundo suas estruturas e funções, podem ser classificadas em: colagenases 1, 2, 3 (MMP-1, 8 e 13, respectivamente), estromelisinas 1 e 2 (MMP-3 e 10), gelatinases (MMP-2 e 9) e MMPs tipo membrana como, MMP-14, 15, 16, 17, 24 e 25. A MMP-2 é a mais importante entre as MMPs devido a sua capacidade em degradar diferentes tipos de colágenos. Além de ser a MMP mais expressa, também é encontrada na maioria dos tecidos e células (NAGASE; VISSE; MURPHY, 2006; PITTAYAPRUEK et al., 2016). Estudos têm relatado sua alta expressão em vários tipos de câncer e sua associação no aumento da metástase, sendo também comprovada sua relação a um mau prognóstico (LUO; LIANG; ZHANG, 2009; NOH et al., 2011). Em estudos relacionados ao OS, foi comprovado o envolvimento de MMP-2 na migração e invasão

(BJORNLAND et al., 2005; JIN et al., 2013; LEI et al., 2015), associada com metástase pulmonar e menor sobrevida (LI et al., 2014; ZHANG et al., 2015). Por esta razão, o bloqueio da ação de MMP-2 torna-se um alvo relevante na tentativa de controle da progressão tumoral e da metástase (LIMA et al., 2018; SEBA et al., 2018; SILVA et al., 2018a).

1.5 Apoptose

A apoptose é um mecanismo de morte celular programada rigidamente regulado, para a manutenção do equilíbrio fisiológico entre a proliferação e morte celular. Considerado como um processo evolutivo essencial para a eliminação de células danificadas, em excesso ou cancerígenas (HUTT et al., 2015; KOFF; RAMACHANDIRAN; BERNAL-MIZRACHI, 2015; KNIGHT et al., 2019). Desta forma, a apoptose pode ser eficaz no bloqueio da progressão do câncer, atuando como uma barreira natural (ADAMS; CORY, 2007).

A via apoptótica é um conjunto de reações bioquímicas que exige energia, sendo caracterizada também por induzir alterações morfológicas muitas das quais devido a ativação de caspases, tais como: formação de vesículas, redução de volume da célula, fragmentação nuclear e condensação da cromatina, fragmentação do DNA e proteínas, bem como modificações da superfície da membrana, que permitem que a célula apoptótica seja reconhecida e fagocitada (KOFF; RAMACHANDIRAN; BERNAL-MIZRACHI, 2015).

Existem duas principais vias apoptóticas, a via intrínseca, que é desencadeada por estímulos externos envolvendo a ativação de BH3-proteínas, levando à permeabilização da membrana externa mitocondrial via canais Bax que ativa SMAC (Second Mitochondria-Derived Activator Of Caspase) o que leva à liberação do citocromo c, que induz a formação do apoptossoma, formado por sete unidades de caspase-9, o que irá ativar as caspases 3 ou 7 ocasionando a apoptose. A via extrínseca é ativada após estímulos dos receptores da família do fator de necrose tumoral (TNF), incluindo o receptor Fas (primeiro sinal de apoptose), TNF-alfa (fator de necrose tumoral) e TRAIL (ligando indutor de apoptose associado ao TNF). Após ligação e oligomerização do ligante, os domínios de morte (FADD e TRADD) são recrutados, eles associam-se a caspase-8 que é clivada e liberada no citoplasma, ativando assim as caspases executoras 3, 6 e 7, levando à apoptose. As vias intrínsecas e extrínsecas resultam na ativação de caspases (proteases de cisteína aspartato-específica) fundamentais para a apoptose, que são responsáveis pela clivagem de proteínas essenciais, em última

análise conduzindo à destruição celular (HUTT, 2015; KNIGHT et al., 2019; GRILO; MANTALARIS, 2019).

A desregulação da via apoptótica, contribui para o desenvolvimento do câncer e resistência à terapia (KOFF; RAMACHANDIRAN; BERNAL-MIZRACHI, 2015). Esta resistência também pode ser causada pela superexpressão de proto-oncogenes (CROCE, 2008) e pela redução da expressão de genes supressores de tumor (ZAHREDDINE; BORDEN, 2013).

1.6 Proteína p53

O fator de transcrição p53 conhecido como "guardião do genoma" é uma proteína supressora de tumores (NIAZI et al., 2018). Ela regula várias funções biológicas como, preservação da integridade genômica contra danos no DNA, indução de parada do ciclo celular para o reparo de quebras da fita de DNA, controle da proliferação, migração, invasão e indução de apoptose (NIAZI et al., 2018; YAMADA; YOSHIDA, 2019).

A ativação da p53 pode levar à sobrevivência ou morte celular, dependendo dos níveis de estresse. Baixos níveis de estresse ou dano desencadeiam a ativação de p53 para induzir parada do ciclo celular durante a fase de transição de G1 a S para o reparo do DNA e sobrevivência celular. Em contraste, altos níveis de estresse ou lesões difíceis de serem revertidas resultam na ativação da p53 que sinaliza às células para se isolarem e sofrerem autodestruição por meio da apoptose, que garante que as células não passem o DNA errôneo para suas células progênitas (NIAZI et al., 2018; KANG; KROEMER; TANG, 2019).

Pela via intrínseca, quando ativada pelos sinais de estresse celular, a p53 regula os fatores de transcrição pró-apoptóticos, como Puma, Bax, Bak, Noxa, Bad, Bid, p53AIP1, APAF1 entre outros, mantendo a expressão basal do fator indutor de apoptose (AIF) reprimindo a expressão de proteínas anti-apoptóticas como Bcl-2, Bcl-xL e Mcl-1. Posteriormente, a p53 se liga diretamente a esses membros pró-apoptóticos e se transloca rapidamente para a mitocôndria, aumentando a permeabilização da membrana externa mitocondrial, desencadeando a morte celular pela liberação do citocromo c e ativação da cascata de caspases (WANG et al., 2014; KANG; KROEMER; TANG, 2019; YAMADA; YOSHIDA, 2019).

De acordo com os estudos de Seba e colaboradores, a p53 exibe papel na regulação da transição epitelial-mesenquimal. Sua ativação pode promover a reversão das células

mesenquimais para epiteliais e a consequente redução da migração e invasão (SEBA et al., 2018). Em muitos tipos de câncer, a p53 encontra-se mutada ou deletada, inativando suas funções antitumorais e antimetastáticas (KANG; KROEMER; TANG, 2019; YAMADA; YOSHIDA, 2019). Nesse contexto, a inativação da p53 possui grande relação com OS e consequente metástase pulmonar (LIU et al., 2000; LIU, KANG; 2017). No entanto, pesquisas mostraram que sua ativação inibiu a migração e invasão *in vitro* e diminuiu o crescimento e metástase pulmonar *in vivo* no OS (NAKASE et al., 2005; SONG et al., 2015).

Devido a estes problemas, muitos estudos têm focado na identificação de genes alvo do p53 que possam retomar sua função supressora de tumor (SILVA et al., 2018b; KANG; KROEMER; TANG, 2019; YAMADA; YOSHIDA, 2019). Como muitas substâncias de baixa massa molecular como chalconas, curcumina e seus híbridos, atuam na ativação de p53 vale a pena investigar o mecanismo molecular pelo qual é regulada (SILVA et al., 2016; LIMA et al., 2018; SEBA et al., 2018; SILVA et al., 2018a). Desta forma, a restauração de p53 pode ser uma abordagem terapêutica para o OS e outros tipos de câncer, visto que o controle de p53 nas células é rigidamente regulado por vários fatores, incluindo exportadores nucleares e proteínas chaperonas que possivelmente controlam seu mecanismo de translocação (SEBA et al., 2018; SILVA et al., 2018b).

1.7 Proteína Hsp40

As proteínas de choque térmico (Hsp) conhecidas como chaperonas moleculares, constituem uma grande família de proteínas envolvidas no enovelamento de proteínas cuja expressão é induzida por choque térmico ou outro tipo de estresse. De todas as principais famílias de Hsp, a Hsp40 tem o maior número de membros, que são classificadas em três subclasses de DNAJ: DNAJA, DNAJB e DNAJC (WU et al., 2017b). As Hsp40 são co-chaperonas que estimulam a atividade de hidrólise de ATP da Hsp70 e regulam o dobramento, desnaturação, translocação e degradação de proteínas. Devido aos poucos estudos relacionados a Hsp40, não são conhecidos os mecanismos moleculares e seu papel no câncer. No entanto investigações recentes indicaram uma relação positiva entre Hsp40 e p53 (WU et al., 2017b; SILVA et al., 2018b).

Foi identificado que a Hsp40 se liga a p53 regulando sua conformação e estabilidade (HIRAKI et al., 2015; SILVA et al., 2018b). Desta forma, a indução de Hsp40 está envolvida na ativação da p53, na qual DNAJB1 (membro da família Hsp40) inibe a ubiquitinação

mediada pelo MDM2 e degradação do p53 e contribui para a ativação de p53 nas células cancerígenas (QI et al., 2014). Além disso, a maior indução de Hsp40 está relacionada ao aumento da atividade de caspase-3, já quando silenciada a atividade da caspase diminui (SILVA et al., 2018b). Outros dados específicos de membros da família Hsp40 como a DNAJA3 mostraram sua interação direta com Hsp70 e p53 e sua indução da apoptose via intrínseca em células de câncer de mama MCF-7 (TRINH; ELWI; KIM, 2010) além da capacidade em suprimir o carcinoma espinocelular de cabeça e pescoço *in vivo* (CHEN et al., 2009). DNAJA3 regula a angiogênese ao desestabilizar o fator 1 induzível por hipóxia (HIF-1) em células de câncer de colo uterino (BAE et al., 2005). O silenciamento de Hsp40 em células de OS, apresentou maior crescimento celular e diminuição da apoptose, o que mostra sua importância na supressão tumoral (EDWARDS; MÜNGER, 2004). A proteína DNAJB4, apresentou atividade supressora de tumor e indução da atividade de caspase-3, sua expressão inibiu a proliferação, crescimento, migração, invasão e diminui a progressão do ciclo celular de células de câncer de pulmão (TSAI et al., 2006; LIN et al., 2010). A alta expressão de DNAJB6 reduz a malignidade tumoral, crescimento e ocasiona a reversão parcial da transição epitélio-mesenquimal em células de câncer de mama *in vivo* (MITRA et al., 2008; MITRA et al., 2010). A DNAJC25 é uma proteína supressora de tumor, sua alta expressão reduz o número de colônias de células de câncer hepático e aumenta o nível de apoptose (LIU et al., 2012). De acordo com os dados apresentados, a Hsp40 é um alvo molecular relevante para os estudos contra a tumorigênese (SILVA et al., 2018b)

1.8 Curcumina e sua atividade antitumoral

A curcumina (Figura 2) é uma substância de cor amarela isolada de rizomas de *Curcuma longa* (Zingiberaceae), popularmente conhecida como açafrão-da-terra ou turmérico. Sua fórmula química de acordo com a IUPAC é [(1*E*, 6*E*)-1,7-*bis*(4-hidroxi-3-metoxifenil)hepta-1,6-dieno-3,5-diona] (SALEHI et al., 2019).

Figura 2. Estrutura da curcumina

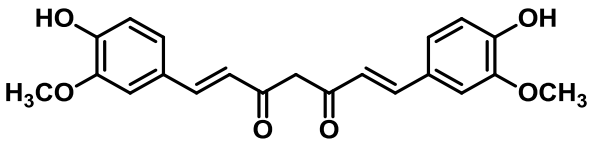

Fonte: autor

O açafrão-da-terra vem sendo utilizado por séculos com fins terapêuticos no Sudeste Asiático, devido aos seus múltiplos efeitos farmacológicos (SALEHI et al., 2019), sendo presente na culinária mundial. A curcumina é considerada pela FDA como GRAS (Geralmente Reconhecido como Seguro) (GUPTA et al., 2012), pois em quantidades elevadas é bem tolerada. Uma revisão sobre o potencial terapêutico *in vivo* da curcumina revelou seus efeitos nos sistemas gastrointestinal, respiratório e cardiovascular, e efeitos anti-inflamatórios, antidiabéticos, hepatoprotetores, neuroprotetores, quimioprotetores, antineoplásicos, antialérgicos e antimicóticos (SALEHI et al., 2019).

Estudos mostraram que a curcumina inibiu o desenvolvimento de células tumorais de pulmão, colorretal, gástrico (FANG et al., 2013), mama (SRIVASTAVA; SRIVASTAVA, 2019), cervical (WANG et al., 2016; PAULRAJ et al., 2015), vulva (WU; LU; CUI, 2015), ovário (GOU et al., 2015) e osteossarcoma (LIMA et al., 2018). Além disso, induziu a apoptose e parada do ciclo celular de células tumorais de ovário (GOU et al., 2015) e ocasionou morte celular por apoptose em células de OS (LIMA et al., 2018). Yallapu e colaboradores relataram que a curcumina foi efetiva contra células de câncer de mama e ovário, apresentando inibição da proliferação e formação de colônias, além da indução de apoptose (YALLAPU et al., 2010). A inibição da migração, invasão e metástase foram relatadas contra células de câncer de pulmão, por meio da ativação da proteína DNAJB4 da família Hsp40 (CHEN et al., 2008). Maher e colaboradores mostraram que a curcumina foi eficaz contra as células tumorais SiHa e HeLa, infectadas com HPV-16 e HPV-18, respectivamente, além de induzir apoptose, regular genes supressores de tumor (p53 e Rb) e diminuir a expressão dos oncogenes E6 e E7 (MAHER et al., 2011).

Uma revisão sobre produtos naturais e seus alvos biológicos, indicou que a atividade da curcumina é correlacionada com a presença da cetona α, β-insaturada (GERSCH et al., 2012). Esse grupo é muito comum em algumas substâncias que possuem atividade antitumoral, pois podem atuar como aceptores de Michael, reagindo com biomoléculas (WANG et al., 2018). Li e colaboradores estudaram a ação de análogos de curcumina e

demostraram que a atividade contra células não-pequenas de pulmão foram dependentes do aceptor de Michael (LI et al., 2015b). Desta forma, esta funcionalidade parece ser interessante para o planejamento de novas susbtâncias antitumorais (WANG et al., 2018).

A bioatividade da curcumina vem sendo associada às propriedades sequestradoras de radicais livres (ou antioxidantes) e a vários mecanismos moleculares, como a modulação da expressão do fator de transcrição p53 e seus genes-alvo (LIN, 2007). Também foi relatado que a curcumina pode ativar os receptores de aril hidrocarbonetos (AhR) que exibe uma atividade semelhante ao supressor de tumor. A curcumina realiza uma translocação nuclear de AhR seguida pelo aumento da expressão de citocromo P450 (KUMAR et al., 2016; SAFE et al., 2018). Além disso, a curcumina é um potencial agente anticâncer por inibição da angiogênese mediada por HIF-1α. Foi demonstrado que a curcumina diminui a expressão de HIF-1α que ocasiona, por exemplo, o aumento do processo EMT, da invasão e do comportamento metastático (BAHRAMI et al., 2018).

A curcumina pode inibir a atividade de várias proteínas relacionadas a resistências do câncer, como a glicoproteína-p (P-gp) (LI et al., 2010; LI et al., 2011; REVALDE et al., 2015). Estas proteínas transmembrana atuam como bombas de efluxo de fármacos, reduzindo ativamente os níveis intracelulares de fármacos. Dessa forma, são necessárias doses progressivamente maiores de fármacos antineoplásicos que consequentemente aumentam o risco de toxicidade (NABEKURA, 2010). A inibição de bombas de efluxo pela curcumina é um fato muito importante, visto que mais de 70% dos pacientes com câncer de ovário, são resistentes à terapia com taxanos (YALLAPU; JAGGI; CHAUHAN, 2010). Foi identificado que este mecanismo de resistência é devido à expulsão do fármaco pela expressão de glicoproteína-p (P-gp) e outros transportadores ABC em células tumorais (LI et al., 2010).

A multirresistência na quimioterapia do câncer é um fenômeno em que as células tumorais não respondem ao tratamento com múltiplos fármacos antineoplásicos de diferentes estruturas e mecanismos de ação. É a principal causa de falha da quimioterapia, sendo a razão da elevada taxa de mortalidade, especialmente em estágio avançado e cânceres metastáticos (BAGULEY, 2010; GILLET; GOTTESMAN, 2010).

A toxicidade e a resistência dos antineoplásicos têm despertado interesse dos pesquisadores no desenvolvimento de antitumorais inovadores. Uma das estratégias empregadas no desenvolvimento de fármacos é a hibridação molecular baseada em produtos naturais. Essa ferramenta consiste na união de dois farmacóforos em uma única estrutura, o que resulta em uma melhor eficácia com ação em múltiplos alvos, redução de efeitos adversos

e resistência. Dentre os produtos naturais mais estudados para o tratamento do câncer, a curcumina é o que tem exibido ação *in vivo* (CHOUDHARY et al., 2018; TEWARI et al., 2019).

Apesar de sua eficácia terapêutica, a curcumina possui baixa biodisponibilidade, a qual está associada à sua baixa solubilidade em água e metabolismo de primeira passagem (SALEHI et al., 2019). Este fato levou à busca de análogos obtidos por modificações estruturais, conduzindo a uma maior potência e biodisponibilidade (LIMA et al., 2018; SILVA et al., 2018a).

Paulraj e colaboradores relataram que análogos de curcumina 1,5-bis(2-hidroxifenil)-1,4-pentadieno-3-ona (MS17) e 1,5-bis(4-hidroxi-3-metoxifenil)-1,4-pentadieno-3-ona (MS13) foram mais potentes que a curcumina contra células de câncer cervical CaSki e HeLa, linhagens positivas para HPV 16 e 18 respectivamente, induzindo a morte celular por apoptose (PAULRAJ et al., 2015). Outro estudo avaliou o análogo de curcumina CH-5 (Figura 3) contra células de osteossarcoma U2OS, MG-63 e Saos-2 onde CH-5 mostrou-se mais ativo que a curcumina, controlando a expressão do fator de transcrição p53. Este mesmo análogo se mostrou eficaz no tratamento de células de câncer gástrico HGC-27, induzindo a morte celular por apoptose e reduzindo a migração e invasão das células tumorais (LIMA et al., 2018).

Figura 3. Estrutura do análogo de curcumina (CH-5)

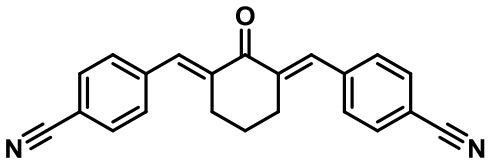

Fonte: autor

Silva e colaboradores sintetizaram uma série de híbridos de curcumina-resveratrol e avaliaram seu potencial contra células de câncer de mama (MCF-7), o híbrido mais ativo (Figura 4) apresentou um valor de CI_{50} de 19,09 μM sendo mais potente que a curcumina, resveratrol ou curcumina combinada com resveratrol, levando ao bloqueio do ciclo celular no início da mitose e, posteriormente, apoptose (SILVA et al., 2018c).

Figura 4. Híbrido de curcumina-resveratrol

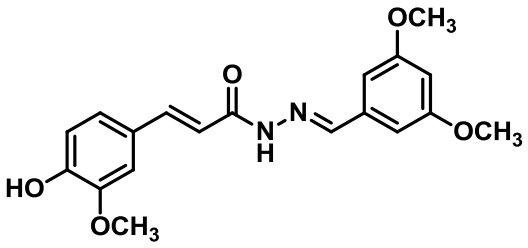

Fonte: autor

Os efeitos antineoplásicos da curcumina, seus análogos e híbridos, podem estar envolvidos nas vias regulatórias transcricionais responsáveis pela regulação dos genes relacionados à tumorigênese, angiogênese, metástase, invasão, proliferação e apoptose (LIN, 2007; SHISHODIA, 2013).

1.9 Cinamaldeído e sua atividade antitumoral

O cinamaldeído (obtido de espécies de *Cinnamomum*) é uma substância constituinte de 50% a 70% do óleo essencial da casca das "canelas", as quais vêm sendo utilizada há milhares de anos para fins medicinais e culinários (HONG et al., 2016, POLAQUINI et al., 2017). É uma substância classificada e aprovada pela FDA (Food and Drug Administration) como GRAS (geralmente reconhecido como seguro) (FABRA et al., 2016). Sua estrutura química (Figura 5) é de natureza fenilpropanoídica, formada por um aldeído aromático α,β-insaturado (POLAQUINI et al., 2017).

Figura 5. Estrutura química do cinamaldeído

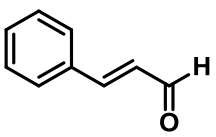

Fonte: autor

A ação do cinamaldeído tem sido amplamente estudada em diversas áreas, revelando seus efeitos antidiabéticos, antidepressivos, antivirais, anti-inflamatórios, antiosteoporóticos e

antineoplásicos (HONG et al., 2016). Suas atividades antitumorais têm sido exploradas contra linhagens tumorigênicas de pulmão (WU et al., 2017a), mama (RAD et al., 2015), câncer colorretal (LU; OBIANOM; AI, 2018), bucal (YU et al., 2019), osteossarcoma, cervical, pele e neuroblastoma (SINGH et al., 2009). Os extratos e óleos essenciais da canela apresentaram efeito antialérgico, antimicrobiano, antioxidante, antiangiogênico, antimutagênico e anti-Alzheimer. Estes dados são interessantes, visto que o componente principal dos extratos e óleos essenciais da canela é o cinamaldeído. Além disso, os extratos de canela reduziram significativamente a migração de células de câncer de colo uterino (SiHa) e induziram apoptose, aumentando as concentrações de cálcio intracelular, ocasionando a alteração do potencial de membrana mitocondrial (HAMIDPOUR et al., 2015; HONG et al., 2016).

A atividade do cinamaldeído tem sido descrita na regulação da invasão, metástase e no efeito antiproliferativo pela inibição da ciclina D1 em vários tipos de tumores (HONG et al., 2016; WU et al., 2017a). Rad e colaboradores demonstraram em seus estudos sobre câncer de mama, que a ação do cinamaldeído está relacionada à morte celular por apoptose mediada pela ativação da caspase-8 (RAD et al., 2015). Outro estudo mostrou sua capacidade em inibir a proliferação celular de câncer cervical (HeLa) pela indução da parada do ciclo celular na fase S (LARASATI et al., 2014). Um estudo de revisão indicou que sua inibição da proliferação tumoral pode ocorrer pela indução da apoptose por espécies reativas de oxigênio (EROs) em células de leucemia HL-60 e ativação de proteínas pró-apoptóticas da família Bcl-2 em células de hepatoma humano (HONG et al., 2016). No entanto, o cinamaldeído possui instabilidade química devido à sua alta reatividade relacionada à presença do grupo aldoxila (aldeído) (LOPACHIN; GAVIN, 2014; HONG et al., 2016; POLAQUINI et al., 2017).

Para superar essa limitação, o estudo com análogos e híbridos do cinamaldeído tem sido de grande interesse para as extensivas pesquisas de muitos cientistas da área da química medicinal. Uma pesquisa de revisão mostrou que substâncias derivadas do cinamaldeído são candidatos para o desenvolvimento de fármacos antineoplásicos como, por exemplo, o derivado 2-hidroxicinamaldeído (Figura 6). Este derivado apresentou efeitos antiproliferativos contra células tumorigênicas e induziu a apoptose em células de câncer de cólon ao diminuir a expressão da proteína anti-apoptótica Bcl-2, aumentando a expressão da proteína Bax e induzindo a translocação citoplasmática do citocromo c. Outros relatos mostraram que baixas concentrações (10 μM) dos derivados 2-hidroxicinamaldeído e 2-benzoiloxicinamaldeído (Figura 6) induzem a apoptose em células de câncer de mama MDA-MB-231 p53-mutante e

câncer de colorretal SW620 por induzir o acúmulo de EROs e ativação de caspase-3, sugerindo que o cinamaldeído induz a apoptose via caspase-3 de modo independente de p53. A ação conjunta de polifenóis e cinamaldeído desencadearam a parada do ciclo celular na fase G2/M e morte celular por apoptose em células de câncer de ovário resistentes à cisplatina (HONG et al., 2016).

Figura 6. Estrutura química do 2-hidroxicinamaldeído e 2-benzoiloxicinamaldeído

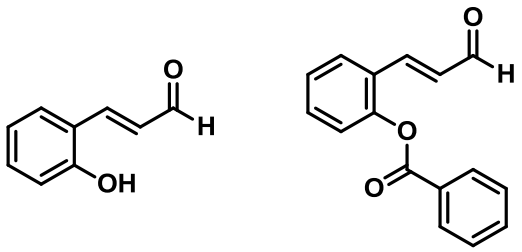

Fonte: autor

Outros trabalhos descreveram que derivados de ácido acetilsalicílico baseados na estrutura do cinamaldeído apresentaram atividade contra linhagens HCT-8 de câncer de colorretal. A avaliação biológica indicou que a substância mais ativa (Figura 7) exibiu um aumento de mais de 10 vezes na atividade antiproliferativa em comparação às substâncias de origem natural e baixa toxicidade nas células não-tumorigênicas, além disso, induziu a parada do ciclo celular e apoptose, mostrando que derivados de cinamaldeído são promissores agentes para o desenvolvimento de fármacos antineoplásicos inovadores (LU; OBIANOM; AI, 2018).

Figura 7. Estrutura química dos derivados de ácido acetilsalicílico baseados no cinamaldeído

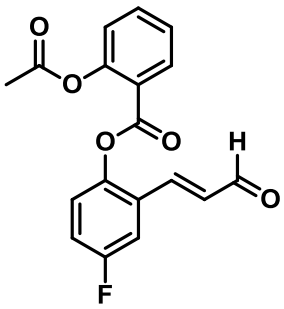

Fonte: autor

1.10 Chalconas e sua atividade antitumoral

As chalconas são substâncias que pertencem à família dos flavonoides que são presentes em frutas, legumes e plantas (JANDIAL et al., 2014; MIRZAEI; EMAMI, 2016). Sua estrutura é composta por dois anéis benzênicos unidos por uma ponte cetônica α,β-insaturada (Figura 8) (MIRZAEI; EMAMI, 2016).

Figura 8. Núcleo chalcônico

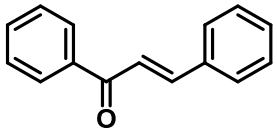

Fonte: autor

A síntese de chalconas ou seu isolamento a partir de fontes naturais estão sendo investigadas em todo o mundo para o desenvolvimento de medicamentos mais potentes e eficientes para o tratamento de diversas doenças (SINGH; ANAND; KUMAR, 2014). Revisões sobre a atividade biológica das chalconas mostraram seus efeitos anti-inflamatórios, antifúngicos, anti-*Leishmania*, antiproliferativos, antimaláricos, antimicrobianos, antiprotozoários, anti-HIV e antidiabéticos (SINGH; ANAND; KUMAR, 2014; MIRZAEI; EMAMI, 2016).

Diversos estudos mostraram que as chalconas inibiram o desenvolvimento de células tumorais de fígado, ovário (BHAT et al., 2005), próstata (BHAT et al., 2005; SYAM et al., 2012), pulmão (BHAT et al., 2005; SYAM et al., 2012), colorretal (BHAT et al., 2005; SYAM et al., 2012; IFTIKHAR et al., 2017), cervical (BHAT et al., 2005; MARQUES et al., 2019), vulva (MARQUES et al., 2019), mama (SYAM et al., 2012; BORTOLOTTO et al., 2017; IFTIKHAR et al., 2017; MARQUES et al., 2019) e osteossarcoma (SILVA et al., 2016). Além disso, a *trans*-chalcona (Figura 8) aumentou o nível de EROs ocasionando a morte de células de câncer de mama (MCF-7) por apoptose, por vias intrínsecas e extrínsecas, pois também aumentou a atividade das caspases-7, -8 e -9 (SYAM et al., 2012). Bortolotto e colaboradores também realizaram estudos com as células MCF-7, na qual, a *trans*-chalcona ocasionou a parada do ciclo celular na fase G1 e induziu apoptose mediado pela via intrínseca, pela inibição de Bcl-2 e indução de Bax (BORTOLOTTO et al., 2017).

Estudos de Silva e colaboradores mostraram que a *trans*-chalcona inibiu o crescimento de células cancerígenas de OS (U2OS), mediado pela indução de apoptose dependente da caspase, além de regular genes envolvidos na migração e invasão celular (SILVA et al., 2016). Outro trabalho deste mesmo autor mostrou que a *trans*-chalcona induziu a expressão de p53, além do gene Hsp40 nas células de OS (U2OS), que está envolvido na estabilidade e ativação da p53, bloqueando sua ubiquitinação mediada por MDM2 através da interação com MDM2 (SILVA et al., 2018b).

Uma revisão sobre a farmacologia das chalconas mostrou que suas estruturas simples e versáteis exibiram atividade anticâncer por morte celular apoptótica por meio de interação com alvos moleculares como MDM2 / p53, tubulina e STAT3 (MENEZES; DIEDERICH, 2019). Outros dados sugerem que as chalconas também têm como alvo, várias vias de sinalização de câncer, como a via proteossômica, o ciclo celular, a apoptose, os receptores e os transportadores de resistência a múltiplos fármacos (JANDIAL et al., 2014).

O potencial anticâncer das chalconas também está associada à sua capacidade de ligação à tubulina e propriedade alquilante, bem como possíveis interações com várias proteínas envolvidas na apoptose e proliferação celular (MIRZAEI; EMAMI, 2016). Também foi relatado que seu mecanismo de ação pode ser via porção carbonila α, β-insaturada como aceitador de Michael, tioredoxina redutase, via Keap1-Nrf2-ARE e inibição da formação de microtúbulos (MENEZES; DIEDERICH, 2019).

No entanto, vários estudos mostram que a estrutura da chalcona pode ser facilmente modificada para potencializar sua ação biológica, como por exemplo, pela adição de uma grande variedade de grupos funcionais como arilos, halogênios, hidroxilas, grupos carboxílicos, benzenos etc (JANDIAL et al., 2014). Além disso, os substituintes metoxi e hidroxi são importantes na atividade antitubulina e citotóxica das chalconas (MIRZAEI; EMAMI, 2016).

Santos e colaboradores relataram que as chalconas 2’-flúor-4’-aminochalcona e 3’-piridil-4’-aminochalcona (Figura 9) foram ativas contra as linhagens de células de câncer de mama MCF-7 e MDA-MB-231, induziram a morte celular por apoptose em ambas as linhagens e aumentaram a expressão da proteína pró-apoptótica p53 na linhagem MCF-7. Estas chalconas ainda foram capazes de inibir a proliferação celular mesmo em condições de acidose, demonstrando serem substâncias promissoras para o tratamento do câncer de mama (SANTOS et al., 2019).

Figura 9. 2'-fluor-4'-aminochalcona e 3'-piridil-4'-aminochalcona

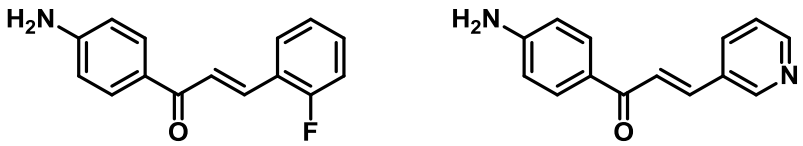

Fonte: autor

Markovic e colaboradores mostraram que híbridos de antraquinona e chalcona (Figura 10) tiveram efeito citotóxico seletivo contra as células de câncer cervical (HeLa), por meio da indução de apoptose dependente de caspase (MARKOVIC et al., 2015).

Figura 10. Híbrido de antraquinona e chalcona

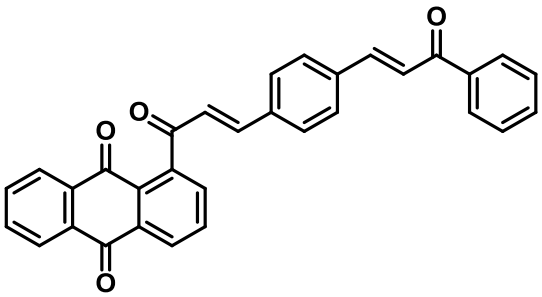

Fonte: autor

Outro estudo com aminochalconas realizado por Seba e colaboradores, mostraram que as 4’-amino-1’-naftil-chalcona e 4’-amino-4’-metil-1’-naftil-chalcona (Figura 11) apresentaram baixa capacidade de inibir a viabilidade das células de OS (U2OS e SAOS-2), no entanto, diminuiram a migração, invasão, atividade da MMP-2 e regularam genes envolvidos na EMT, além de induzir a expressão de p53 que pode estar relacionada aos efeitos anti-metastáticos (SEBA et al., 2018).

Figura 11. 4'-amino-1'-naftil-chalcona e 4'-amino-4'-metil-1'-naftil-chalcona

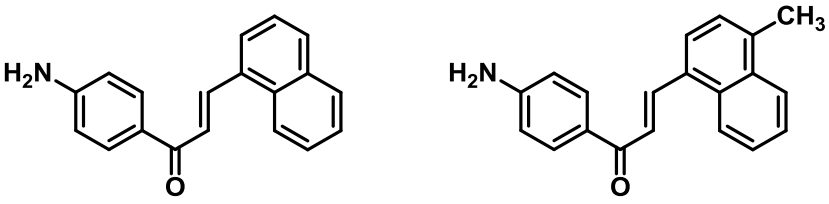

Fonte: autor

Silva e colaboradores analisaram o efeito da 4’-hidroxi-chalcona (Figura 12) contra células cancerígenas de OS (U2OS) que suprimiu a proteína Sp1 e induziu p53 (SILVA et al., 2016). Este mesmo autor mostrou que a 2’-hidroxi-5’-flúor-chalcona (Figura 12) induziu a expressão de p53, além do gene Hsp40 nas células de OS (U2OS). Além disso, 2-hidroxi-5-flúor chalcona exibiu a maior atividade da caspase quando comparado a *trans*-chalcona (SILVA et al., 2018b).

Figura 12. 4'-hidroxi-chalcona e 2'-hidroxi-5'-flúor-chalcona

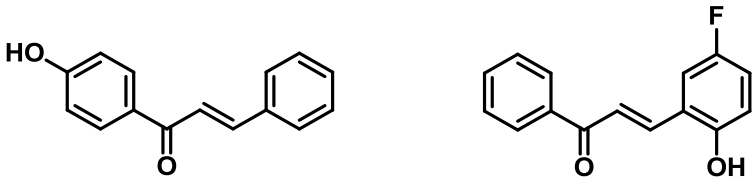

Fonte: autor

2. JUSTIFICATIVAS

O câncer é uma das principais causas de mortes no mundo. Apesar dos tratamentos existentes, infelizmente não são totalmente eficazes e possuem alta toxicidade, ocasionando variados efeitos adversos, reversíveis ou não.

Devido a isso, a busca por novos fármacos baseados em produtos naturais tem crescido mundialmente, visto que a curcumina, cinamaldeído e chalconas têm demonstrado atividade anticâncer em diversos trabalhos da literatura. Além disso, a ferramenta da hibridação molecular é muito interessante e útil na potencialização da ação destas substâncias para a busca de novos fármacos contra o câncer.

3. OBJETIVOS

3.1 Objetivos Gerais

O presente trabalho teve dois objetivos gerais: avaliar o efeito de híbridos curcumina-cinamaldeído sobre a viabilidade celular de linhagens de câncer feminino e de osteossarcoma; selecionar o híbrido mais ativo e investigar os possíveis mecanismos celulares e moleculares em células de osteossarcoma.

3.2 Objetivos Específicos

Capítulo II

- Determinar a CI_{50} de doze híbridos curcumina-cinamaldeído contra linhagens de câncer feminino: câncer de mama (MCF-7 e MDA-MB-231); câncer de colo do útero (C33, HeLa, SiHa, CaSki) e câncer de vulva (A431);
- Avaliar a inibição da formação de colônias após o tratamento com o híbrido mais ativo (**5a**) contra a célula mais sensível (A431);
- Avaliar a seletividade de **5a** testando seu efeito contra células de queratinócitos não-tumorigênicos (HaCaT);
- Avaliar a estabilidade de **5a** sob condições fisiológicas;
- Predizer *in silico* propriedades farmacocinéticas e *drug-likeness* de **5a**;

Capítulo III

- Determinar a CI_{50} do híbrido **3HC(5a)** contra linhagens de osteossarcoma U2OS (p53 selvagem) e SAOS-2 (p53 ausente);
- Avaliar a atividade pró-apoptótica de **3HC** em U2OS;
- Avaliar a capacidade de migração e invasão da linhagem U2OS após tratamento com **3HC** e seu efeito sobre a atividade da MMP-2;
- Avaliar o perfil de expressão de p53 e DNAJB1(Hsp40) na linhagem U2OS após tratamento com **3HC**.

Obs: **5a** e **3HC** é a mesma substância. No primeiro artigo (Capítulo II) a substância selecionada foi a **5a** e no segundo artigo (Capítulo III) chamamos **5a** de **3HC**.

4. REFERÊNCIAS

ADAMS, J. M.; CORY, S. The Bcl-2 apoptotic switch in cancer development and therapy. **Oncogene**, v. 26, p. 1324–1337, 2007.

ALBERTS, B.; JOHNSON, A.; LEWIS, J.; RAFF, M.; ROBERTS, K.; WALTER, P. **Biologia Molecular da Célula**. 6. ed. – Porto Alegre : Artmed, 2017.

ANDERSON, M. E. Update on survival in osteosarcoma. **Orthopedic Clinics of North America**, v. 47, p. 283–292, 2016.

ARALDI, R. P.; SANT'ANA, T. A.; MÓDOLO, D. G.; MELO, T. C.; SPADACCI-MORENA, D. D.; STOCCO, R. C.; CERUTTI, J. M.; SOUZA, E. B. The human papillomavirus (HPV)-related cancer biology: An overview. **Biomedicine & Pharmacotherapy**, v. 106, p. 1537–1556, 2018.

BAE, M. K.; JEONG, J. W.; KIM, S. H.; KIM, S. Y.; KANG, H. J.; KIM, D. M.; BAE, S. K.; YUN, I. L.; TRENTIN, G. A.; ADCOCK, M. R.; KIM, K. W. Tid-1 interacts with the von Hippel-Lindau protein and modulates angiogenesis by destabilization of HIF-1α. **Cancer Research**, v. 6, p. 2520–2525, 2005.

BAGULEY, B. C. Multiple drug resistance mechanisms in cancer. **Molecular Biotechnology**, v. 46, p. 308–316, 2010.

BAHRAMI, A.; ATKIN, S. L.; MAJEED, M.; SAHEBKAR, A. Effects of curcumin on hypoxia-inducible factor as a new therapeutic target. **Pharmacological research**, v. 137, p. 159–169, 2018.

BHAT, B. A.; DHAR, K. L.; PURI, S. C.; SAXENA, A. K.; SHANMUGAVELB, M.; QAZI, G. N. Synthesis and biological evaluation of chalcones and their derived pyrazoles as potential cytotoxic agents. **Bioorganic & Medicinal Chemistry Letters**, v. 15, p. 3177–3180, 2005.

BJORNLAND, K.; FLATMARK, K.; PETTERSEN, S.; AAASEN, A. O.; FODSTAD, O.; MAELANDSMO, G. M. Matrix metalloproteinases participate in osteosarcoma invasion. **Journal of Surgical Research**, v. 127, p. 151–156, 2005.

BORTOLOTTO, L. F. B.; BARBOSA, F. R.; SILVA, G.; BITENCOURT, T. A.; BELEBONI, R. O.; BAEK, S. J.; MARINS, M.; FACHIN, A. L. Cytotoxicity of *trans*-chalcone and licochalcone A against breast cancer cells is due to apoptosis induction and cell cycle arrest. **Biomedicine & Pharmacotherapy**, v. 85, p. 425–433, 2017.

CARR, S. V. Surrogacy and ethics in women with cancer. **Best Practice & Research Clinical Obstetrics and Gynaecology**, v. 18, p. 30113–30115, 2018.

CHEN, H. W.; LEE, J. Y.; HUANG, J. Y.; WANG, C. C.; CHEN, W. J.; SU, S. F.; HUANG, C. W.; HO, C. C.; CHEN, J. J. W.; TSAI, M. F.; YU, S. L.; YANG, P. C. Curcumin inhibits lung cancer cell invasion and metastasis through the tumor suppressor HLJ1. **Cancer Research**, v. 68, p. 7428–7438, 2008.

CHEN, C. Y.; CHIOU, S. H.; HUANG, C. Y.; JAN, C. I.; LIN, S. C.; HU, W. Y.; CHOU, S. H.; LIU, C. J.; LO, J. F. Tid1 functions as a tumour suppressor in head and neck squamous cell carcinoma. **The Journal of Pathology: A Journal of the Pathological Society of Great Britain and Ireland**, v. 219, p. 347–355, 2009.

CHOUDHARY, S.; SINGH, P. K.; VERMA, H.; SINGH, H.; SILAKARI, O. Success stories of natural product-based hybrid molecules for multifactorial diseases. **European Journal of Medicinal Chemistry**, v. 151, p. 62–97, 2018.

CROCE, C. M. Oncogenes and cancer. **The New England Journal of Medicine**, v. 358, p. 502–511, 2008

ECCLES, S. A.; WELCH, D. R. Metastasis: recent discoveries and novel treatment strategies. **The Lancet**, v. 369, p. 1742–1757, 2007.

EDWARDS, K. M.; MÜNGER, K. Depletion of physiological levels of the human TID1 protein renders cancer cell lines resistant to apoptosis mediated by multiple exogenous stimuli. **Oncogene**, v. 23, p. 8419–8431, 2004.

FABRA, M. J.; CASTRO-MAYORGA, J. L.; RANDAZZO, W.; LAGARÓN, J. M.; LÓPEZ-RUBIO, A.; AZNAR, R.; SÁNCHEZ, G. Efficacy of cinnamaldehyde against enteric viruses and its activity after incorporation into biodegradable multilayer systems of interest in food packaging. **Food and Environmental Virology**, v. 8, p. 125–132, 2016.

FANG, X.; FANG, L.; GOU, S.; CHENG, L. Design and synthesis of dimethylaminomethyl-substituted curcumin derivatives/analogues: Potent antitumor and antioxidant activity, improved stability and aqueous solubility compared with curcumin. **Bioorganic & Medicinal Chemistry Letters**, v. 23, p. 1297–1301, 2013.

GAFFNEY, D. K.; HASHIBE, M.; KEPKA, D.; MAURER, K. A.; WERNER, T. L. Too many women are dying from cervix cancer: Problems and solutions. **Gynecologic Oncology**, v. 151, p. 547–554, 2018.

GERSCH, M.; KREUZER, J.; SIEBER, S. A. Electrophilic natural products and their biological targets. **Natural Product Reports**, v. 29, p. 659–682, 2012.

GILLET, J. P.; GOTTESMAN, M. M. Mechanisms of multidrug resistance in cancer. **Methods Molecular Biology**, v. 596, p. 47–76, 2010.

GINSBURG, O.; BRAY, F.; COLEMAN, M. P.; VANDERPUYE, V.; ENIU, A.; KOTHA, S. R.; SARKER, M.; HUONG, T. T.; ALLEMANI, C.; DVALADZE, A.; GRALOW, J.; YEATES, K.; TAYLOR, C.; OOMMAN, N.; KRISHNAN, S.; SULLIVAN, R.; KOMBE, D.; BLAS, M. M.; PARHAM, G.; KASSAMI, N.; CONTEH, L. The global burden of women's cancers: a grand challenge in global health. **Lancet**, v. 389, p. 847–860, 2017.

GLOBOCAN–IARC. **BRAZIL**. Disponível em: < https://gco.iarc.fr/today/data/factsheets/populations/76-brazil-fact-sheets.pdf>. Acesso em: 04 dez. 2019.

GLOBOCAN–IARC. **MUNDO**. Disponível em: < https://gco.iarc.fr/today/data/factsheets/populations/900-world-fact-sheets.pdf>. Acesso em: 29 mar. 2020.

GOU, Q.; LIU, L.; WANGA, C.; WUA, Q.; SUNA, L.; YANGA, X.; XIEA, Y.; LIB, P.; GONG, C. Polymeric nanoassemblies entrapping curcumin overcome multidrug resistance in ovarian cancer. **Colloids and Surfaces B: Biointerfaces**, v. 126, p. 26–34, 2015.

GRILO, A.; MANTALARIS, A. Apoptosis: A mammalian cell bioprocessing perspective. **Biotechnology Advances**, v. 19, p. 459–475, 2019.

GUPTA, S. C.; PATCHVA, S.; KOH, W.; AGGARWAL, B. B. Discovery of curcumin, a component of golden spice, and its miraculous biological activities. **Clinical and Experimental Pharmacology and Physiology**, v. 39, p. 283–299, 2012.

HANSON, S.; GILBERT, D.; LANDY, R.; OKOLI, G.; GUELL, C. Cancer risk in socially marginalised women: An exploratory study. **Social Science & Medicine**, v. 220, p. 150–158, 2019.

HAMIDPOUR, R.; HAMIDPOUR, M.; HAMIDPOUR, S.; SHAHLARI, M. *Cinnamon* from the selection of traditional applications to its novel effects on the inhibition of angiogenesis in cancer cells and prevention of Alzheimer's disease, and a series of functions such as antioxidant, anticholesterol, antidiabetes, antibacterial, antifungal, nematicidal, acaracidal, and repellent activities. **Journal of Traditional and Complementary Medicine**, v. 5, p. 66–70, 2015.

HIRAKI, M.; HWANG, S.; CAO, S.; RAMADHAR, T. R.; BYUN, S.; YOON, K. W.; LEE, J. H.; CHU, K.; GURKAR, A. U.; KOLEV, V.; ZHANG, J.; NAMBA, T.; MURPHY, M. E.; NEWMAN, D. J.; MANDINOVA, A.; CLARDY, J.; LEE, S. W. Small-molecule reactivation of mutant p53 to wild-type-like p53 through the p53-Hsp40 regulatory axis. **Chemistry & Biology**, v. 22, p. 1206–1216, 2015.

HONG, S.; ISMAIL, I. A.; KANG, S.; HAN, D. C.; KWON, B. Cinnamaldehydes in Cancer Chemotherapy. **Phytotherapy Research**, v. 30, p. 754–767, 2016.

HOUSSAMI, N.; MACASKILL, P.; MINCKWITZ, G. V.; MARINOVICH, M. L.; MAMOUNAS, E. Meta-analysis of the association of breast cancer subtype and pathologic complete response to neoadjuvant chemotherapy. **European Journal of Cancer**, v. 48, p. 3342–3354, 2012.

HUTT, K. J. The role of BH3-only proteins in apoptosis within the ovary. **Reproduction**, v. 149, p. R81–R89, 2015.

IARC – International Agency for Research on Cancer. **Latest global cancer data: Cancer burden rises to 18.1 million new cases and 9.6 million cancer deaths in 2018**. Disponível em: <https://www.iarc.fr/wp-content/uploads/2018/09/pr263_E.pdf>. Acesso em: 04 dez. 2019.

IFTIKHAR, S.; KHAN, S.; BILAL, A.; MANZOOR, S.; ABDULLAH, M.; EMWAS, A.; SIOUD, S.; GAO, X.; CHOTANA, G. A.; FAISAL, A.; SALEEM, R. S. Z. Synthesis and evaluation of modified chalcone based p53 stabilizing agents. **Bioorganic & Medicinal Chemistry Letters**, v. 27, p. 4101–4106, 2017.

INCA – Instituto Nacional de Câncer José Alencar Gomes da Silva. Estimativa | 2018 – **Incidência de Câncer no Brasil**. Disponível em: <http://www1.inca.gov.br/estimativa/2018/estimativa-2018.pdf>. Acesso em: 27 dez. 2019a.

INCA – Instituto Nacional de Câncer José Alencar Gomes da Silva. Exposições – **A mulher e o câncer de mama no Brasil**. Disponível em: <https://www.inca.gov.br/exposicoes/mulher-e-o-cancer-de-mama-no-brasil#>. Acesso em: 11 dez. 2019b.

INCA – Instituto Nacional de Câncer José Alencar Gomes da Silva. **Tipos de câncer – Câncer do colo do útero**. Disponível em: <https://www.inca.gov.br/tipos-de-cancer/cancer-do-colo-do-utero>. Acesso em: 11 jdez. 2019c.

INCA – Instituto Nacional de Câncer José Alencar Gomes da Silva. **Tipos de câncer – Câncer de corpo do útero**. Disponível em: <https://www.inca.gov.br/tipos-de-cancer/cancer-do-corpo-do-utero>. Acesso em: 11 jdez. 2019d.

INCA – Instituto Nacional de Câncer José Alencar Gomes da Silva. **Tipos de câncer - Câncer de mama**. Disponível em: <https://www.inca.gov.br/tipos-de-cancer/cancer-de-mama>. Acesso em: 11 dez. 2019e.

INCA – Instituto Nacional de Câncer José Alencar Gomes da Silva. **Tipos de câncer - Osteossarcoma - versão para Profissionais de Saúde**. Disponível em: <https://www.inca.gov.br/tipos-de-cancer/cancer-infantojuvenil/osteossarcoma/profissional-de-saude>. Acesso em: 11 dez. 2019f.

JAFFE, N.; PURI, A.; GELDERBLOM, H. Osteosarcoma: evolution of treatment paradigms. **Sarcoma**, v. 2013, p. 1–7, 2013.

JANDIAL, D. D.; BLAIR, C. A.; ZHANG, S.; KRILL, L. S.; ZHANG, Y.; ZI X. Molecular targeted approaches to cancer therapy and prevention using chalcones. **Current Cancer Drug Targets**, v. 14, p. 181–200, 2014.

JIN, J.; CAI, L.; LIU, Z. M.; ZHOU, X. S. miRNA-218 inhibits osteosarcoma cell migration and invasion by down-regulating of TIAM1, MMP2 and MMP9. **Asian Pacific Journal of Cancer Prevention**, v. 14, p. 3681–3684, 2013.

KANG, R.; KROEMER, G.; TANG, D. The tumor suppressor protein p53 and the ferroptosis network. **Free Radical Biology and Medicine**, v. 133, p. 162–168, 2019.

KANSARA, M.; TENG, M. W.; SMYTH, M. J.; THOMAS, D. M. Translational biology of osteosarcoma. **Nature Reviews Cancer**, v. 14, p. 722–735, 2014.

KNIGHT, T.; LUEDTKE, D.; EDWARDS, H.; TAUB, J. W.; GE, Y. A delicate balance – The BCL-2 family and its role in apoptosis, oncogenesis, and cancer therapeutics. **Biochemical Pharmacology**, v. 162, p. 250–261, 2019.

KOFF, J. L.; RAMACHANDIRAN, S.; BERNAL-MIZRACHI, L. A time to kill: targeting apoptosis in cancer. **International Journal of Molecular Sciences**, v. 16, p. 2942–2955, 2015.

KUMAR, G.; MITTAL, S.; SAK, K.; TULI, H. S. Molecular mechanisms underlying chemopreventive potential of curcumin: Current challenges and future perspectives. **Life Sciences**, v. 148, p. 313-328, 2016.

LARASATI, Y. A.; PUTRI, D. P.; UTOMO, R. Y.; HERMAWAN, A.; MEIYANTO, E. Combination of cisplatin and cinnamon essential oil inhibits HeLa cells proliferation through cell cycle arrest. **Journal of Applied Pharmaceutical Science**, v. 4, p. 14–19, 2014.

LAURENT, J. S.; LUCKETT, R.; FELDMAN, S. HPV vaccination and the effects on rates of HPV-related cancers. **Current Problems in Cancer**, v. 42, p 493–506, 2018.

LEI, P.; HE, H.; HU, Y.; LIAO, Z. Small interfering RNA-induced silencing of galectin-3 inhibits the malignant phenotypes of osteosarcoma in vitro. **Molecular Medicine Reports**, v. 12, p. 6316–6322, 2015.

LI, Y.; REVALDE, J. L.; REID, G.; PAXTON, J. W. Interactions of dietary phytochemicals with ABC transporters: possible implications for drug disposition and multidrug resistance in cancer. **Drug Metabolism Reviews**, v. 42, p. 590–611, 2010.

LI, Y.; REVALDE, J. L.; REID, G.; PAXTON, J. W. Modulatory effects of curcumin on multi-drug resistance-associated protein 5 in pancreatic cancer cells. **Cancer Chemotherapy and Pharmacology**, v. 68, p. 603–610, 2011.

LI, H.; ZHANG, K.; LIU, L. H.; OUYANG, Y.; BU, J.; GUO, H. B.; XIAO, T. A systematic review of matrix metalloproteinase 9 as a biomarker of survival in patients with osteosarcoma. **Tumor Biology**, v. 35, p. 5487–5491, 2014.

LI, S.; SUN, W.; WANG, H.; ZUO, D.; HUA, Y.; CAI, Z. Research progress on the multidrug resistance mechanisms of osteosarcoma chemotherapy and reversal. **Tumor Biology**, v. 36, p. 1329–1338, 2015a.

LI, Y.; ZHANG, L.; DAI, F.; YAN, W.; WANG, H.; TU, Z.; ZHOU, B. Hexamethoxylated mono-carbonyl analogs of curcumin cause G2/M cell cycle arrest in NCI-H460 cells via Michael acceptor-dependent redox intervention. **Journal of Agricultural and Food Chemistry**, v. 63, p. 7731–7742, 2015b.

LIN, J. K. Molecular targets of curcumin. **Advances in Experimental Medicine and Biology**, v. 595, p. 227–243, 2007.

LIN, S. Y.; HSUEH, C. M.; YU, S. L.; SU, C. C.; SHUM, W. Y.; YEH, K. C.; CHANG, G. C.; CHEN, J. J. HLJ1 is a novel caspase-3 substrate and its expression enhances UV-induced apoptosis in non-small cell lung carcinoma. **Nucleic Acids Research**, v. 38, p. 6148–6158, 2010.

LIMA, F. T.; SEBA, V.; SILVA, G.; TORREZAN, G. S.; POLAQUINI, C. R.; PINHANELLI, V. C.; BAEK, S. J.; FACHIN, A. L.; REGASINI, L. O.; MARINS, M. The curcumin analog CH-5 exerts anticancer effects in human osteosarcoma cells via modulation of transcription factors p53/Sp1. **International Journal of Molecular Sciences**, v. 19, p. e1909, 2018.

LIU, G.; MCDONNELL, T. J.; LUNA, R. M. O.; KAPOOR, M.; MIMS, B.; EL-NAGGAR, A. K.; LOZANO, G. High metastatic potential in mice inheriting a targeted p53 missense mutation. **Proceedings of the National Academy of Sciences of the USA**, v. 97, p. 4174–4179, 2000.

LIU, T.; JIANG, W.; HAN, D.; YU, L. DNAJC25 is downregulated in hepatocellular carcinoma and is a novel tumor suppressor gene. **Oncology Letters**, v. 4, p. 1274–1280, 2012.

LIU, D. D.; KANG, Y. Ets2 anchors the prometastatic function of mutant p53 in osteosarcoma. **Genes & Development**, v. 31, p. 1823–1824, 2017.

LOPACHIN, R. M.; GAVIN, T. Molecular mechanisms of aldehyde toxicity: a chemical perspective. **Chemical Research in Toxicology**, v. 27, p. 1081−1091, 2014.

LU, S.; OBIANOM, O. N.; AI, Y. Novel cinnamaldehyde-based aspirin derivatives for the treatment of colorectal cancer. **Bioorganic & Medicinal Chemistry Letters**, v. 28, p. 2869–2874, 2018.

LUO, Y.; LIANG, F.; ZHANG, Z. Y. PRL1 promotes cell migration and invasion by increasing MMP2 and MMP9 expression through Src and ERK1/2 pathways. **Biochemistry**, v. 48, p. 1838–1846, 2009.

MAHER, D. M.; BELL, M. C.; O'DONNELL, E. A.; GUPTA, B. K.; JAGGI, M.; CHAUHAN, S. C. Curcumin suppresses human papillomavirus oncoproteins, restores p53, Rb, and PTPN13 proteins and inhibits benzo[*a*]pyrene-induced upregulation of HPV E7. **Molecular Carcinogenesis**, v. 50, p. 47–57, 2011.

MARKOVIC, V.; DEBELJAK, N.; STANOJKOVIC, T.; KOLUNDZIJA, B.; SLADIC, D.; VUJCIC, M.; JANOVIC, B.; TANIC, N.; PEROVIC, M.; TESIC, V.; ANTIC, J.; JOKSOVIC, M. D. Anthraquinone–chalcone hybrids: synthesis, preliminary antiproliferative evaluation and DNA-interaction studies. **European Journal of Medicinal Chemistry**, v. 89, p. 401–410, 2015.

MARQUES, B, C.; SANTOS, M. B.; ANSELMO, D. B.; MONTEIRO, D. A.; GOMES, E.; SAIKI, M. F. C.; RAHAL, P.; ROSALEN, P. L.; SARDI, J. C. O.; REGASINI, L. O. Methoxychalcones: effect of methoxyl group toward antifungal, antibacterial and antiproliferative activities. **Medicinal chemistry (Shariqah (United Arab Emirates))**, v. 15, doi: 10.2174/1573406415666190724145158, 2019.

MENEZES, J. C. J. M. D. S; DIEDERICH, M. F. Natural dimers of coumarin, chalcones, and resveratrol and the link between structure and pharmacology. **European Journal of Medicinal Chemistry**, v. 182, p. 111637, 2019.

MINISTÉRIO DA SAÚDE. **HPV: sintomas, causas, prevenção e tratamento**. Disponível em: <http://portalms.saude.gov.br/saude-de-a-z/hpv>. Acesso em: 11 dez. 2019.

MIRZAEI, H.; EMAMI, S. Recent advances of cytotoxic chalconoids targeting tubulin polymerization: Synthesis and biological activity. **European Journal of Medicinal Chemistry**, v. 121, p. 610–639, 2016.

MITRA, A.; FILLMORE, R. A.; METGE, B. J.; RAJESH, M.; XI, Y.; KING, J.; JU, J.; PANNEL, L.; SHEVDE, L. A.; SAMANT, R. S. Large isoform of MRJ (DNAJB6) reduces malignant activity of breast cancer. **Breast Cancer Research**, v. 10, p. R22, 2008.

MITRA, A.; MENEZES, M. E.; SHEVDE, L. A.; SAMANT, R. S. DNAJB6 induces degradation of β-catenin and causes partial reversal of mesenchymal phenotype. **Journal of Biological Chemistry**, v. 285, p. 24686–24694, 2010.

NABEKURA, T. Overcoming multidrug resistance in human cancer cells by natural compounds. **Toxins**, v. 2, p. 1207–1224, 2010.

NAGASE, H.; VISSE, R.; MURPHY, G. Structure and function of matrix metalloproteinases and TIMPs. **Cardiovascular Research**, v. 69, p. 562–573, 2006.

NAKASE, M.; INUI, M.; OKUMURA, K.; KAMEI, T.; NAKAMURA, S.; TAGAWA, T. p53 gene therapy of human osteosarcoma using a transferrin-modified cationic liposome. **Molecular Cancer Therapeutics**, v. 4, p. 625–631, 2005.

NIAZI, S.; PUROHIT, M.; NIAZI, J. H. Role of p53 circuitry in tumorigenesis: A brief review. **European Journal of Medicinal Chemistry**, v. 158, p. 7–24, 2018.

NOH, S.; JUNG, J. J.; JUNG, M.; KIM, T. S.; PARK, C. H.; LIM, S. J.; JEUNG, H. C.; CHEOL, H.; CHUNG, H. C.; RHA, S. Y. Mmp-2 as a putative biomarker for carcinomatosis in gastric cancer. **Hepatogastroenterology**, v. 58, p. 2015–2019, 2011.

OPAS – Brasil. **Folha informativa – Câncer**. Disponível em: <https://www.paho.org/bra/index.php?option=com_content&view=article&id=5588:folha-informativa-cancer&Itemid=839>. Acesso em: 11 dez. 2019.

OYERVIDES-MUÑOZ, M. A.; PÉREZ-MAYA, A. A.; RODRÍGUEZ-GUTIÉRREZ, H. F.; GÓMEZ-MACIAS, G. S.; FAJARDO-RAMÍREZ, O. R.; TREVIÑO, V.; BARRERA-SALDAÑA, H. A.; GARZA-RODRÍGUEZ, M. L. Understanding the HPV integration and its progression to cervical cancer. **Infection, Genetics and Evolution**, v. 61, p. 134–144, 2018.

PAULRAJ, F.; ABAS, F.; LAJIS, N. H.; OTHMAN, I.; HASSAN, S. S.; NAIDU, R. The Curcumin analogue 1,5-*Bis*(2-hydroxyphenyl)-1,4-pentadiene-3-one induces apoptosis and downregulates E6 and E7 oncogene expression in HPV16 and HPV18-infected cervical cancer cells. **Molecules**, v. 20, p. 11830–11860, 2015.

PASTUSHENKO, I.; BLANPAIN, C. EMT transition states during tumor progression and metastasis. **Trends in Cell Biology**, v. 29, p. 212–226, 2018.

PITTAYAPRUEK, P.; MEEPHANSAN, J; PRAPAPAN, O.; KOMINE, M.; OHTSUKI, M. Role of matrix metalloproteinases in photoaging and photocarcinogenesis. **International Journal of Molecular Sciences**, v. 17, p. 868, 2016.

POLAQUINI, C. R.; TORREZAN, G. S.; SANTOS, V. R.; NAZARÉ, A. C.; CAMPOS, D. L.; ALMEIDA, L. A.; SILVA, I. C.; FERREIRA, H.; PAVAN, F. R.; DUQUE, C.; REGASINI, L. O. Antibacterial and antitubercular activities of cinnamylideneacetophenones. **Molecules**, v. 22, p. 1685, 2017.

PROVENZANO, E.; ULANER; G. A.; CHIN, S. Molecular classification of breast cancer. **PET Clinics**, v. 13, p. 325–338, 2018.

PUGAZHENDHI, A.; EDISON, T. N. J. I.; VELMURUGAN, B. K.; JACOB, J. A.; KARUPPUSAMY, I. Toxicity of doxorubicin (Dox) to different experimental organ systems. **Life Sciences**, v. 200, p. 26–30, 2018.

QI, M.; ZHANG, J.; ZENG, W.; CHEN, X. DNAJB1 stabilizes MDM2 and contributes to cancer cell proliferation in a p53-dependent manner. **Biochimica et Biophysica Acta (BBA)-Gene Regulatory Mechanisms**, v. 1839, p. 62–69, 2014.

RAD, S. K.; KANTHIMATHI, M. S.; MALEK, S. N. A.; LEE, G. S.; LOOI, C. Y.; WONG, W. F. *Cinnamomum cassia* suppresses caspase-9 through stimulation of AKT1 in MCF-7 cells but not in MDA-MB-231 cells. **PLoS One**, v. 10, p. e0145216, 2015.

REVALDE, J. L.; LI, Y.; HAWKINS, B. C.; ROSENGREN, R. J.; PAXTON, J. W. Heterocyclic cyclohexanone monocarbonyl analogs of curcumin can inhibit the activity of ATP-binding cassette transporters in cancer multidrug resistance. **Biochemical Pharmacology**, v. 93, p. 305–317, 2015.

SAFE, S.; HAN, H.; GOLDSBY, J.; MOHANKUMAR, K.; CHAPKIN, R. S. Aryl hydrocarbon receptor (AhR) ligands as selective AhR modulators: genomic studies. **Current Opinion in Toxicology**, v. 11, p. 10–20, 2018.

SALEHI, B.; STOJANOVIC-RADIC, Z.; MATEJIC, J.; SHARIFI-RAD, M.; KUMAR, N. V. A.; MARTINS, N.; SHARIFI-RAD, J. The therapeutic potential of curcumin: A review of clinical trials. **European Journal of Medicinal Chemistry**, v. 163, p. 527–545, 2019.

SANNINO, G.; MARCHETTO, A.; KIRCHNER, T.; GRÜNEWALD, T. G. P. Epithelial-to-mesenchymal and mesenchymal-to-epithelial transition in mesenchymal tumors: a paradox in sarcomas? **Cancer Research**, v. 77, p. 4556–4561, 2017.

SANTOS, M. B.; ANSELMO, D. B.; OLIVEIRA, J. G.; JARDIM-PERASSI, B. V.; MONTEIRO, D. A.; SILVA, G.; GOMES, E.; FACHIN, A. L.; MARINS, M.; ZUCCARI, D. A. P. C.; REGASINI, L. O. Antiproliferative activity and p53 upregulation effects of

chalcones on human breast cancer cells. **Journal of Enzyme Inhibition and Medicinal Chemistry**, v. 34, p. 1093–1099, 2019.

SEBA, V.; SILVA, G.; SANTOS, M. B.; BAEK, S. J.; FRANÇA, S. C.; FACHIN, A. L.; REGASINI, L. O.; MARINS, M. Chalcone derivatives 4'-amino-1'-naphthyl-chalcone (D14) and 4'-amino-4'-methyl-1-naphthyl-chalcone (D15) suppress migration and invasion of osteosarcoma cells mediated by p53 regulating EMT-related genes. **International Journal Molecular Science**, v. 19, p. 2838, 2018.

SEYFRIED, T. N.; HUYSENTRUYT, L. C. On the origin of cancer metastasis. **Critical Reviews in Oncogenesis**, v. 18, 43–73, 2013.

SHISHODIA, S. Molecular mechanismsn of curcumin action: Gene expression. **BioFactors**, v. 39, p. 37–55, 2013.

SILVA, G.; MARINS, M.; FACHIN, A. L.; LEE, S.; BAEK, S. J. Anti-cancer activity of *trans*-chalcone in osteosarcoma: involvement of sp1 and p53. **Molecular Carcinogenesis**, v. 55, p. 1438–1448, 2016.

SILVA, G; LIMA, F. T.; SEBA, V.; LOURENÇO, A. L. M.; LUCAS, T. G.; ANDRADE, B. V.; TORREZAN, G. S.; POLAQUINI, C. R.; GARCIA, M. E.; COUTO, L. B.; BESTETTI, R. B.; FRANÇA, S. C.; FACHIN, A. L.; REGASINI, L. O.; MARINS, M. Curcumin analog CH-5 suppresses the proliferation, migration, and invasion of the human gastric cancer cell line HGC-27. **Molecules**, v. 23, p. e279, 2018a.

SILVA, G.; MARINS, M.; CHAICHANASAK, N.; YOON, Y.; FACHIN, A. L.; PINHANELLI, V. C.; REGASINI, L. O.; SANTOS, M. B.; AYUSSO, G. M.; MARQUES, B. C.; WU, W. W.; PHUE, J.; SHEN, R.; BAEK, S. J. *Trans*-chalcone increases p53 activity via DNAJB1/HSP40 induction and CRM1 inhibition. **PLoS ONE**, v. 13, p. e0202263, 2018b.

SILVA, M. F.; COELHO, L. F.; GUIRELLI, I. M.; PEREIRA, R. M.; FERREIRA-SILVA, G. A.; GRARAVELLI, G. Y.; HORVATH, R. O.; CAIXETA, E. S.; IONTA, M.; VIEGAS,

C. Synthetic resveratrol-curcumin hybrid derivative inhibits mitosis progression in estrogen positive MCF-7 breast cancer cells. **Toxicology in Vitro**, v. 50, p. 75–85, 2018c.

SINGH, R.; KOPPIKAR, S. J.; PAUL, P.; GILDA, S.; PARADKAR, A. R.; KAUL-GHANEKAR, R. Comparative analysis of cytotoxic effect of aqueous cinnamon extract from *Cinnamomum zeylanicum* bark with commercial cinnamaldehyde on various cell lines. **Pharmaceutical Biology**, v. 47, p. 1174–1179, 2009.

SINGH, P.; ANAND, A.; KUMAR, V. Recent developments in biological activities of chalcones: A mini review. **European Journal of Medicinal Chemistry**, v. 85, p. 758–777, 2014.

SONG, R.; TIAN, K.; WANG, W.; WANG, L. p53 suppresses cell proliferation, metastasis, and angiogenesis of osteosarcoma through inhibition of the PI3K/AKT/mTOR pathway. **International Journal of Surgery**, v. 20, p. 80–87, 2015.

SRIVASTAVA, N. S.; SRIVASTAVA, R. A. K. Curcumin and quercetin synergistically inhibit cancer cell proliferation in multiple cancer cells and modulate Wnt/β-catenin signaling and apoptotic pathways in A375 cells. **Phytomedicine**, v. 52, p. 117–128, 2019.

SYAM, S.; ABDELWAHAB, S. I.; AL-MAMARY, M. A.; MOHAN, S. Synthesis of chalcones with anticancer activities. **Molecules**, v. 17, p. 6179-6195, 2012.

TEWARI, D.; RAWAT, P.; SINGH, P. K. Adverse drug reactions of anticancer drugs derived from natural sources. **Food and Chemical Toxicology**, v. 123, p. 522–535, 2019.

TEYMOURI, M.; PIRRO, M.; JOHNSTON, T. P.; SAHEBKAR, A. Curcumin as a multifaceted compound against human papilloma virus infection and cervical cancers: A review of chemistry, cellular, molecular, and preclinical features. **BioFactors**, v. 43, p. 331–346, 2017.

TRINH, D. L. N; ELWI, A. N.; KIM, S. Direct interaction between p53 and Tid1 proteins affects p53 mitochondrial localization and apoptosis. **Oncotarget**, v. 1, p. 396-404, 2010.

TSAI, M. F.; WANG, C. C.; CHANG, G. C.; CHEN, C. Y.; CHEN, H. Y.; CHENG, C. L.; YANG, Y. P.; WU, C. Y.; SHIH, F. Y.; LIU, C. C.; LIN, H. P.; JOU, Y. S.; LIN, S. C.; LIN, C. W.; CHEN, W. J.; CHAN, W. K.; CHEN, J. J. W.; YANG, P. C. A new tumor suppressor DnaJ-like heat shock protein, HLJ1, and survival of patients with non–small-cell lung carcinoma. **Journal of the National Cancer Institute**, v. 98, p. 825–838, 2006.

WANG, L. L. Biology of osteogenic sarcoma. **The Cancer Journal**, v. 11, p. 294–305, 2005.

WANG, D. B.; KINOSHITA, C.; KINOSHITA, Y.; MORRISON, R. S. p53 and mitochondrial function in neurons. **Biochimica et Biophysica Acta**, v. 1842, p. 1186–1197, 2014.

WANG, R.; ZHANG, X.; CHEN, C.; CHEN, G.; ZHONG, Q.; ZHANG, Q.; ZHENG, S.; WANG, G.; CHEN, Q. Synthesis and evaluation of 1,7-diheteroarylhepta-1,4,6-trien-3-ones as curcumin-based anticancer agents. **European Journal of Medicinal Chemistry,** v. 110, p. 164–180, 2016.

WANG, J.; YUN, D.; YAO, J.; FU, W; HUANG, F.; CHEN, L.; WEI, T.; YU, C.; XU, H.; ZHOU, X.; HUANG, Y.; WU, J.; QIU, P.; LI, W. Design, synthesis and QSAR study of novel isatin analogues inspired Michael acceptor as potential anticancer compounds. **European Journal of Medicinal Chemistry**, v. 144, p. 493–503, 2018.

WEINBERG, D.; GOMEZ-MARTINEZ, R. A. Vulvar cancer. **Obstetrics and Gynecology Clinics of North America**, v. 46, p. 125–135, 2019.

WHO – World Health Organization. **Human papillomavirus (HPV) and cervical cancer**. Disponível em: <https://www.who.int/en/news-room/fact-sheets/detail/human-papillomavirus-(hpv)-and-cervical-cancer>. Acesso em: 11 dez. 2019.

WU, J.; LU, W.; CUI, L. Inhibitory effect of curcumin on invasion of skin squamous cell carcinoma A431 cells. **Asian Pacific Journal of Cancer Prevention**, v. 16, p. 2813–2818, 2015.

WU, C.; ZHUANG, Y.; JIANG, S.; TIAN, F.; TENG, Y.; CHEN, X.; ZHENG, P.; LIU, S.; ZHOU, J.; WU, J.; WANG, R.; ZOU, X. Cinnamaldehyde induces apoptosis and reverses epithelial-mesenchymal transition through inhibition of Wnt/β-catenin pathway in non-small cell lung cancer. **The International Journal of Biochemistry & Cell Biology**, v. 84, p. 58–74, 2017a.

WU, J.; LIU, T.; RIOS, Z.; MEI, Q.; LIN, X.; CAO, S. Heat shock proteins and cancer. **Trends in Pharmacological Sciences**, v. 38, p. 226–256; 2017b.

YALLAPU, M. M.; GUPTA, B. K.; JAGGI, M.; CHAUHAN, S. C. Fabrication of curcumin encapsulated PLGA nanoparticles for improved therapeutic effects in metastatic cancer cells. **Journal of Colloid and Interface Science**, v. 351, p. 19–29, 2010.

YALLAPU, M. M.; JAGGI, M.; CHAUHAN, S. C. Scope of nanotechnology in ovarian cancer therapeutics. **Journal of Ovarian Research**, v. 3, p. 19, 2010.

YAMADA, K.; YOSHIDA, K. Mechanical insights into the regulation of programmed cell death by p53 via mitochondria. **Biochimica et Biophysica Acta (BBA) - Molecular Cell Research**, v. 1866, p. 839–848, 2019.

YU, C.; CHU, S.; YANG, S.; HSIEH, Y.; LEE, C.; CHEN, P. Induction of apoptotic but not autophagic cell death by *Cinnamomum cassia* extracts on human oral cancer cells. **Journal of Cellular Physiology**, v. 234, p. 5289–5303, 2019.

ZAHREDDINE, H.; BORDEN, K. Mechanisms and insights into drug resistance in cancer. **Frontiers in Pharmacology**, v. 4, p.28, 2013.

ZAWACKA-PANKAU, J.; SELIVANOVA, G. Pharmacological reactivation of p53 as a strategy to treat cancer. **Journal of Internal Medicine**, v. 277, p. 248–259, 2015.

ZHANG, M.; ZHANG, X. Association of MMP-2 expression and prognosis in osteosarcoma patients. **International Journal of Clinical and Experimental Pathology**, v. 8, p. 14965–14970, 2015.

Capítulo II

5. ARTIGO CIENTÍFICO

Curcumin-Cinnamaldehyde Hybrids as Antiproliferative Agents against Women Cancer Cells

Daiane B. Anselmo[1·] Carlos R. Polaquini[1·] Beatriz C. Marques[1 ·] Gabriela M. Ayusso[1·] Letícia R. Assis[1·] Guilherme S. Torrezan[1 ·] Paula Rahal[2·] Marília F. Calmon[2·] Mozart A. Marins[3·] Luis O. Regasini[1]

✉ Luis O. Regasini

luis.regasini@unesp.br

[1]Laboratory of Antibiotics and Chemotherapeutics, Department of Chemistry and Environmental Sciences, Institute of Biosciences, Humanities and Exact Sciences, São Paulo State University (Unesp), São José do Rio Preto, SP, 15054-000, Brazil

[2]Laboratory of Genomic Studies, Department of Biology, Institute of Biosciences, Humanities and Exact Sciences, São Paulo State University (Unesp), São José do Rio Preto, SP, 15054-000, Brazil

[3]Laboratory of Molecular Genetics and Bioinformatics, Biotechnology Unit, University of Ribeirão Preto (Unaerp), Ribeirão Preto, SP, 14096-900, Brazil

Abstract

Curcumin and cinnamaldehyde are natural products with *in vitro* and *in vivo* antineoplastic activity. In this study, two series of curcumin-cinnamaldehyde hybrids were evaluated by MTT assay to determine their antiproliferative activity against women cancer cell lines, including breast cancer (MCF-7 and MDA-MB-231), cervical cancer (C33, HeLa, SiHa and CaSki) and vulvar cancer (A431). Hybrid **5a** demonstrated potent antiproliferative activity

against all women cancer cell lines, with IC_{50} values of 2.7–36.5 μM. Hybrid **5a** was more active than curcumin and cinnamaldehyde against CaSki, SiHa, C33 and A431 cell lines, displaying higher selectivity index (SI = 8.5) than curcumin (SI = 0.8) toward non-tumorigenic HaCaT cell line. Clonogenic experiments indicated hybrid **5a** inhibited A431 colonies formation in concentration-dependent manner. In addition, **5a** was more stable than curcumin and cinnamaldehyde (parent compounds) in phosphate buffer (pH 7.4) for 24 h at 37 °C. *In silico* investigations suggested **5a** has good drug-likeness properties, according to Lipinski's, Veber's, Muegge's and Ghose's rules. These results corroborate the use of molecular hybridization based on natural products to discovery new drug-like hits.

Keywords curcumin · cinnamaldehyde · antiproliferative · hybridization · cancer

5.1. INTRODUCTION

Cancer is one of pivotal causes of death around the world (Tewari et al., 2019). Its incidence has increased about 18.1 million new cases and 9.6 million deaths in 2018 (Iarc, 2019), and the women are more susceptible to mortality than men (Tewari et al., 2019). Breast cancer is the main women cancer (Bray et al., 2018), and the triple negative type is the most severe, because there is not targeted pharmacotherapy (Ren et al., 2019). Cervical cancer is the fourth place in women cancer incidence (Bray et al., 2018). Its main causative agent is Human Papilloma Virus (HPV), mainly HPV-16 and HPV-18. These two types are classified as high risk, and responsible for 70% of cervical cancers (Bolatti et al., 2016), as well as also may be associated with correlated with vulva cancer (Weinberg and Gomez-Martinez, 2019). Vulva cancer was responsible for 44.235 cases and 15.222 deaths worldwide in the year 2018 (Globocan–Iarc, 2020).

Curcumin (from *Curcuma longa*) and cinnamaldehyde (from *Cinnamomum* species) have been used as food additive and are considered as safe by FDA (Gupta et al., 2012; Fabra et al., 2016). Curcumin and cinnamaldehyde have potent activity against breast cancer (Wani et al., 2014; Srivastava and Srivastava, 2019) and cervical cancers (Singh et al., 2009; Paulraj et al., 2015). The mode of action of curcumin includes induction of apoptosis, regulation of tumor suppressor genes such as p53 and Rb, as well as decreased of HPV E6 and E7

oncogenes expression (Maher et al., 2011). Cinnamaldehyde has antiproliferative effect and decreases the number of breast cancer cell colonies (Nagle et al., 2012). Although curcumin and cinnamaldehyde have shown to be promising antitumor agents, their poor chemical stabilities have not allowed advances of their clinical studies (Hong et al., 2016; Nelson et al., 2017). In our previous work, we demonstrated that curcumin analogs with the β-diketone moiety (chelatogenic group) replaced by monoketone showed potent antiproliferative activity (Lima et al., 2018; Oliveira et al., 2018; Silva et al., 2018). In addition, we also reported that the replacement of cinnamaldehyde aldoxyl (reactive functionality) by acetophenone moiety resulted in more stable antibacterial and antitubercular analogs (Polaquini et al., 2017).

In this study, we selected curcumin and cinnamaldehyde as parent compounds for molecular hybridization. Two series of curcumin-cinnamaldehyde hybrids (CCHs) were designed by removal of the undesirable functionalities of parent compounds, including β-diketone and aldoxyl of curcumin and cinnamaldehyde, respectively. We focused the in exploration of number of double bonds between aromatic rings A and B, as well as in role of hydroxyl and methoxyl substituents on ring A. Series I and II of CCHs were constituted by α,β-unsaturated ketones and α,β,γ,δ-unsaturated ketones, respectively (Scheme 1).

Scheme 1 Design of curcumin-cinnamaldehyde hybrids (CCHs) of series I and II

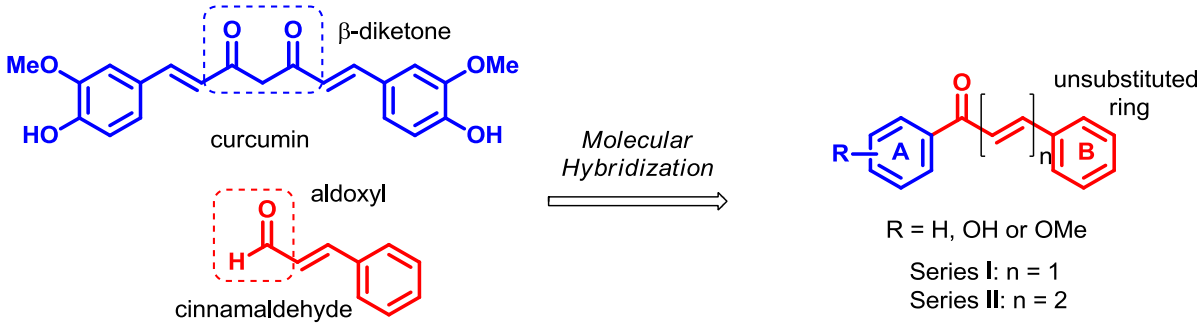

Source: author

Antiproliferative activity of CCHs was evaluated against a panel women cancer cells, including cervical, breast and vulvar cancers. The most active hybrid (**5a**) was investigated regarding its toxicity and selectivity toward non-tumorigenic keratinocytes. We also investigated inhibition of **5a** on vulvar cell colonies formation. The chemical stability of hybrid **5a** was evaluated. *In silico* investigations using Molinspiration® explorer toolkit contributed to prediction of drug-likeness properties of **5a**.

5.2. MATERIAL AND METHODS

5.2.1 Synthesis of Curcumin-Cinnmaldehyde Hybrids (CCHs) **1a – 6a** and **1b – 6b**

Curcumin, cinnamaldehyde and all starting reagents were purchased from Merck®. Synthesis of CCHs was achieved by Claisen-Schmidt aldol condensation reactions under basic catalysis and ethanol as protic solvent. Hybrids of series I (**1a**−**6a**) were synthesized by reaction between benzaldehyde and respective acetophenone as previously described by Marques and co-authors with minor modifications (Marques et al., 2019). Hybrids of series II (**1b**−**6b**) were synthesized by reaction between cinnamaldehyde and corresponding acetophenone as previously reported by Polaquini and co-authors with minor modifications (Polaquini et al., 2017).

5.2.2 Cells and their Culture

Panel of human cell lines was constituted by: breast cancer cell lines MCF-7 (ATCC® HTB-22 ™) and MDA-MB-231 (ATCC® HTB-26 ™); cervical cancer cell lines: C33 – HPV-negative (ATCC® HTB-31 ™), HeLa - positive for HPV-18 (ATCC® CCL-2 ™), CaSki – positive for HPV-16 (ATCC® CRM-CRL-1550 ™) and SiHa – positive for HPV-16 (ATCC® HTB-35 ™); and vulvar cancer cell line A431 (SIGMA-85090402); immortalized non-tumor human keratinocyte cells (HaCaT - CLS 300493). Cell lines were maintained in DMEM (Dulbecco's Modified Eagle Medium, Gibco Life Technologies) supplemented with 10% (v/v) heat inactivated FBS (fetal bovine serum) (Cultilab), 100 U/mL penicillin, and 100 μg/mL streptomycin (Invitrogen) in plastic flasks (Corning) at 37 °C under humidified 5% CO_2 atmosphere.

5.2.3 MTT assay

Cell viability assay was performed using protocol described by Nazaré and co-authors, with minor modifications (Nazaré et al., 2018). An aliquot of 1×10^4 cells/well was seeded into

96-well cell culture plate with total volume of 100 µL for 24 h. Cells were treated with compounds (hybrids and parent compounds) in concentrations ranging from 200 to 1.56 µM. After 48 h, medium was removed and 100 µL of MTT [3-(4,5-dimethylthiazol-2-yl)-2,5-diphenyltetrazolium bromide] (1mg/mL) was added and plates were incubated at 37 °C for 30 min. MTT was removed and 100 µL of DMSO was added, and the mixture was maintained under agitation for 5 min at 60 rpm. Absorbance was measured at 570 nm on FLUOstar Omega microplate reader (BMG LABTECH). DMSO 0.1% was used as solvent for substances and vehicle control. Curcumin was used as a comparative agent because it has greater antiproliferative activity than cinnamaldehyde. In addition, other studies also use curcumin for comparison with new substances (Li et al., 2015; Hsieh et al., 2017; Marques et al., 2019). Results were plotted as the percentage of cell viability inhibition (CVI) calculated as follows: CVI (%) = [1 - (absorbance of cells treated with compounds/absorbance of cells trated with DMSO 0.1%)] × 100. We carried out the experiments in triplicate and three independent events for statistical analysis.

5.2.4 Clonogenic Formation Assay

Clonogenic assay, using A431 and HaCaT cell lines, was performed according to Franken and co-authors (Franken et al., 2006), with minor modifications (Pereira et al., 2016). Briefly, 5×10^3 cells/well were seeded in 12-well plates and incubated at 37 °C under humidified 5% CO_2 atmosphere for 24 h. After incubation, cells were treated with hybrid **5a** at its respective ¼ IC_{50} and IC_{50} values obtained from MTT assays. After 48 h, cells were recovered in compound-free medium subsequently for 15 days, allowing cell growth and formation colonies. For qualitative observation, colonies were counted. Images of colonies were obtained using iPhone digital camera (Apple). For quantitative analyses, cell viability was measured by MTT assay. 0.1% DMSO was used as vehicle control. We carried out experiments in triplicate and three independent events for statistical analysis.

5.2.5 Statistical Analyses

Experiments were performed three times and quantitative data are expressed as mean ± SD. Statistical analyses were performed by one-way analysis of variance (ANOVA) followed by Tukey's Test using GraphPad Prism 7 (GraphPad Software, Inc.) and Microsoft Office Excel 2007 computer software. $p < 0.0001$ was statistically significant.

5.2.6 Chemical stability assay

Chemical stability of hybrid **5a** (at λ_{max} 314 nm), curcumin (at λ_{max} 426 nm) and cinnamaldehyde (at λ_{max} 288 nm) was analyzed by monitoring their UV–visible absorptions (Perkin Elmer® Lambda 25 UV/Visible Spectrophotometer) in phosphate buffer (pH 7.4) at 37 °C. Minor modifications in this protocol and their detailed procedures were reported in our previous work (Polaquini et al., 2019).

5.2.7 Drug-likeness Properties

In silico investigations about drug-likeness properties of hybrid **5a** were performed using free Molinspiration® toolkit to explore Lipinski's, Veber's, Muegge's and Ghose's rules (Molinspiration, 2019).

5.3. RESULTS AND DISCUSSION

Two series of CCHs investigated were synthesized by Claisen-Schmidt condensation reaction, with yields of 60–95% (Scheme 2). Structure of hybrids were confirmed by their NMR spectra analyses. Spectra were presented in Supplementary Material. For all CCHs, NMR data, including chemical shifts, integrations multiplicities and coupling constants, corresponded to the proposed structures (Polaquini et al., 2017; Marques et al., 2019).

Scheme 2. Synthesis of CCHs of series I and II

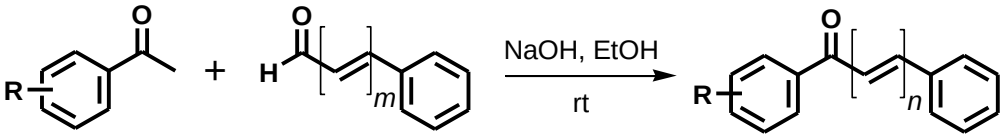

R = H, OMe or OH
m = 0 or 1
n = 1 (series I) or 2 (series II)

Source: author

Antiproliferative effect of curcumin, cinnamaldehyde and CCHs was evaluated against human cancer cells from breast (MCF-7 and MDA-MB-231 lines), cervix (C33 HPV-negative, HeLa positive for HPV-18, CaSki positive for HPV-16 and SiHa positive for HPV-16 lines), and vulva (A431 line). These cell lines were selected due to high frequency of these cancers in women (Bray et al., 2018). Antiproliferative potency was expressed as IC_{50} values (concentration able to inhibit 50% of cell viability), which were obtained from MTT assay. In addition, we calculated average of IC_{50} values (mIC_{50}) to analyze global effect of CCHs and its parent compounds against the panel of women cancer cells. For hybrids with IC_{50} values > 100 μM against at least one cancer cell line was attributed mIC_{50} value > 100 μM (Table 1).

Table 1. Antiproliferative activity of parent compounds and CCHs expressed as IC_{50} values (in µM)

Compounds		R	R^1	MCF-7 (breast)	MDA-MB-231 (breast)	HeLa (cervical)	CaSki (cervical)	SiHa (cervical)	C33 (cervical)	A431 (vulva)	mIC_{50}[a]
curcumin[b],[c]		–	–	14.9±2.9	31.0±4.3	29.7±3.3	16.6±2.9	54.1±0.6	29.0±2.4	10.4±0.5	26.5
cinnamaldehyde[b]		–	–	>100	>100	>100	>100	>100	>100	>100	>100
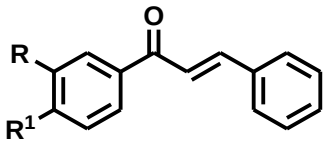 Series I	**1a**	OMe	OH	46.8±1.3	66.3±2.2	59.2±7.7	61.4±0.9	62.6±0.2	47.1±3.0	27.1±2.7	53.0
	2a	H	H	17.1±5.6	39.9±3.1	52.9±5.2	25.2±2.4	30.1±3.7	37.1±0.9	4.1±1.1	29.5
	3a	OMe	H	42.0±4.6	42.7±7.4	49.7±4.8	57.3±3.1	51.6±5.1	32.6±5.6	12.5±2.3	45.9
	4a	H	OH	30.1±6.3	50.1±7.0	51.8±5.1	27.4±2.5	44.0±5.1	20.0±2.3	7.7±1.7	33.0
	5a	OH	H	22.3±2.9	35.2±3.5	36.5±3.7	15.5±1.5	11.9±1.5	11.3±1.4	2.7±0.2	19.3
	6a	H	OMe	41.5±6.6	48.8±0.7	67.1±6.0	34.7±6.3	41.0±2.7	34.5±5.3	33.8±5.3	43.1
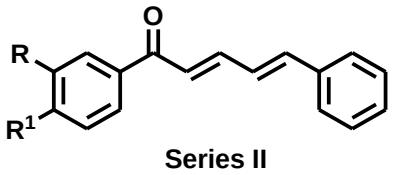 Series II	**1b**	OMe	OH	65.5±6.0	60.3±9.8	59.1±2.4	66.9±4.9	65.0±4.9	41.1±1.8	12.3±2.0	52.9
	2b	H	H	62.3±1.1	94.5±6.6	>100	>100	97.7±0.3	33.6±3.7	29.1±2.8	>100
	3b	OMe	H	>100	>100	>100	91.5±6.8	39.1±3.2	>100	51.0±0.9	>100
	4b	H	OH	41.5±6.6	35.1±3.7	58.6±7.1	50.8±6.0	81.6±0.7	38.2±2.1	41.8±1.2	49.7
	5b	OH	H	38.8±6.2	51.0±0.7	64.2±0.8	37.8±3.2	31.6±3.8	30.0±2.2	12.0±4.6	37.9
	6b	H	OMe	>100	>100	>100	>100	>100	82.7±1.5	35.4±3.4	>100

[a] Average of sum of all IC_{50} values [b] Parent compounds. [c] Comparative agent (Li et al., 2015; Hsieh et al., 2017; Marques et al., 2019).

Source: author

Assays of antiproliferative activity of curcumin were performed for two reasons. Curcumin has been used as positive control or comparative agent in MTT assays (Li et al., 2015; Hsieh et al., 2017; Marques et al., 2019) due to cell viability reduction through apoptosis pathway (Maher et al., 2011), as well as it was selected as parent compound for molecular hybridization design. Curcumin displayed activity against all cell lines, with IC_{50} values of 10.4–54.1 μM (mIC_{50} = 26.5 μM). Against MCF-7 (breast line), curcumin exhibited IC_{50} value of 14.9 μM after 48 h. This result was similar to Srivastava and Srivastava work (Srivastava and Srivastava 2019), which described an IC_{50} value of 18 μM for curcumin against MCF-7 after 72 h. Wang and collaborators reported an IC_{50} value of 12.1 μM against HeLa after 72 h of curcumin treatment (Wang et al., 2016). Paulraj and co-authors described IC_{50} values of 26.7 μM and 15.8 μM against HeLa and CaSki, respectively, after 72 h (Paulraj et al., 2015). Wu and collaborators showed curcumin (at 15 μM) inhibited 54% of A431 cell viability, after 48 h (Wu et al., 2015).

On the other hand, cinnamaldehyde, another parent compound of hybridization design, presented IC_{50} > 100 μM against all cell lines. These results were similar to the studies of Wani and collaborators, which reported IC_{50} values around of 160 μM and 80 μM against MCF-7 and MDA-MB-231 cells, respectively, after 24 h (Wani et al., 2014). Singh and co-authors described that after a treatment with cinnamaldehyde at a concentration of 80 μM for 24 h, there was a 53% reduction in A431 cells. This same treatment was performed against SiHa cells, in which cinnamaldehyde reduced 65% of the cells (Singh et al., 2009).

In order to investigate initial efficacy of molecular hybridization design, hybrids **1a** and **1b** were evaluated. Both the hybrids have guaiacol ring (*meta*-OMe and *para*-OH on benzene ring), which is also found in curcumin structure. Guaiacol (ring A) is spaced to unsubstituted ring B in **1a** and **1b** by α,β-unsaturated and α,β,γ,δ-unsaturated ketones, respectively. Hybrids **1a** and **1b** displayed activity against all cell lines, with IC_{50} values of 12.3–66.9 μM and 27.1–66.3 μM, respectively. Hybrids **1a** and **1b** demonstrated mIC_{50} values of 53.0 and 52.9 μM, respectively. These values we encouraged to study analogs of guaiacolic hybrids **1a** and **1b**, aiming the evaluation of role of substituents (hydroxyl and methoxyl) on ring A, using hybrids **2a**–**6a** and **2b**–**6b**.

We compared activity of **1a** and **1b** with their unsubstituted analogs **2a** and **2b**, respectively. Hybrid **2b** (mIC_{50} > 100 μM) showed to be less active than **1b** (mIC_{50} = 52.9 μM). Among cancer cell lines, HeLa and CaSki were not sensitive to **2b** (IC_{50} > 100 μM). On the other hand, hybrid **1a** (mIC_{50} = 53.0 μM) was less active than **2a** (mIC_{50} = 29.5 μM).

Altogether, these results suggested that the *meta*-OMe and *para*-OH substituents are relevant for antiproliferative activity.

In order to investigate effects of *meta*-OMe and *para*-OH substituents, separately, we evaluated pairs of compounds **3a**/**3b** and **4a**/**4b**, respectively. In general, hydroxy-hybrids **4a**/**4b** were more potent than methoxy-hybrids **3a**/**3b**, demonstrating mIC_{50} values of 33.0 µM/49.7 µM and 45.9 µM/100 µM, respectively. These results suggest hydroxyl at *para* is more relevant for antiproliferative activity than methoxyl at *meta*.

We evaluated the regioisomers of pairs **3a**/**3b** and **4a**/**4b**, which were designed by replacement of OMe and OH positions, furnishing hybrids **6a**/**6b** and **5a**/**5b**, respectively. Hydroxy-hybrids **5a**/**5b** (mIC_{50} = 19.3 µM and 37.9 µM) displayed more potent antiproliferative activity than methoxy-hybrids **6a**/**6b** (mIC_{50} = 43.1 µM and > 100 µM), corroborating importance of hydroxyl substituent for bioactivity. Hybrid **5a** presented the lowest IC_{50} value among CCHs (IC_{50} = 2.7 µM against vulva cancer cells), as well as mIC_{50} value of 19.3 µM, both are lower than those described for curcumin (IC_{50} = 10.4 µM and mIC_{50} = 26.5 µM).

Finally, hybrids of series I (mIC_{50} values = 19.3–53.0 µM) displayed higher antiproliferative activity than hybrids of series II (mIC_{50} values = 37.9–>100 µM). These mIC_{50} values indicated one double carbon-carbon bond as spacer is more relevant for antiproliferative activity than two double carbon-carbon bonds. In this context, hybrids of series I exhibited electrophilic carbon β, which can act as Michael acceptor in reactions with bionucleophiles from cancer cells. This moiety has been recognized as pharmacophoric moiety of antineoplastic drugs, including afatinib, osimertinib and rociletinib (Jackson et al., 2017).

Altogether, bioactivity of CCHs corroborated the use of curcumin as cinnamaldehyde as parent compounds to molecular hybridization, design which has been widely used to discovery antineoplastic agents. Wang and co-authors used isatin and curcumin as parent compounds to design series of hybrids with antineoplastic activities. Activity of isatin-curcumin hybrids was attributed to α,β-unsaturated ketone side chain as Michael acceptor (Wang et al., 2018). In this way, our results corroborated the potential of natural products containing Michel acceptor moieties, including: zerumbone (Shin et al., 2011), xanthohumol (Liu et al., 2017), withaferin A (Liu et al., 2016) and celastrol (Raja et al., 2011), to discover of novel antineoplastic agents.

Hybrid **5a** was the most potent CCH and selected for subsequent assays. In order to determine effect of **5a** toward non-tumorigenic cells, we selected human spontaneously transformed keratinocyte from histologically normal skin (HaCaT line). Hybrid **5a** exhibited IC_{50} = 23.0 µM against HaCaT cells, which is three times less toxic than curcumin (IC_{50} = 7.6 µM) (Table 2). To compare effect of hybrid **5a** and its parent compounds toward tumorigenic and non-tumorigenic cells, we determined their selectivity index (SI). This value was calculated by ratio between IC_{50} (HaCaT line) and IC_{50} (A431 line). Curcumin and hybrid **5a** presented SI values of 0.7 and 8.5, respectively, suggesting hybrid **5a** was nine times more selective than curcumin (Table 2). Cinnamaldehyde presented values of IC_{50} > 100 µM against A431 and HaCaT cells, and it was not possible the SI value calculation. Mai and collaborators have reported compounds exhibiting IC_{50} values ≤ 10 µM against tumorigenic cells and SI values ≥ 5 are selective and promising hits for *in vivo* trials (Mai et al., 2014). Hybrid **5a** presented IC_{50} and SI values according to the Mai and collaborators' boundaries (Mai et al., 2014), displaying to be promising antineoplastic hit.

Table 2. IC_{50} values (in µM) of parent compounds and hybrid **5a** against A431 and HaCaT cell lines and respective selectivity index (SI)[a]

Compounds	HaCaT	A431	SI
curcumin[b]	7.6±2.1	10.4±0.5	0.7
cinnamaldehyde[b]	>100	>100	nc
hybrid **5a**	23.0±3.9	2.7±0.2	8.5

[a] SI: ratio between IC_{50} for HaCaT and IC_{50} for A431. [b] Parent compounds. nc = not calculated

Source: author

Inhibitory effect of hybrid **5a** on A431 against HaCaT colony formation was performed by clonogenic assay. This experiment evaluated the antiproliferative activity of compounds for long period of time (Franken et al., 2006). A431 and HaCaT cells were treated with hybrid **5a** at concentrations corresponding to its IC_{50} (2.7 and 23 µM) and ¼ IC_{50} (0.7 and 6.2 µM) values respectively (Fig.1). A431 colony formation was significantly reduced by hybrid **5a** in concentration-dependent manner compared to vehicle control (0.1% DMSO). Number of A431colonies decreased 60% in samples treated with **5a** (at ¼ IC_{50}) and colony formation did not observe in samples treated at IC_{50} value. Number of HaCaT colonies were

reduced 44% by **5a** (at ¼ IC_{50}), when compared to vehicle control. Comparison of inhibitory effect against A431 and HaCaT colony formation suggested **5a** (at ¼ IC_{50}) was able to induce higher antiproliferative activity after 15 days against tumorigenic than non-tumorigenic cells, corroborating its selectivity.

Figure 1. Qualitative and quantitative data of inhibitory effect of hybrid **5a** against cell colony formation of A431 and HaCaT lines, after 15 days. Cells were treated with hybrid **5a** at concentrations corresponding to its IC_{50} (2.7 and 23 µM) and ¼ IC_{50} (0.7 and 6.2 µM) values, respectively. Significant differences were determined using ANOVA followed by Tukey test for results ****p<0.0001 vs. vehicle control.

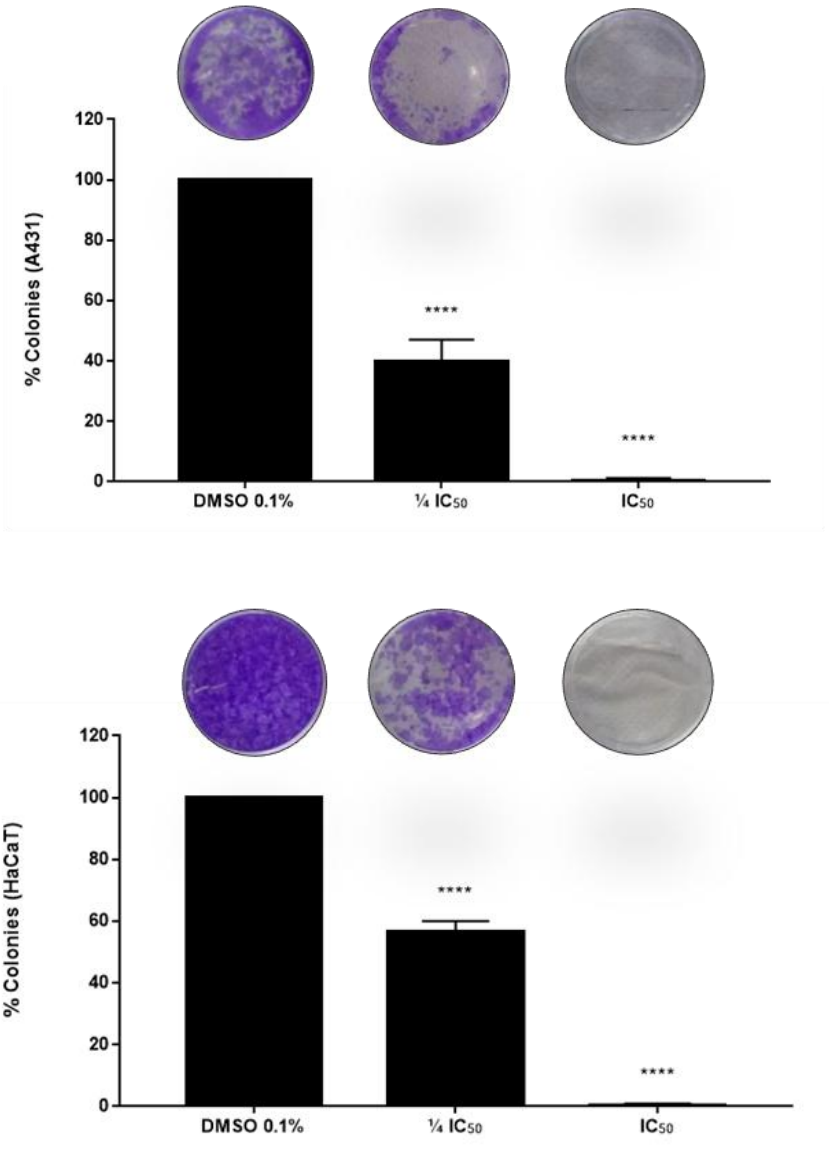

Source: author

The chemical stability of hybrid **5a** was evaluated at pH 7.4 by monitoring its UV–Vis absorption decreasing at 37 °C and compared with curcumin and cinnamaldehyde demonstrated poor stability under physiological conditions (Hong et al., 2016; Nelson et al., 2017). Curcumin and cinnamaldehyde were rapidly degraded, reducing at 60 and 40%, respectively, after 24 h (Fig. 2). On the other hand, hybrid **5a** was more stable than its parent compounds, reducing 21%.

Figure 2. Chemical stability of hybrid **5a** and parent compounds (pH 7.4) by monitoring the decrease in their maximum absorbance at 37 ºC for 24 h. Data are represented as means ± SEMs and expressed as percentage (%).

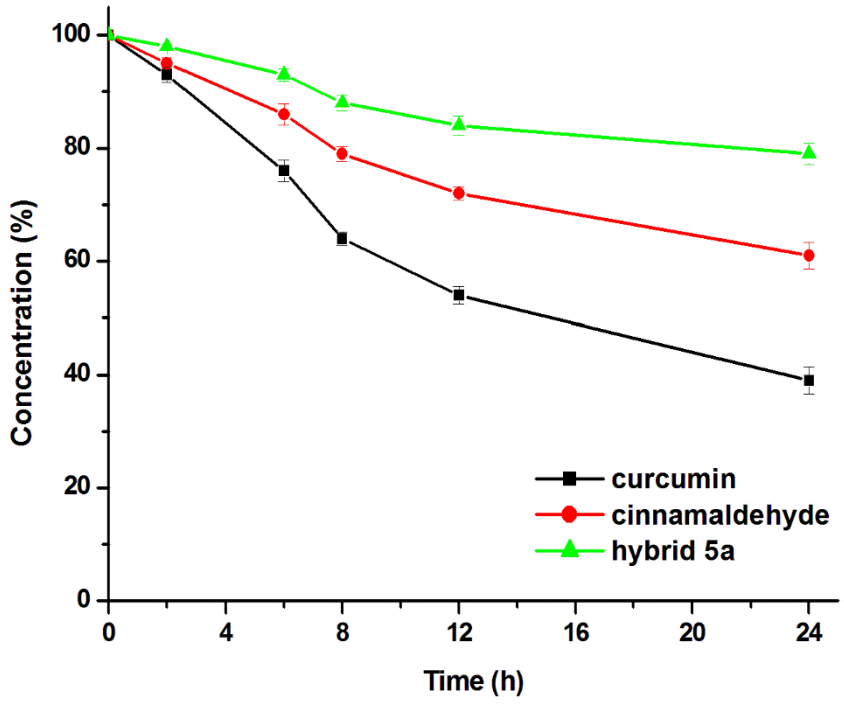

Source: author

Drug-likeness properties may be defined as set of structural and physico-chemical features, which indicate if a hit compound is similar to drugs (Polkam et al., 2016), corroborating its further chemical and biological studies. Several drug-likeness sets to filter hit compounds have been described such as Lipinski's (Lipinski et al., 1997),Veber's (Veber

et al., 2002), Muegge's (Muegge et al., 2001; Muegge 2003) and Ghose's rules (Ghose et al., 1999). Among these, "Rule-of-Five" established by Lipinski and collaborators is one of the best known and widely used filters (Lipinski et al., 1997). Lipinski's rules include values of logarithm of compound partition coefficient between *n*-octanol and water (log $P_{o/w} \leq 5.0$), weight molecular (MW ≤ 500 Da), number of hydrogen bond acceptors (HBA ≤ 10), number of hydrogen bond donors (HBD ≤ 5).

Hybrid **5a** demonstrated log $P_{o/w}$ = 3.31, MW = 224.26 Da, HBD = 1 and HBA = 2. Veber and collaborators (Veber et al., 2002) reported two drug-likeness properties, such as sum of HBA and HBD (HBA + HBD ≤ 12) and number of rotatable bonds (NROBT ≤ 10). Hybrid **5a** presented HBA + HBD = 3 and NROBT = 3. Muegge and co-authors developed rapid and simple criteria to select pharmacophore points. The main central is related to number or functionalities and rings on drug structure, which can corroborate as pharmacophores (Muegge et al., 2001; Muegge 2003). Hybrid **5a** exhibited two functional groups, carbonyl (as part of enone bridge) and hydroxyl (as part of phenolic ring A), which may be pharmacophoric motifs. Moreover, hybrid **5a** displayed two rings phenol (ring A) and unsubstituted benzene ring (ring B) as result of molecular hybridization between curcumin and cinnamaldehyde. Ghose and collaborators (Ghose et al., 1999) analyzed Comprehensive Medicinal Chemistry (CMC) database and classify ranges of molecular properties of drugs, including antineoplastic drugs. Among these, drugs presented total number of atoms considered in the range of 20–70 (average value of 48). Hybrid **5a** possess number of atoms of 29. Thus, hybrid **5a** did not violate Lipinski's, Veber's, Muegge's and Ghose's boundaries, corroborating its drug-likeness properties.

5.4. CONCLUSIONS

In conclusion, we evaluated two series of CCHs as part of continuous search for antineoplastic compounds based on natural products and molecular hybridization. Hybrids of series I were more potent antiproliferative agents than series II, which can be related to electrophilic carbon β as Michael acceptor. Hybrid **5a** was found to be a hit with activity against breast, cervical and vulvar cancer cells and able to inhibit vulvar colony formation after 15 days. *In vitro* investigations with non-tumorigenic cells (HaCaT) indicated **5a** was nine times more toxic to cancer cells than normal cells, as well as stable at pH 7.4. In

addition, a brief *in silico* investigation corroborated drug-likeness properties of **5a**. These results corroborate curcumin and cinnamaldehyde as parent compounds for design of antiproliferative hybrids.

5.5. ACKNOWLEDGEMENTS

The authors gratefully acknowledge financial support from Coordination for Improvement of Higher Education Personnel (CAPES, Coordenação de Aperfeiçoamento de Pessoal de Nível Superior, Finance Code 001), Brazilian Council for Scientific and Technological Development (CNPq, Conselho Nacional de Desenvolvimento Científico e Tecnológico, Grants #471129/2013-5, 306251/2016-7 and 429322/2018-6); São Paulo Research Foundation (FAPESP, Fundação de Amparo à Pesquisa do Estado de São Paulo, Grants # 2014/18330-0 and 2018/15083-2). D. B. A. thanks CAPES (finance code 001) for her scholarships. All authors thank Center of Biomolecular Innovation (FAPESP Grant # 2009/53989-4), National Institute of Science and Technology – Biodiversity and Natural Products INCT-BioNat (Grants FAPESP # 2014/50926-0 and CNPq # 465637/2014-0) and National Institute of Science and Genomics Technology for Citrus Improvement INCT-Citrus (Grants FAPESP # 2014/50880-0 and CNPq # 465440/2014- 2).

5.6. REFERENCES

Bolatti EM, Chouhy D, Casal PE, Pérez GR, Stella EJ, Sanchez A, Gorosito M, Bussy RF, Giri AA (2016) Characterization of novel human papillomavirus types 157, 158 and 205 from healthy skin and recombination analysis in genus γ-Papillomavirus. Infect Genet Evol 42: 20–29.

Bray F, Ferlay J, Soerjomataram I, Siegel RL, Torre LA, Jemal A (2018) Global cancer statistics 2018: GLOBOCAN estimates of incidence and mortality worldwide for 36 cancers in 185 countries. CA Cancer J Clin 68: 394–424.

Fabra MJ, Castro-Mayorga JL, Randazzo W, Lagarón JM, López-Rubio A, Aznar R, Sánchez G (2016) Efficacy of cinnamaldehyde against enteric viruses and its activity after incorporation into biodegradable multilayer systems of interest in food packaging. Food Environ Virol 8: 125–132.

Franken NAP, Rodermond HM, Stap J, Haveman J, Bree CV (2006) Clonogenic assay of cells *in vitro*. Nat Protoc 1: 2315–2319.

Ghose AK, Viswanadhan VN, Wendoloski JJ (1999) A knowledge-based approach in designing combinatorial or medicinal chemistry libraries for drug discovery. 1. A qualitative and quantitative characterization of known drug databases. J Combin Chem 1: 55–68.

Globocan–Iarc. Mundo. https://gco.iarc.fr/today/data/factsheets/populations/900-world-fact-sheets.pdf Accessed 29 March 2020.

Gupta SC, Patchva S, Koh W, Aggarwal BB (2012) Discovery of curcumin, a component of golden spice, and its miraculous biological activities. Clin Exp Pharmacol Physiol 39: 283–299.

Hong S, Ismail IA, Kang S, Han DC, Kwon B. (2016) Cinnamaldehydes in cancer chemotherapy. Phytother Res 30: 754–767.

Hsieh M, Chang L, Hung H, Lin H, Shih M, Tsai C, Kuo S, Lee K (2017) New *bis*(hydroxymethyl) alkanoate curcuminoid derivatives exhibit activity against triple-negative breast cancer *in vitro* and *in vivo*. Eur J Med Chem 131: 141–151.

Iarc – International Agency for Research on Cancer (2019) Latest global cancer data: Cancer burden rises to 18.1 million new cases and 9.6 million cancer deaths in 2018. https://www.iarc.fr/wp-content/uploads/2018/09/pr263_E.pdf Accessed 25 November 2019.

Jackson PA, Widen JC, Harki DA, Brummond KM (2017) Covalent modifiers: A chemical perspective on the reactivity of α,β-unsaturated carbonyls with thiols via hetero-Michael addition reactions. J Med Chem 60: 839–885.

Li Q, Chen J, Luo S, Xu J, Huang Q, Liu T (2015) Synthesis and assessment of the antioxidant and antitumor properties of asymmetric curcumin analogues. Eur J Med Chem 93: 461–469.

Lima FT, Seba V, Silva G, Torrezan GS, Polaquini CR, Pinhanelli VC, Baek SJ, Fachin AL, Regasini LO, Marins M (2018) The curcumin analog CH-5 exerts anticancer effects in human osteosarcoma cells via modulation of transcription factors p53/Sp1. Int J Mol Sci 19: 1909.

Lipinski CA, Lombardo F, Dominy BW, Feeney PJ (1997) Experimental and computational approaches to estimate solubility and permeability in drug discovery and development settings. Adv Drug Deliv Rev 23: 3–25.

Liu W, Barnette AR, Andreansky S, Landgraf R (2016) ERBB2 Overexpression establishes ERBB3-dependent hypersensitivity of breast cancer cells to withaferin A. Mol Cancer Ther 15: 2750–2757.

Liu R, Heiss EH, Schachner D, Jiang B, Liu W, Breuss JM, Dirsch VM, Atanasov AG (2017) Xanthohumol blocks proliferation and migration of vascular smooth muscle cells *in vitro* and reduces neointima formation *in vivo*. J Nat Prod 80: 2146–2150.

Maher DM, Bell MC, O'Donnell EA, Gupta BK, Jaggi M, Chauhan SC (2011) Curcumin suppresses human papillomavirus oncoproteins, restores p53, Rb, and PTPN13 proteins and inhibits benzo[*a*]pyrene-induced upregulation of HPV E7. Mol Carcinog 50: 47–57.

Mai CW, Yaeghoobi M, Abd-Rahman N, Kang YB, Pichika MR (2014) Chalcones with electron-withdrawing and electron-donating substituents: anticancer activity against TRAIL resistant cancer cells, structure-activity relationship analysis and regulation of apoptotic proteins. Eur J Med Chem 77: 378–387.

Marques BC, Santos MB, Anselmo DB, Monteiro DA, Gomes E, Saiki MFC, Rahal P, Rosalen PL, Sardi JCO, Regasini LO (2019) Methoxychalcones: effect of methoxyl group toward antifungal, antibacterial and antiproliferative activities. Med Chem 15: 1.

Molinspiration (2019) Molinspiration cheminformatics. http://www.molinspiration.com Accessed 24 November 2019.

Muegge I, Heald SL, Brittelli D (2001) Simple selection criteria for drug-like chemical matter. J Med Chem 44: 1841–1846.

Muegge I (2003) Selection criteria for drug-like compounds. Med Res Rev 23: 302–321.

Nagle AA, Gan F, Jones G, So C, Wells G, Chew E (2012) Induction of tumor cell death through targeting tubulin and evoking dysregulation of cell cycle regulatory proteins by multifunctional cinnamaldehydes. PloS One 7: e50125.

Nazaré AC, Polaquini CR, Cavalca LB, Anselmo DB, Saiki MFC, Monteiro DA, Zielinska A, Rahal P, Gomes E, Scheffers D, Ferreira H, Regasini LO (2018). Design of antibacterial agents: alkyl dihydroxybenzoates against *Xanthomonascitri* subsp. *citri*. Int J Mol Sci 19: 3050.

Nelson KM, Dahlin JL, Bisson J, Graham J, Pauli GF, Walters MA (2017) The essential medicinal chemistry of curcumin: miniperspective. J Med Chem 60: 1620–1637.

Oliveira ABB, Matos RPA, Stuqui B, Torrezan GS, Polaquini CR, Regasini LO, Calmon MF, Rahal P (2018) Cytotoxicity and antitumoral activity by apoptosis induction of AC13: A brominated curcumin analogue. Pharmacogn Mag 14: 611–616.

Paulraj F, Abas F, Lajis NH, Othman I, Hassan SS, Naidu R (2015) The curcumin analogue 1,5-*bis*(2-hydroxyphenyl)-1,4- pentadiene-3-one induces apoptosis and downregulates E6 and E7 oncogene expression in HPV16 and HPV18-infected cervical cancer cells. Molecules 20: 11830–11860.

Pereira RM, Ferreira-Silva GA, Pivatto M, Santos LA, Bolzani VS, Paula DAC, Oliveira, JC, Júnior CV, Ionta M (2016) Alkaloids derived from flowers of *Senna spectabilis*, (−)-cassine and (−)-spectaline, have antiproliferative activity on HepG2 cells for inducing cell cycle arrest in G1/S transition through ERK inactivation and downregulation of cyclin D1 expression. Toxicol In Vitro 31: 86–92.

Polaquini CR, Torrezan GS, Santos VR, Nazaré AC, Campos DL, Almeida LA, Silva IC, Ferreira H, Pavan FR, Duque C, Regasini LO (2017) Antibacterial and antitubercular activities of cinnamylideneacetophenones. Molecules 22: 1685.

Polaquini CR, Morão LG, Nazaré AC, Torrezan GS, Dilarri G, Cavalca LB, Campos DL, Silva IC, Pereira JA, Scheffers D, Duque C, Pavan FR, Ferreira H (2019) Antibacterial activity of 3,3’-dihydroxycurcumin (DHC) is associated with membrane perturbation. Bioorg Chem 90: 103031.

Polkam N, Ramaswamy VR, Rayam P, Allaka TR, Anantaraju HS, Dharmarajan S, Perumal Y, Gandamalla D, Yellu NR, Balasubramanian S, Anireddy JS (2016) Synthesis, molecular properties prediction and anticancer, antioxidant evaluation of new edaravone derivatives. Bioorg Med Chem Lett 26: 2562–2568.

Raja SM, Clubb RJ, Ortega-Cava C, Williams SH, Bailey TA, Duan L, Zhao X, Reddi AL, Nyong AM, Natarajan A, Band V, Band H (2011) Anticancer activity of celastrol in combination with ErbB2-targeted therapeutics for treatment of ErbB2-overexpressing breast cancers. Cancer Biol Ther 11: 263–276.

Ren Y, Hao S, Jin X, Ye F, Gong Y, Jiang Y, Shao Z (2019) Effects of adjuvant chemotherapy in T1N0M0 triple-negative breast cancer. The Breast 43: 97–104.

Shin J, Ohnishi K, Murakami A, Lee J, Kundu JK, Na H, Ohigashi H, Surh Y (2011) Zerumbone induces heme oxygenase-1 expression in mouse skin and cultured murine epidermal cells through activation of Nrf2. Cancer Prev Res 4: 860–870.

Silva G, Lima FT, Seba V, Lourenço ALM, Lucas TG, Andrade BV, Torrezan GS, Polaquini CR, Garcia ME, Couto LB, Bestetti RB, França SC, Fachin AL, Regasini LO, Marins M (2018) Curcumin analog CH-5 suppresses the proliferation, migration, and invasion of the human gastric cancer cell line HGC-27. Molecules 23: 279.

Singh R, Koppikar SJ, Paul P, Gilda S, Paradkar AR, Kaul-Ghanekar R (2009) Comparative analysis of cytotoxic effect of aqueous cinnamon extract from *Cinnamomum zeylanicum* bark with commercial cinnamaldehyde on various cell lines. Pharm Biol 47: 1174–1179.

Srivastava NS, Srivastava RAK (2019) Curcumin and quercetin synergistically inhibit cancer cell proliferation in multiple cancer cells and modulate Wnt/β-catenin signaling and apoptotic pathways in A375 cells. Phytomedicine 52: 117–128.

Tewari D, Rawat P, Singh PK (2019) Adverse drug reactions of anticancer drugs derived from natural sources. Food Chem Toxicol 123: 522–535.

Veber DF, Johnson SR, Cheng HY, Smith BR, Ward KW, Kopple KD (2002) Molecular properties that influence the oral bioavailability of drug candidates. J Med Chem 45: 2615–2623.

Wang R, Zhang X, Chen C, Chen G, Zhong Q, Zhang Q, Zheng S, Wang G, Chen Q (2016) Synthesis and evaluation of 1,7-diheteroarylhepta-1,4,6-trien-3-ones as curcumin-based anticancer agents. Eur J Med Chem 110: 164–180.

Wang J, Yun D, Yao J, Fu W, Huang F, Chen L, Wei T, Yu C, Xu H, Zhou X, Huang Y, Wu J, Qiu P, Li W (2018) Design, synthesis and QSAR study of novel isatin analogues inspired Michael acceptor as potential anticancer compounds. Eur J Med Chem 144: 493–503.

Wani KD, Kadu BS, Mansara P, Gupta P, Deore AV, Chikate RC, Poddar P, Dhole SD, Kaul-Ghanekar R (2014) Synthesis, characterization and *in vitro* study of biocompatible

cinnamaldehyde functionalized magnetite nanoparticles (CPGF Nps) for hyperthermia and drug delivery applications in breast cancer. PloS One 9: e107315.

Weinberg D, Gomez-Martinez RA (2019) Vulvar Cancer. Obstet Gynecol Clin North Am 46: 125–135.

Wu J, Lu W, Cui L (2015) Inhibitory effect of curcumin on invasion of skin squamous cell carcinoma A431 cells. Asian Pac J Cancer Prev 16: 2813–2818.

5.7. Supplementary Material

5.7.1. Spectroscopy Data Analyses

^{1}H NMR and ^{13}C NMR spectra were recorded on a Bruker Avance III 14.1 T (600 MHz) spectrometer. Compounds were solubilized in deuterated chloroform ($CDCl_3$) or dimethylsulfoxide (DMSO-d_6). Chemical shifts (δ) and coupling constants (J) were expressed in ppm and Hz, respectively. Multiplicities were reported as singlet (s), doublet (d), doublet of doublet (dd) and doublet of doublet of doublets (ddd).

(*E*)-1-(4-hydroxy-3-methoxyphenyl)-3-phenylprop-2-en-1-one (**1a**) (Weber et a., 2006; Badavath et al., 2016)

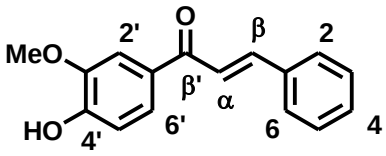

Yellow solid

Yield: 89%

^{1}H NMR (600 MHz; DMSO-d_6): 3.88 (s; 3'-OMe), 6.94 (d; 8.4; H-5'), 7.44−7.46 (H-3, H-4 and H-5), 7.64 (d; 1.8; H-2'), 7.71 (d; 15.6; H-α), 7.81 (dd; 1.8 and 8.4; H-6'), 7.87 (dd; 1.8 and 7.5; H-2 and H-6), 7.93 (d; 15.6; H-β), 10.1 (s; 4'-OH).

^{13}C NMR (150 MHz; DMSO-d_6): 56.2 (3'-OMe), 112.1 (C-2'), 115.5 (C-5'), 122.5 (C-α), 124.2 (C-6'), 129.2 (C-3 and C-5), 129.3 (C-2 and C-6), 129.9 (C-1'), 130.8 (C-4), 135.3 (C-1), 143.2 (C-β), 148.3 (C-4'), 152.4 (C-3'), 187.6 (C-β').

(*E*)-1-phenyl-3-phenylprop-2-en-1-one (**2a**) (Weber et al., 2006; Weldon et al., 2014)

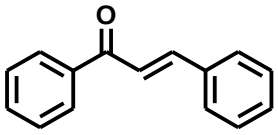

Yellow solid

Yield: 95%

^{1}H NMR (600 MHz; $CDCl_3$): 7.40−7.42 (H-3, H-4 and H-5), 7.49 (dd; 7.8 and 8.4; H-3’ and H-5’), 7.53 (d; 15.6; H-α), 7.56−7.58 (H-4’), 7.63 (dd; 1.8 and 6.3; H-2 and H-6), 7.81 (d; 15.6; H-β), 8.02 (dd; 1.2 and 8.4; H-2’ and H-6’).

^{13}NMR (150 MHz; $CDCl_3$): 122.1 (C-α), 128.4 (C-3 and C-5), 128.5 (C-2 and C-6), 128.7 (C-3’ and C-5’), 129.0 (C-2’ and C-6’), 130.6 (C-4), 132.8 (C-4’), 134.9 (C-1), 138.2 (C-1’), 144.9 (C-β), 190.6 (C-β’).

(*E*)-1-(3-methoxyphenyl)-3-phenylprop-2-en-1-one (**3a**) (Marques et al., 2019)

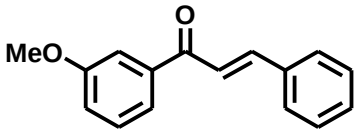

Yellow solid

Yield: 85%

^{1}H NMR (600 MHz; $CDCl_3$): 3.86 (s; 3’-OMe), 7.12 (dd; 2.4 and 8.1; H-4’), 7.39−7.41 (H-3, H-4, H-5 and H-5’), 7.51 (d; 15.6; H-α), 7.54 (dd; 1.8 and 2.4; H-2’), 7.60 (ddd; 1.2, 1.8 and 7.3; H-6’), 7.63 (dd; 1.2 and 6.6; H-2 and H-6), 7.81 (d; 15.6; H-β).

^{13}C NMR (150 MHz; $CDCl_3$): 55.5 (3’-OMe), 112.9 (C-2’), 119.3 (C-4’), 121.1 (C-6’), 122.1 (C-α), 128.5 (C-3 and C-5), 129.0 (C-2 and C-6), 129.6 (C-5’), 130.6 (C-4), 134.9 (C-1), 139.6 (C-1’), 144.9 (C-β), 159.9 (C-3’), 190.2 (C-β’).

(*E*)-1-(4-hydroxyphenyl)-3-phenylprop-2-en-1-one (**4a**) (Syam et al., 2012; Fandakli et al., 2018)

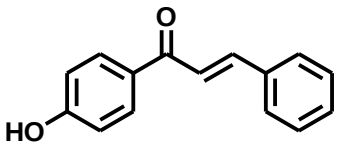

Yellow solid

Yield: 93%

^{1}H NMR (600 MHz; DMSO-d_6): 6.93 (d; 8.4; H-3’ and H-5’), 7.44−7.45 (H-3, H-4 and H-5), 7.70 (d; 15.6; H-α), 7.86 (dd; 1.2 and 7.5; H-2 and H-6), 7.91 (d; 15.6; H-β), 8.09 (d; 8.4; H-2’ and H-6’), 10.46 (s; 4’-OH).

^{13}C NMR (150 MHz; DMSO-d_6): 115.9 (C-3’ and C-5’), 122.6 (C-α), 129.1 (C-3 and C-5), 129.3 (C-2 and C-6), 129.6 (C-1’), 130.8 (C-4), 131.7 (C-2’ and C-6’), 135.4 (C-1), 143.2 (C-β), 162.7 (C-4’), 187.6 (C-β’).

(*E*)-1-(3-hydroxyphenyl)-3-phenylprop-2-en-1-one (**5a**) (Fandakli et al., 2018)

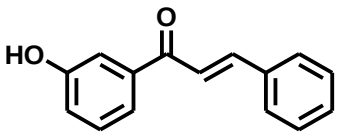

Yellow solid

Yield: 89%

^{1}H NMR (600 MHz; DMSO-d_6): 7.08 (dd; 1.8 and 8.4; H-4'), 7.38 (dd; 7.8 and 8.4; H-5'), 7.45−7.48 (H-3, H-4, H-5 and H-2'), 7.64 (d; 7.8; H-6'), 7.73 (d; 15.6; H-α), 7.86 (d; 15.6; H-β), 7.87−7.88 (H-2 and H-6), 9.83 (s; 3'-OH).

^{13}C NMR (150 MHz; DMSO-d_6): 115.1 (C-2'), 120.1 (C-4'), 120.8 (C-6'), 122.7 (C-α), 129.3 (C-3 and C-5), 129.4 (C-2 and C-6), 130.3 (C-4), 131.0 (C-5'), 135.1 (C-1), 139.5 (C-1'), 144.3 (C-β), 158.2 (C-3'), 189.6 (C-β').

(*E*)-1-(4-methoxyphenyl)-3-phenylprop-2-en-1-one (**6a**) (Syam et al., 2012; Marques et al., 2019)

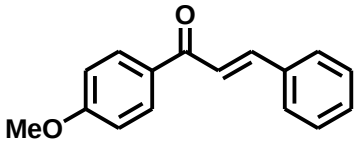

Yellow solid

Yield: 73%

^{1}H NMR (600 MHz; $CDCl_3$): 3.87 (s; 4'-OMe), 6.97 (d; 8.4; H-3' and H-5'), 7.40−7.41 (H-3, H-4 and H-5), 7.54 (d; 15.6; H-α), 7.63 (dd; 1.8 and 6.0; H-2 and H-6); 7.80 (d; 15.6; H-β), 8.04 (d; 8.4; H-2' and H-6').

^{13}C NMR (150 MHz; $CDCl_3$): 55.5 (4'-OMe), 113.9 (C-3' and C-5'), 121.9 (C-α), 128.4 (C-3 and C-5), 128.9 (C-2 and C-6), 130.3 (C-4), 130.8 (C-2' and C-6'), 131.1 (C-1'), 135.1 (C-1), 144.0 (C-β), 163.5 (C-4'), 188.7 (C-β')

(2*E*,4*E*)-1-(4-hydroxy-3-methoxyphenyl)-5-phenylpenta-2,4-dien-1-one (**1b**) (Polaquini et al., 2017)

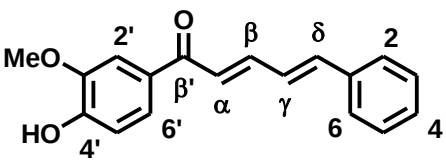

Yellow crystal

Yield: 95%

^{1}H NMR (600 MHz; DMSO-d_6): 3.86 (s; 3'-OMe), 6.92 (d; 8.4; H-5'), 7.17−7.27 (H-γ and H-δ), 7.35 (dd; 1.8 and 7.2; H-4), 7.42 (dd; 7.2 and 7.8; H-3 and H-5), 7.43 (d; 15.0; H-α), 7.47−7.52 (H-β), 7.56 (d; 1.8; H-2'), 7.59 (dd; 1.8 and 7.8; H-2 and H-6), 7.62 (dd; 1.8 and 8.4; H-6'), 10.07 (s; 4'-OH).

^{13}C NMR (150 MHz; DMSO-d_6): 56.1 (3'-OMe), 111.9 (C-2'), 115.5 (C-5'), 123.7 (C-6'), 126.0 (C-γ), 127.6 (C-2 and C-6), 127.9 (C-α), 129.4 (C-3 and C-5), 129.5 (C-4), 130.0 (C-1'), 136.6 (C-1), 141.3 (C-δ), 143.5 (C-β), 148.2 (C-4'), 152.3 (C-3'), 187.5 (C-β').

(2*E*,4*E*)-1,5-diphenylpenta-2,4-dien-1-one (**2b**) (Weldon et al., 2014; Silva et al., 2016; Pan et al., 2019)

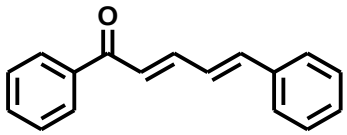

Yellow solid

Yield: 87%

^{1}H NMR (600 MHz; $CDCl_3$): 6.98−7.04 (H-γ and H-δ), 7.08 (d; 15.0; H-α), 7.31 (dd; 1.2 and 7.8; H-4), 7.36 (dd; 7.2 and 7.8; H-3 and H-5), 7.46−7.50 (H-2, H-6, H-3' and H-5'), 7.56 (dd; 1.2 and 7.2; H-4'), 7.58−7.62 (H-β), 7.97 (dd; 1.2 and 7.8; H-2' and H-6').

^{13}C NMR (150 MHz; $CDCl_3$): 125.4 (C-γ), 127.0 (C-α), 127.3 (C-2 and C-6), 128.4 (C-3 and C-5), 128.6 (C-3' and C-5'), 128.9 (C-2' and C-6'), 129.3 (C-4), 132.7 (C-4'), 136.1 (C-1), 138.2 (C-1'), 142.0 (C-δ), 144.9 (C-β), 190.5 (C-β').

(2*E*,4*E*)-1-(3-methoxyphenyl)-5-phenylpenta-2,4-dien-1-one (**3b**) (Polaquini et al., 2017; Pan et al., 2019)

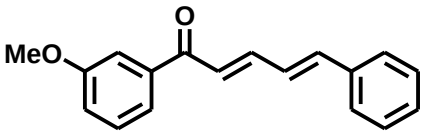

Yellow crystal

Yield: 60%

^{1}H NMR (600 MHz; $CDCl_3$): 3.90 (s; 3'-OMe), 7.03−7.09 (H-γ and H-δ), 7.10 (d; 15.0; H-α), 7.15 (ddd; 1.2, 2.4 and 8.2; H-4'), 7.35 (dd; 2.4 and 7.2; H-4), 7.40 (dd; 7.2 and 7.8; H-3

and H-5), 7.42 (dd; 7.8 and 8.2; H-5'), 7.53−7.54 (H-2, H-6 and H-2'), 7.58 (ddd; 1.2, 1.8 and 7.8; H-6'), 7.61−7.66 (H-β).

^{13}C NMR (150 MHz; $CDCl_3$): 55.5 (3'-OMe), 112.6 (C-2'), 119.3 (C-4'), 121.0 (C-6'), 125.4 (C-γ), 127.0 (C-α), 127.3 (C-2 and C-6), 128.9 (C-3 and C-5), 129.3 (C-4), 129.6 (C-5'), 136.1 (C-1), 139.6 (C-1'), 142.0 (C-δ), 144.9 (C-β), 159.9 (C-3'), 190.2 (C-β').

(2*E*,4*E*)-1-(4-hydroxyphenyl)-5-phenylpenta-2,4-dien-1-one (**4b**) (Silva et al., 2016; Polaquini et al., 2017)

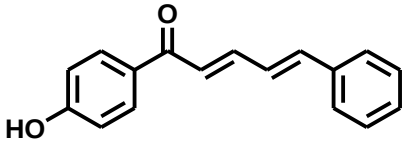

Yellow solid

Yield: 71%

^{1}H NMR (600 MHz; DMSO-d_6): 6.90 (d; 8.4; H-3' and H-5'), 7.16−7.26 (H-γ and H-δ), 7.35 (d; 7.2; H-4), 7.38 (d; 14.4; H-α), 7.42 (dd; 7.2 and 7.8; H-3 and H-5), 7.46−7.51 (H-β), 7.59 (d; 7.8; H-2 and H-6), 7.94 (d; 8.4; H-2' and H-6'), 10.38 (s; 4'-OH).

^{13}C NMR (150 MHz; DMSO-d_6): 115.9 (C-3' and C-5'), 126.0 (C-γ), 127.6 (C-2 and C-6), 127.9 (C-α), 129.4 (C-3 and C-5), 129.5 (C-4), 129.6 (C-1'), 131.3 (C-2' and C-6'), 136.6 (C-1), 141.3 (C-δ), 143.6 (C-β), 162.6 (C-4), 187.6 (C-β').

(2*E*,4*E*)-1-(3-hydroxyphenyl)-5-phenylpenta-2,4-dien-1-one (**5b**) (Polaquini et al., 2017)

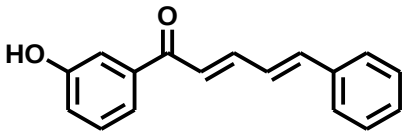

Brown solid

Yield: 84%

^{1}H NMR (600 MHz; DMSO-d_6): 7.06 (d; 8.4; H-4'), 7.19−7.29 (H-γ and H-δ), 7.31 (d; 14.4; H-α), 7.34−7.38 (H-4, H-2' and H-5'), 7.41 (dd; 7.2 and 7.8; H-3 and H-5), 7.47 (d; 7.8; H-6'), 7.50−7.54 (H-β), 7.60 (d; 7.2; H-2 and H-6), 9.84 (s, 3'-OH).

^{13}C NMR (150 MHz; DMSO-d_6): 114.9 (C-2'), 119.6 (C-4'), 120.6 (C-6'), 126.1 (C-γ), 127.7 (C-2 and C-6), 127.8 (C-α), 129.4 (C-3 and C-5), 129.7 (C-4), 130.4 (C-5'), 136.5 (C-1), 139.6 (C-1'), 142.1 (C-δ), 144.8 (C-β), 158.2 (C-3'), 189.6 (C-β').

(2*E*,4*E*)-1-(4-methoxyphenyl)-5-phenylpenta-2,4-dien-1-one (**6b**) (Weldon et al., 2014; Silva et al., 2016; Pan et al., 2019)

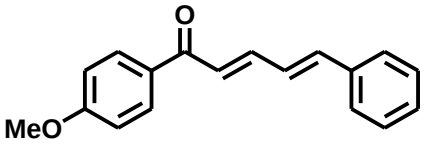

Yellow solid

Yield: 66%

^{1}H NMR (600 MHz; $CDCl_3$): 3.87 (s; 4'-OMe), 6.96 (d; 8.4; H-3' and H-5'), 6.99−7.04 (H-γ and H-δ), 7.10 (d; 14.4; H-α), 7.31 (dd; 2.4 and 7.8; H-4), 7.36 (dd; 7.2 and 7.8; H-3 and H-5), 7.49 (d; 7.2; H-2 and H-6), 7.57−7.61 (H-β), 7.99 (d; 8.4; H-2' and H-6').

^{13}C NMR (150 MHz; $CDCl_3$): 55.5 (4'-OMe), 113.8 (C-3' and C-5'), 125.3 (C-γ), 127.1 (C-α), 127.3 (C-2 and C-6), 128.9 (C-3 and C-5), 129.1 (C-4), 130.7 (C-2' and C-6'), 131.1 (C-1'), 136.2 (C-1), 141.4 (C-δ), 144.0 (C-β), 163.4 (C-4'), 188.7 (C-β').

5.8. REFERENCES

Badavath VN, Baysal I, Ucar G, Sinha BN, Jayaprakash V (2015) Monoamine oxidase inhibitory activity of novel pyrazoline analogues: curcumin based design and synthesis. ACS Med Chem Lett 7: 56-61.

Fandakli S, Dogan IS, Sellitepe HE, Yasar A, Yayli N (2018) Synthesis, theoretical calculation and α-glucosidase inhibition of new chalcone oximes. Org Commun 11: 23-34.

Marques BC, Santos MB, Anselmo DB, Monteiro DA, Gomes E, Saiki MFC, Rahal P, Rosalen PL, Sardi JCO, Regasini LO (2019) Methoxychalcones: effect of methoxyl group toward antifungal, antibacterial and antiproliferative activities. Med Chem 15: 1.

Pan G, Zhang X, Zhu X, Guo R, Wang Y (2019) Synthesis of (*E*, *E*)-Dienones and (*E*, *E*)-Dienals via Palladium-Catalyzed γ, δ-Dehydrogenation of Enones and Enals. iScience 20: 229-236.

Polaquini CR, Torrezan GS, Santos VR, Nazaré AC, Campos DL, Almeida LA, Silva IC, Ferreira H, Pavan FR, Duque C, Regasini LO (2017) Antibacterial and antitubercular activities of cinnamylideneacetophenones. Molecules 22: 1685.

Silva EMP, Melo T, Sousa BC, Resende DISP, Magalhães LM, Segundo MA, Silva AMS, Domingues MRM (2016) Do cinnamylideneacetophenones have antioxidant properties and a protective effect toward the oxidation of phosphatidylcholines?. Eur J Med Chem 121: 331-337.

Syam S, Abdelwahab SI, Al-Mamary MA, Mohan S (2012) Synthesis of chalcones with anticancer activities. Molecules 17: 6179-6195.

Weber WM, Hunsaker LA, Roybal CN, Bobrovnikova-Marjon EV, Abcouwer SF, Royer RE, Decka LM, Jagt DLV (2006) Activation of NFκB is inhibited by curcumin and related enones. Bioorg Med Chem 14: 2450-2461.

Weldon DJ, Saulsbury MD, Goh J, Rowland L, Campbell P, Robinson L, Miller C, Christian J, Amis L, Taylor N, Dill C, Davis Jr. W, Evans SL, Brantley E (2014) One-pot synthesis of cinnamylideneacetophenones and their in vitro cytotoxicity in breast cancer cells. Bioorg Med Chem Lett 24: 3381-3384.

Figure S 1. ^{1}H NMR spectrum of compound **1a** (600 MHz, DMSO-d_6)

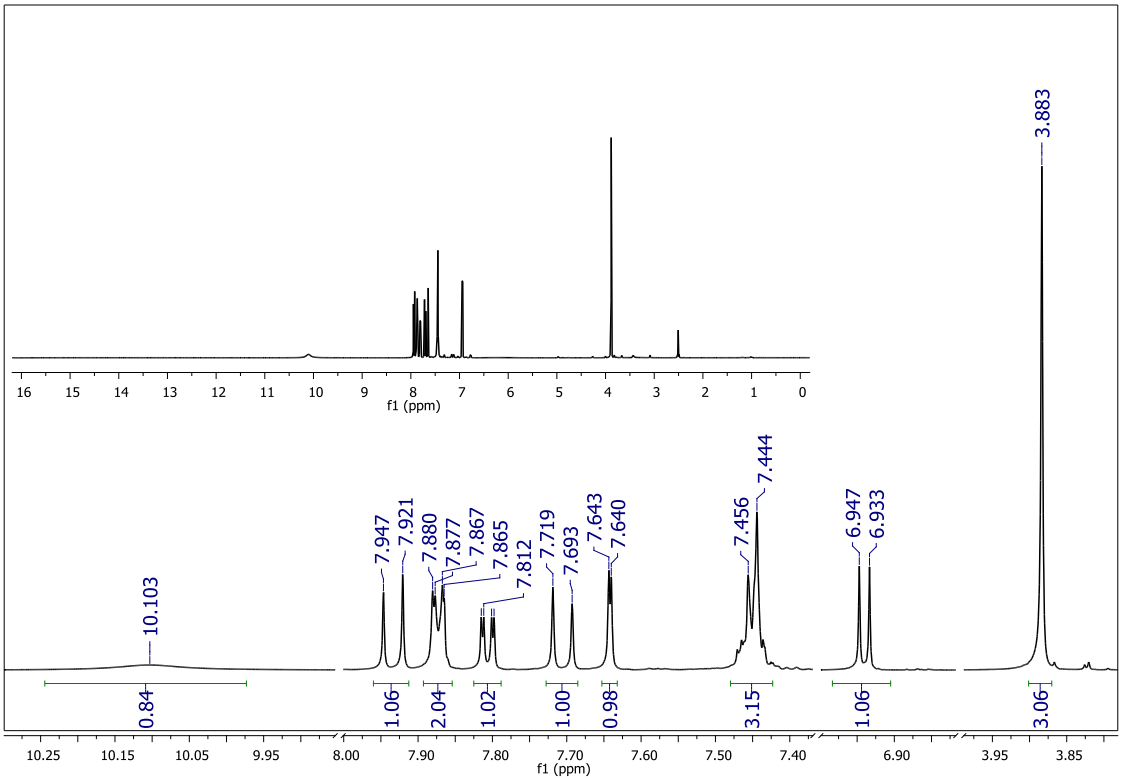

Figure S 2. ^{13}C NMR spectrum of compound **1a** (150 MHz, DMSO-d_6)

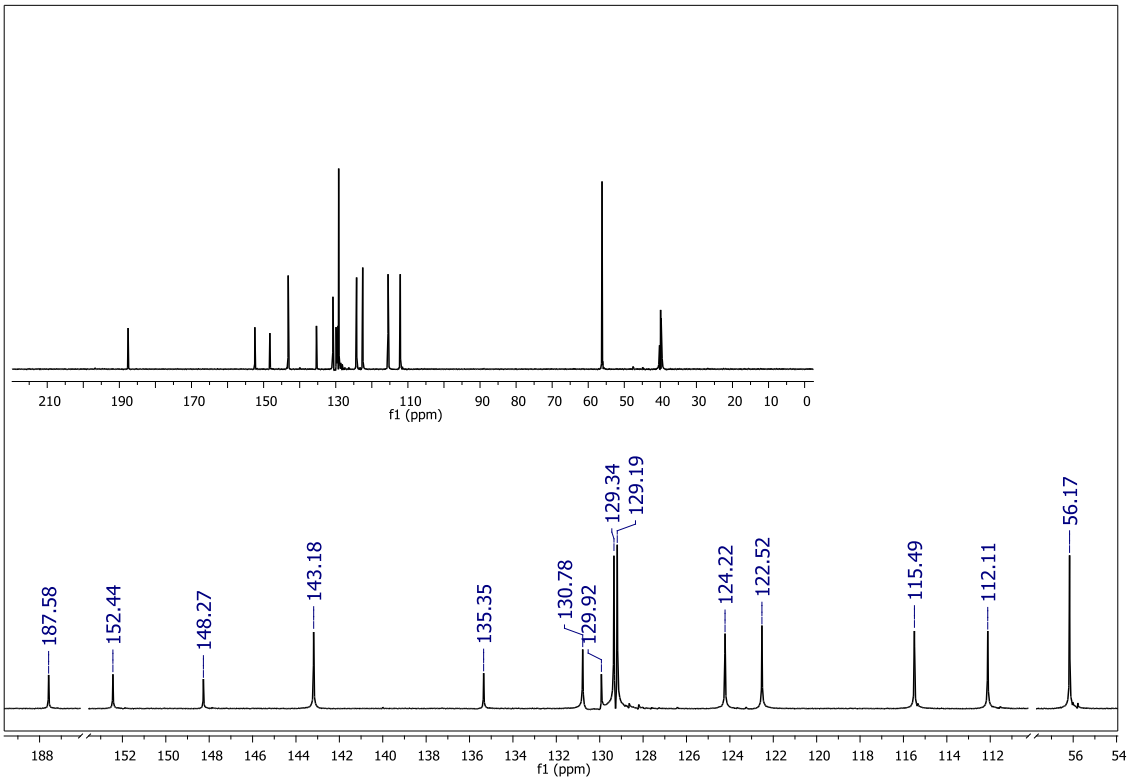

Figure S 3. ^{1}H NMR spectrum of compound **2a** (600 MHz, $CDCl_3$)

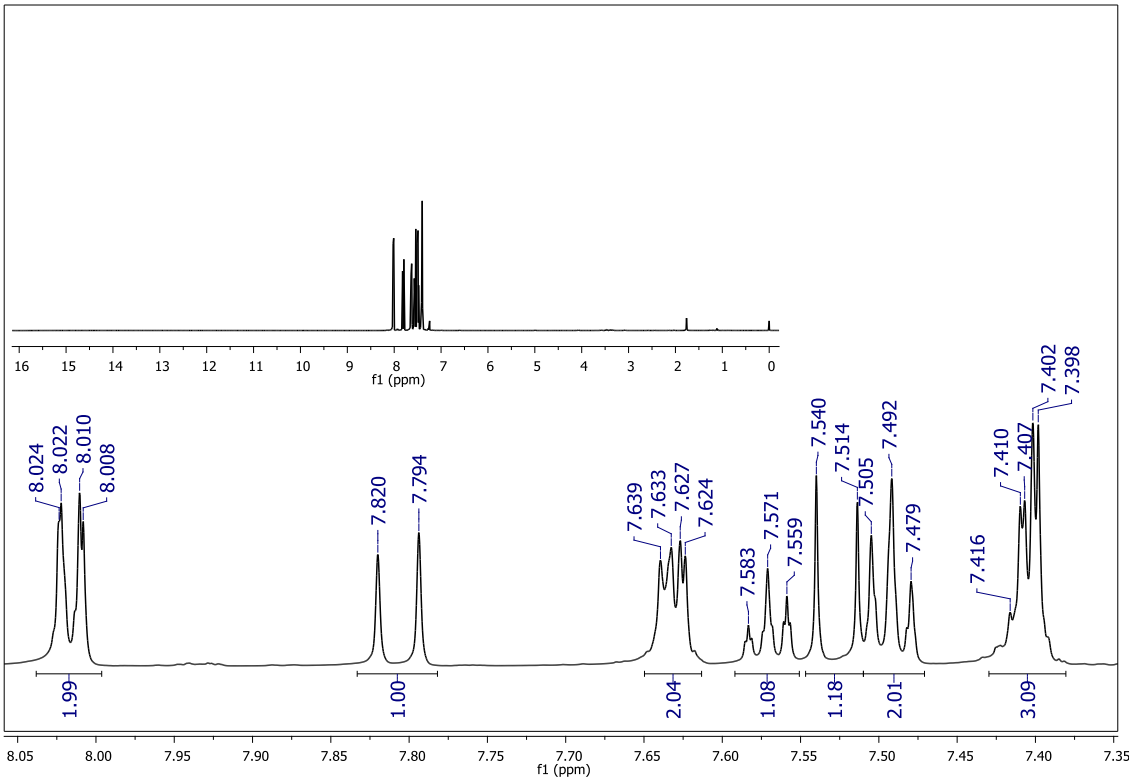

Figure S 4. ^{13}C NMR spectrum of compound **2a** (150 MHz, $CDCl_3$)

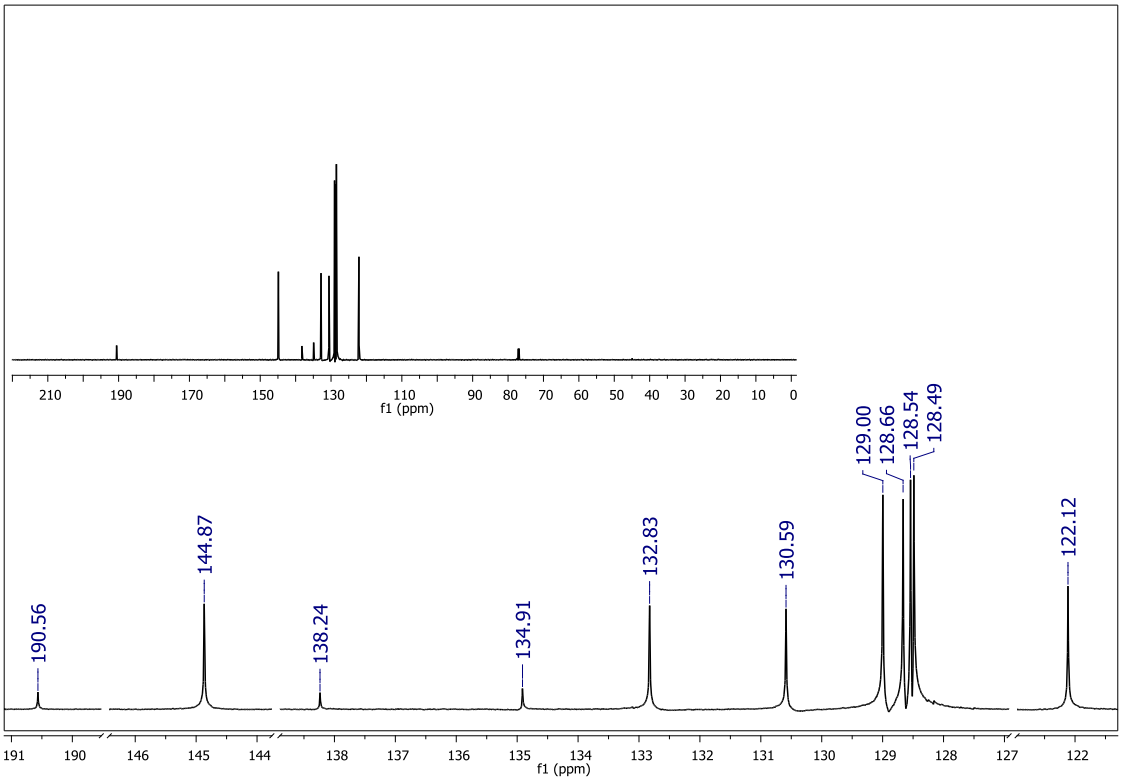

Figure S 5. ^{1}H NMR spectrum of compound **3a** (600 MHz, $CDCl_3$)

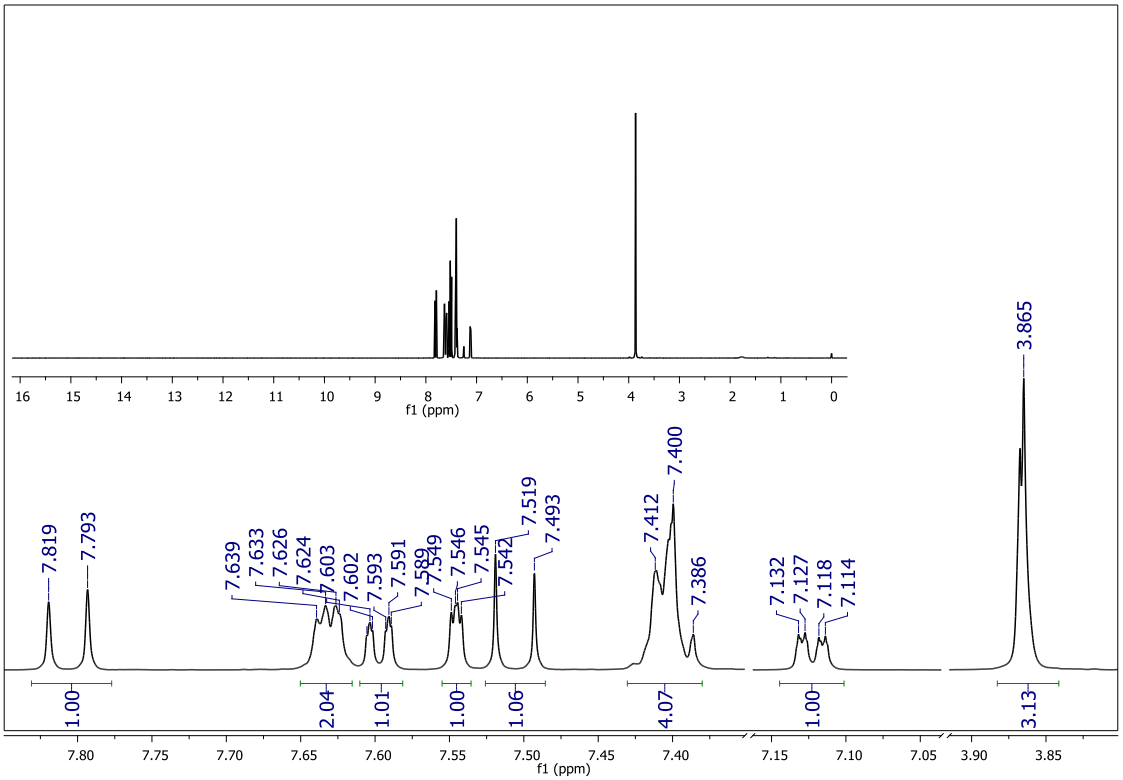

Figure S 6. ^{13}C NMR spectrum of compound **3a** (150 MHz, $CDCl_3$)

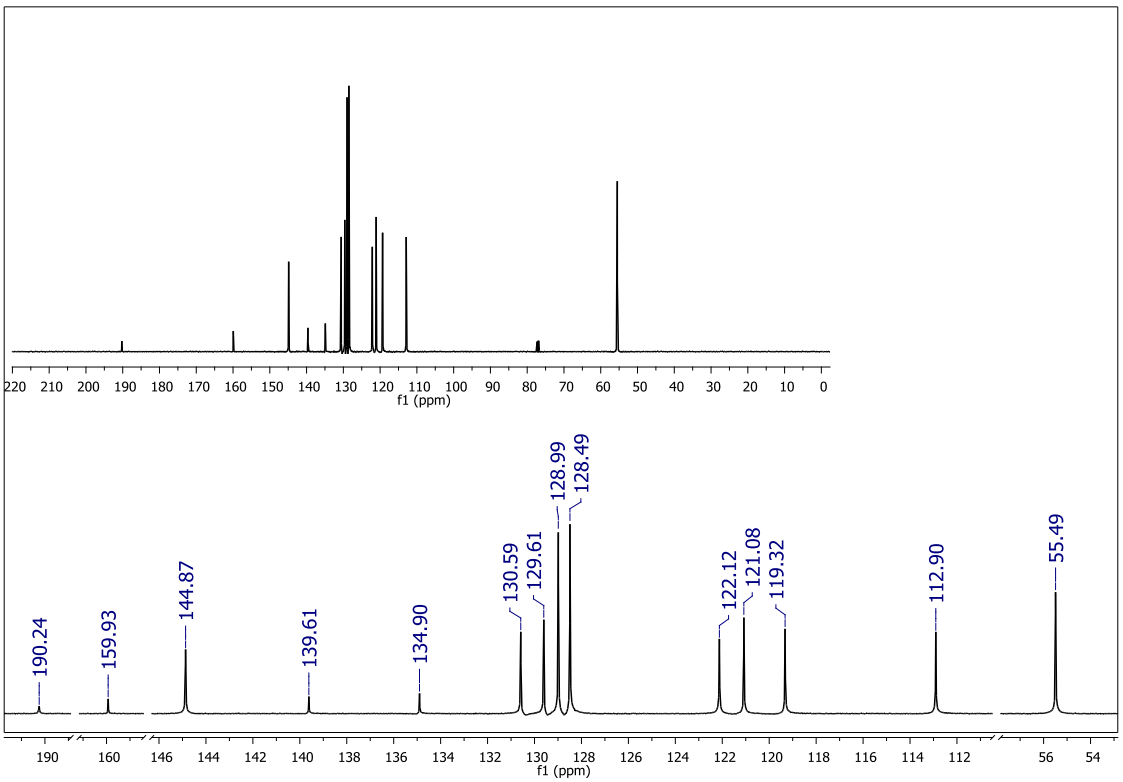

Figure S 7. ^{1}H NMR spectrum of compound **4a** (600 MHz, DMSO-d^{6})

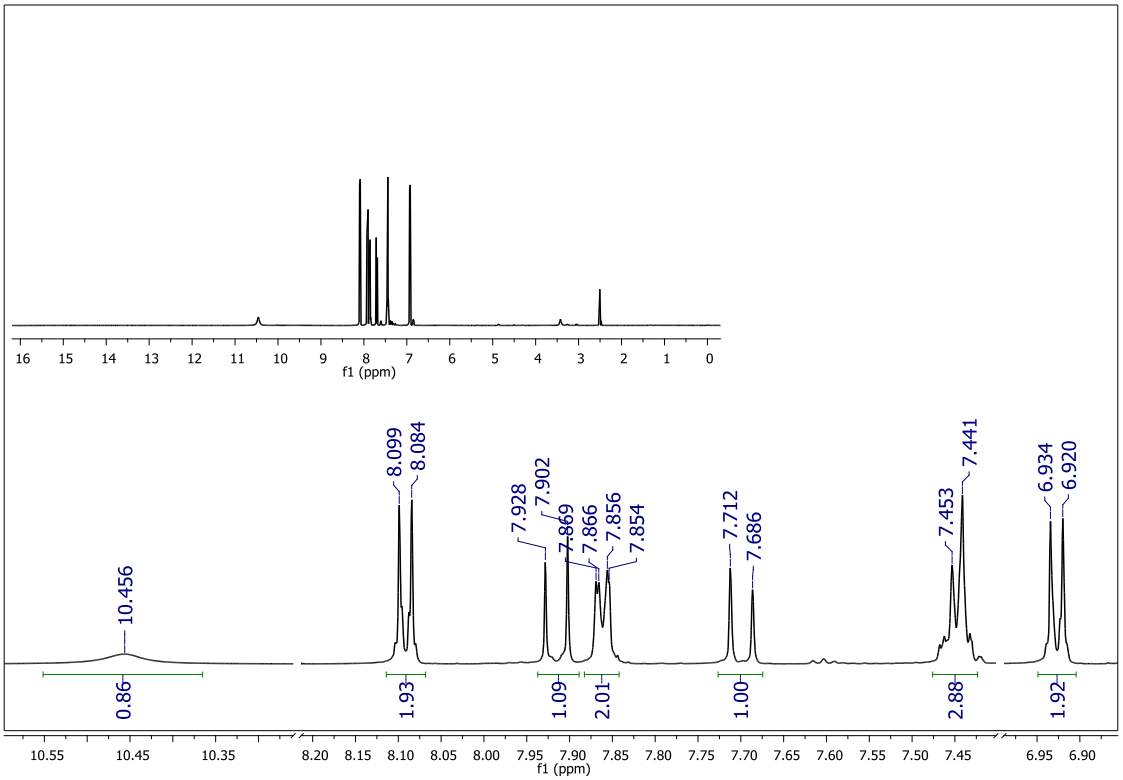

Figure S 8. ^{13}C NMR spectrum of compound **4a** (150 MHz, DMSO-d$_{6}$)

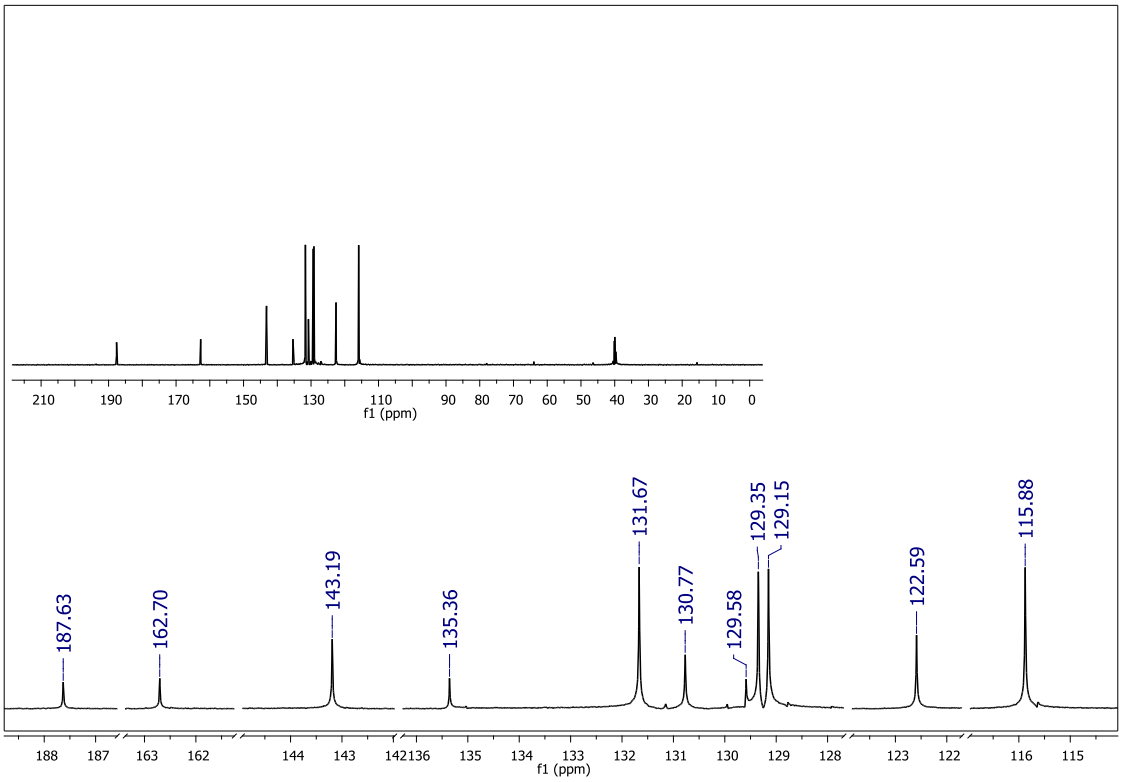

Figure S 9. ^{1}H NMR spectrum of compound **5a** (600 MHz, DMSO-d_6)

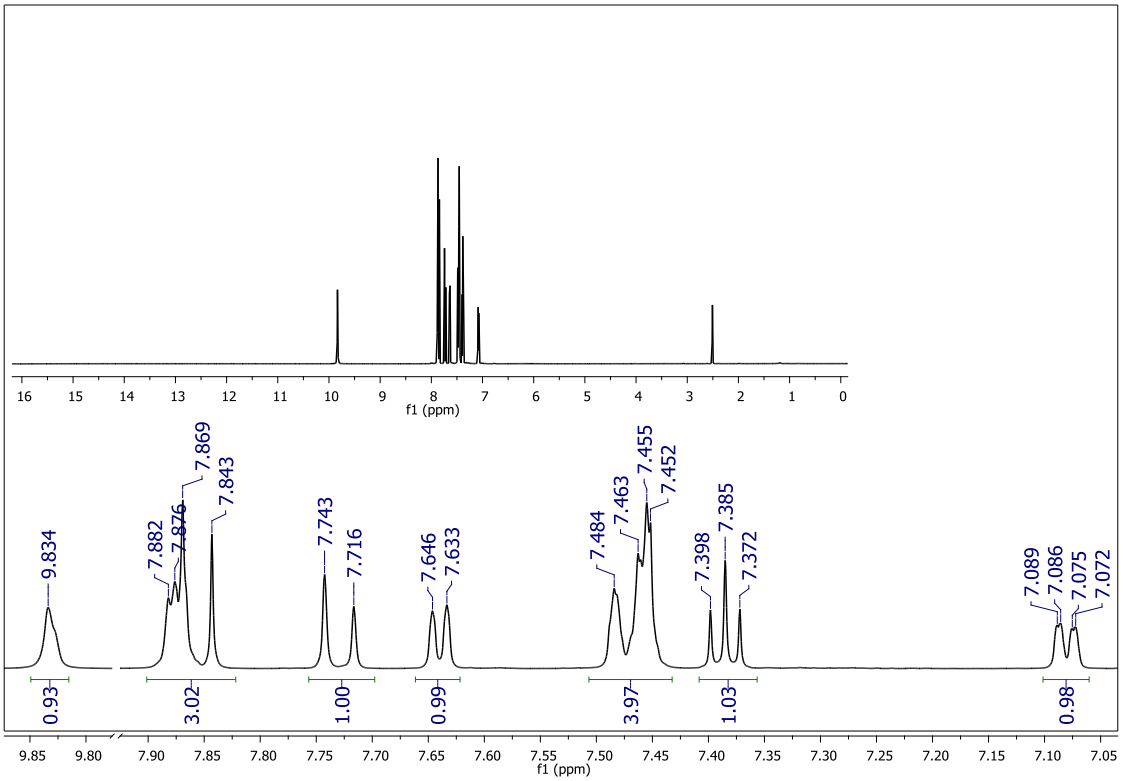

Figure S 10. ^{13}C NMR spectrum of compound **5a** (150 MHz, DMSO-d_6)

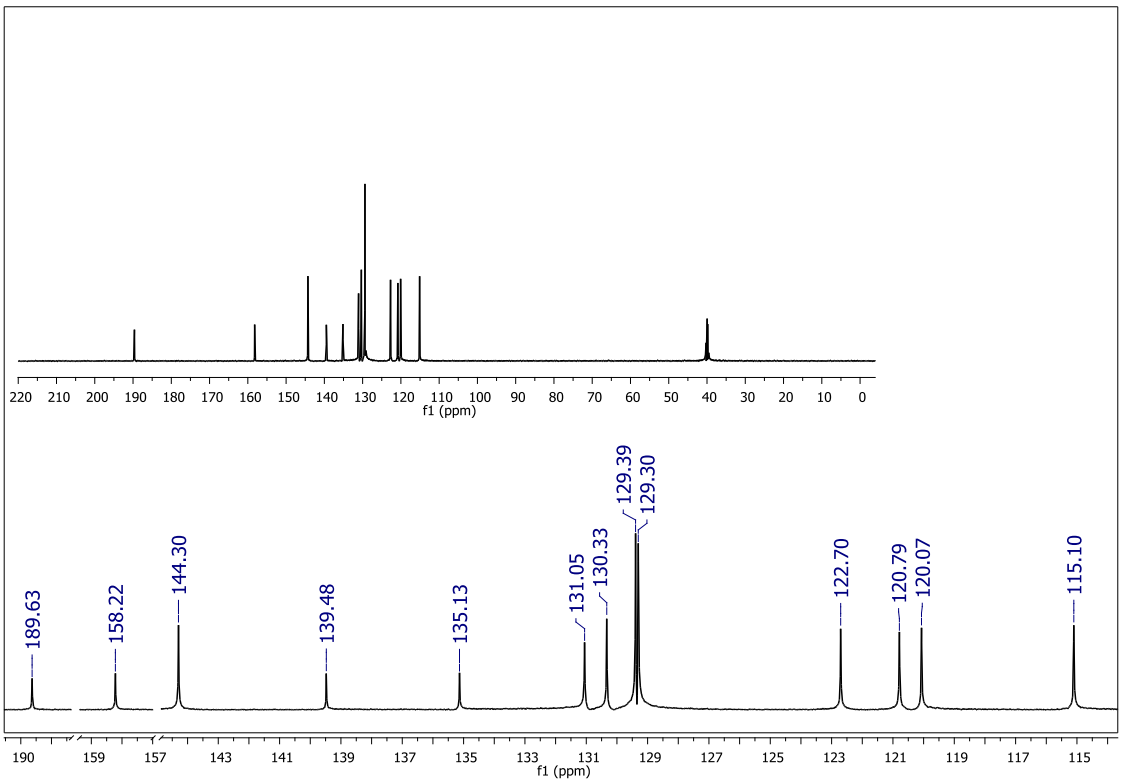

Figure S 11. ^{1}H NMR spectrum of compound **6a** (600 MHz, $CDCl_3$)

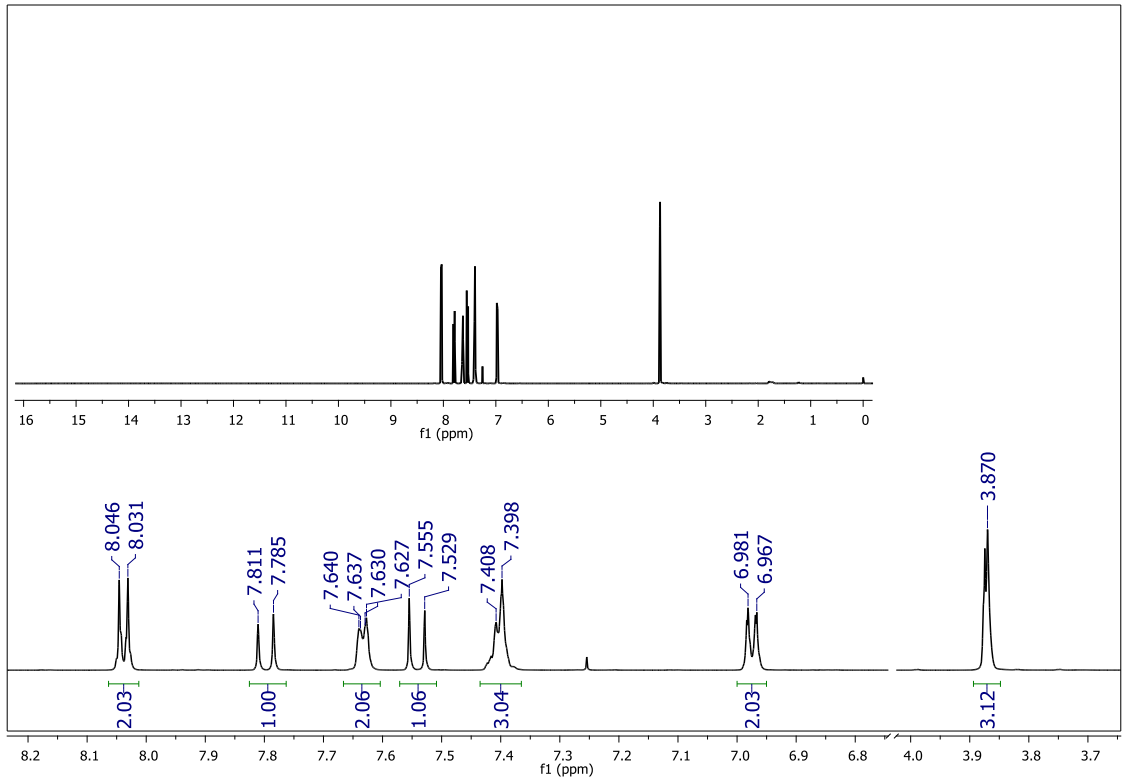

Figure S 12. ^{13}C NMR spectrum of compound **6a** (150 MHz, $CDCl_3$)

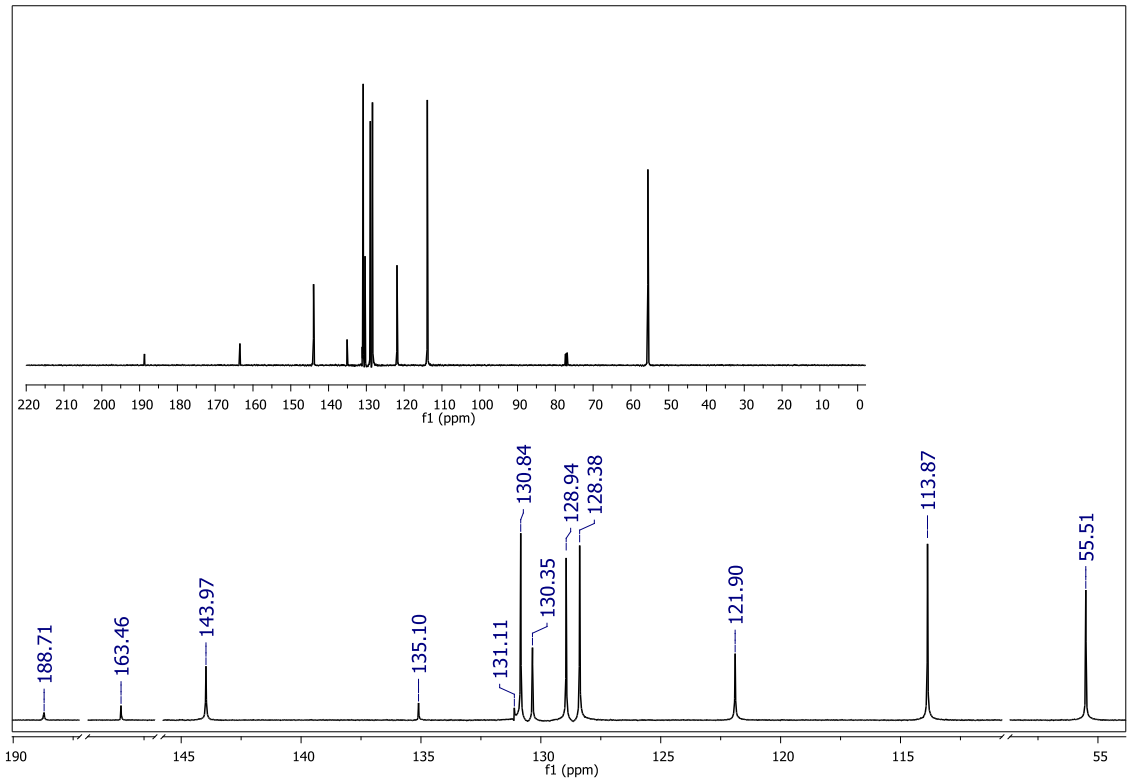

Figure S 13. ^{1}H NMR spectrum of compound **1b** (600 MHz, DMSO-d_6)

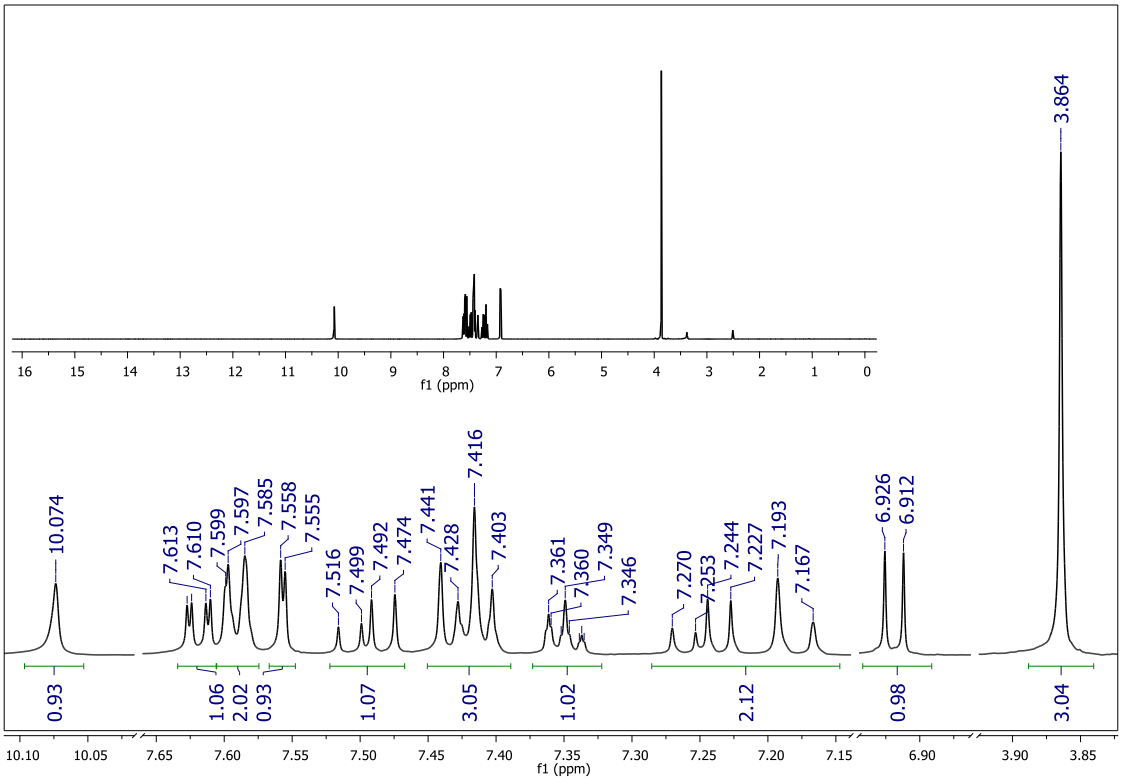

Figure S 14. ^{13}C NMR spectrum of compound **1b** (150 MHz, DMSO-d_6)

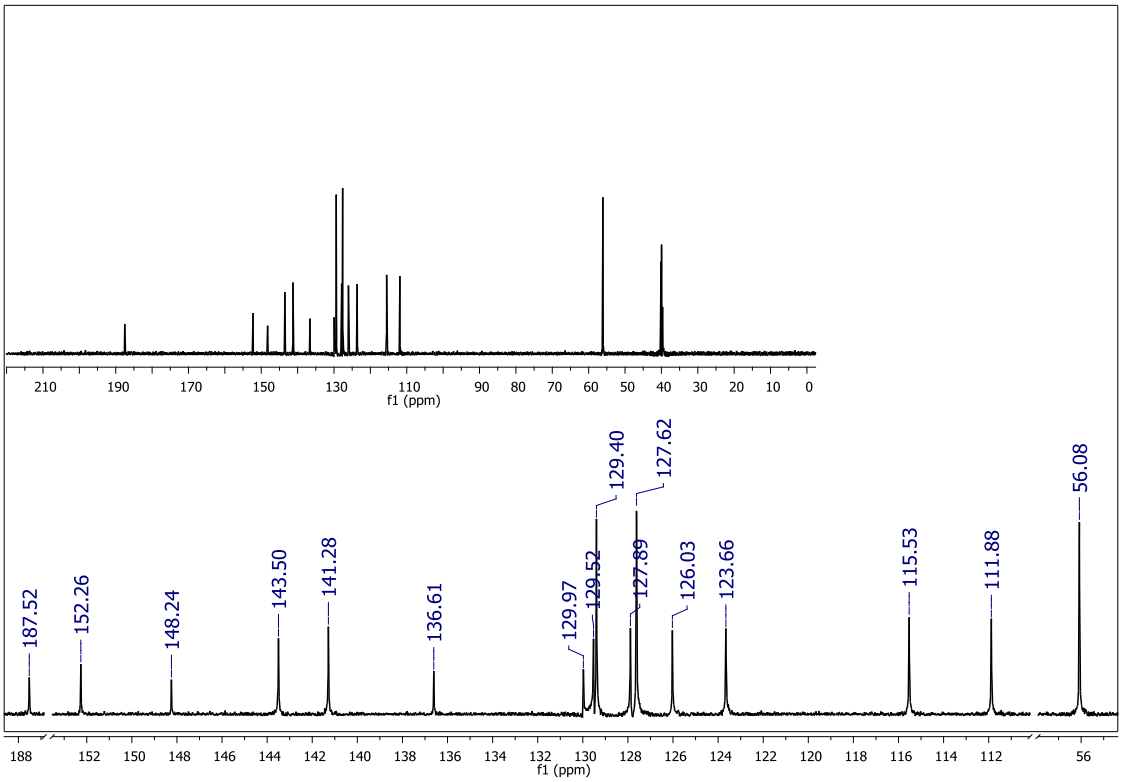

Figure S 15. ^{1}H NMR spectrum of compound **2b** (600 MHz, $CDCl_3$)

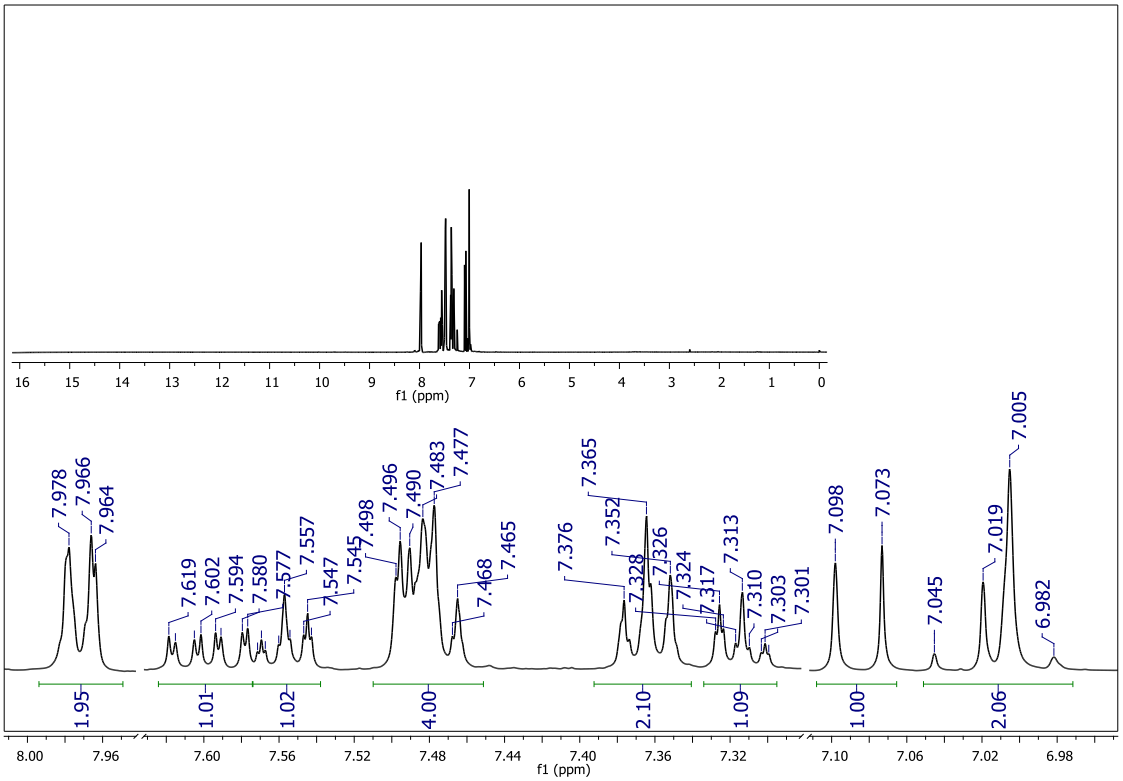

Figure S 16. ^{13}C NMR spectrum of compound **2b** (150 MHz, $CDCl_3$)

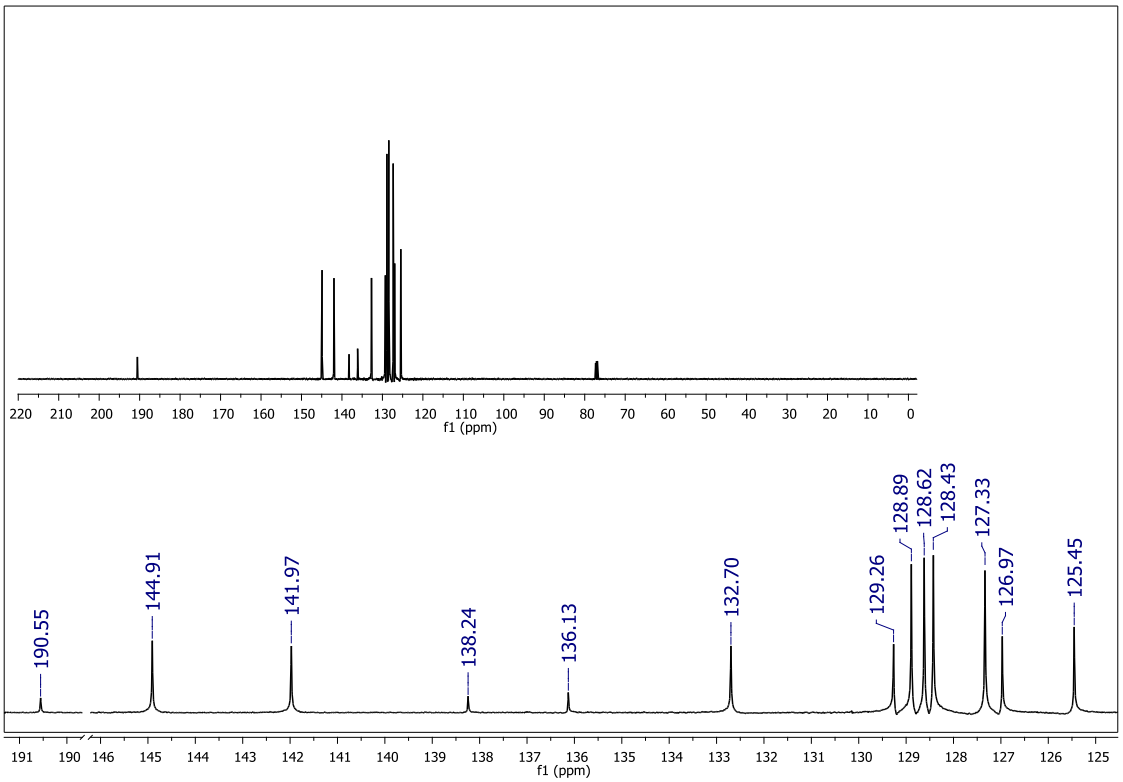

Figure S 17. ^{1}H NMR spectrum of compound **3b** (600 MHz, $CDCl_3$)

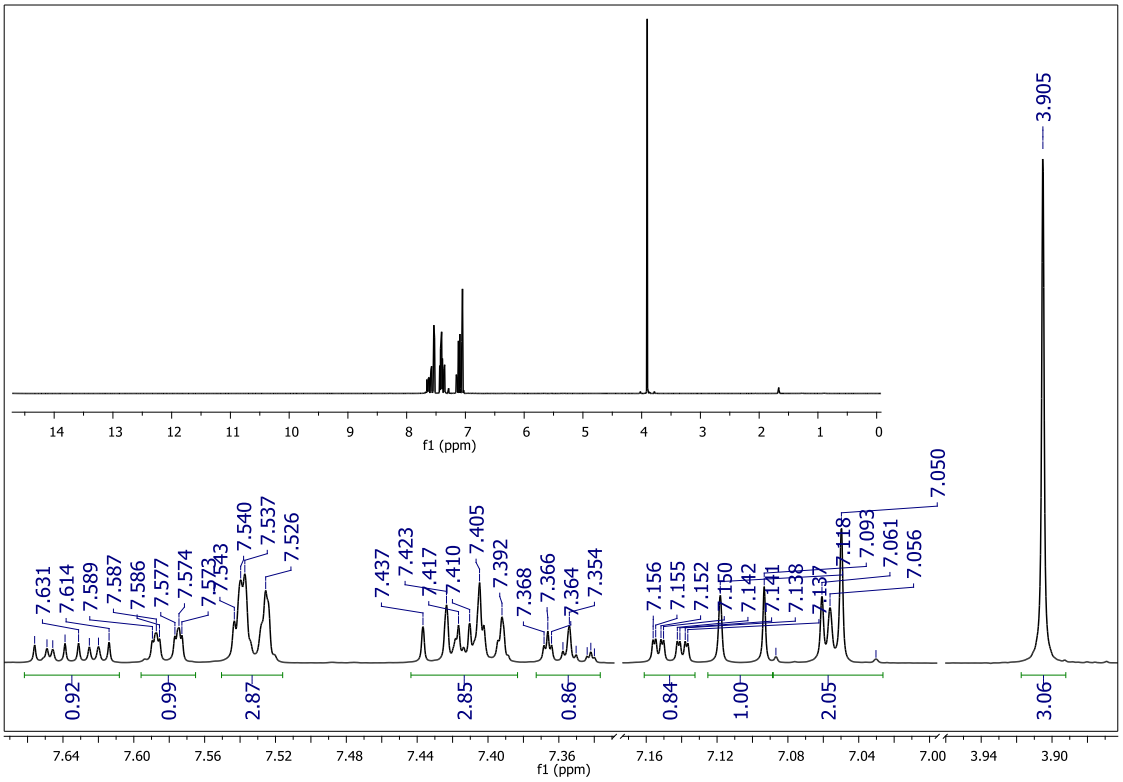

Figure S 18. ^{13}C NMR spectrum of compound **3b** (150 MHz, $CDCl_3$)

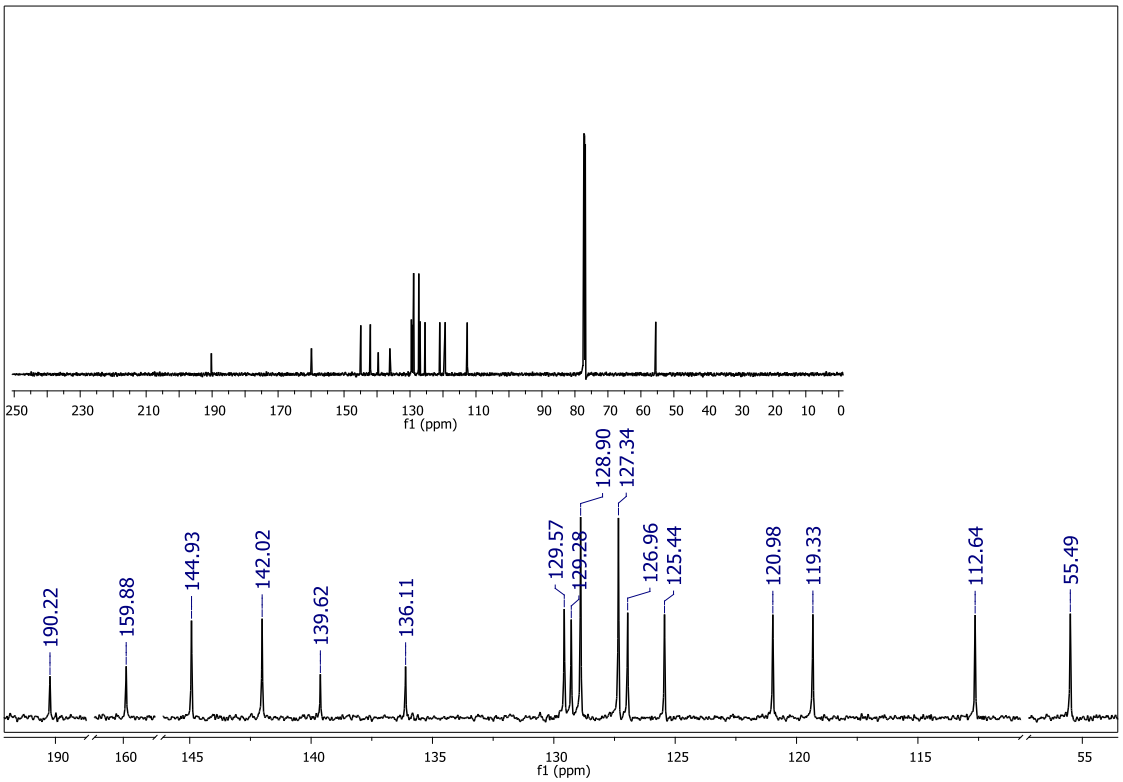

Figure S 19. ^{1}H NMR spectrum of compound **4b** (600 MHz, DMSO-d_6)

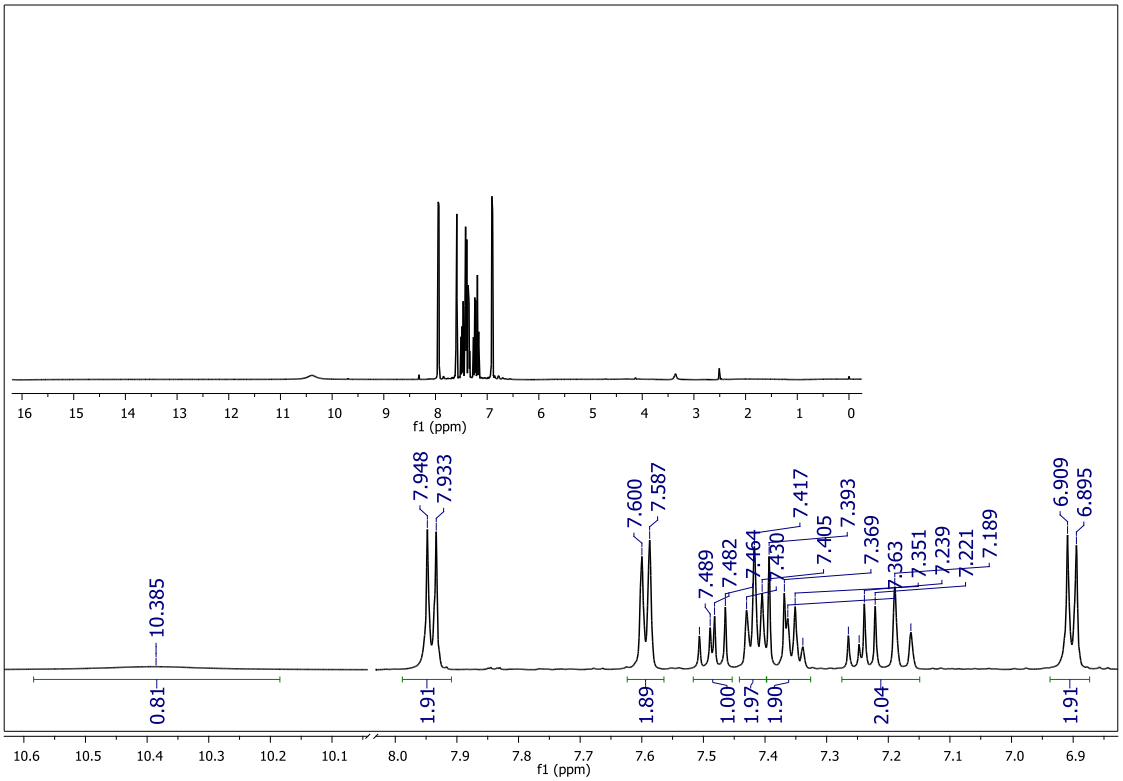

Figure S 20. ^{13}C NMR spectrum of compound **4b** (150 MHz, DMSO-d_6)

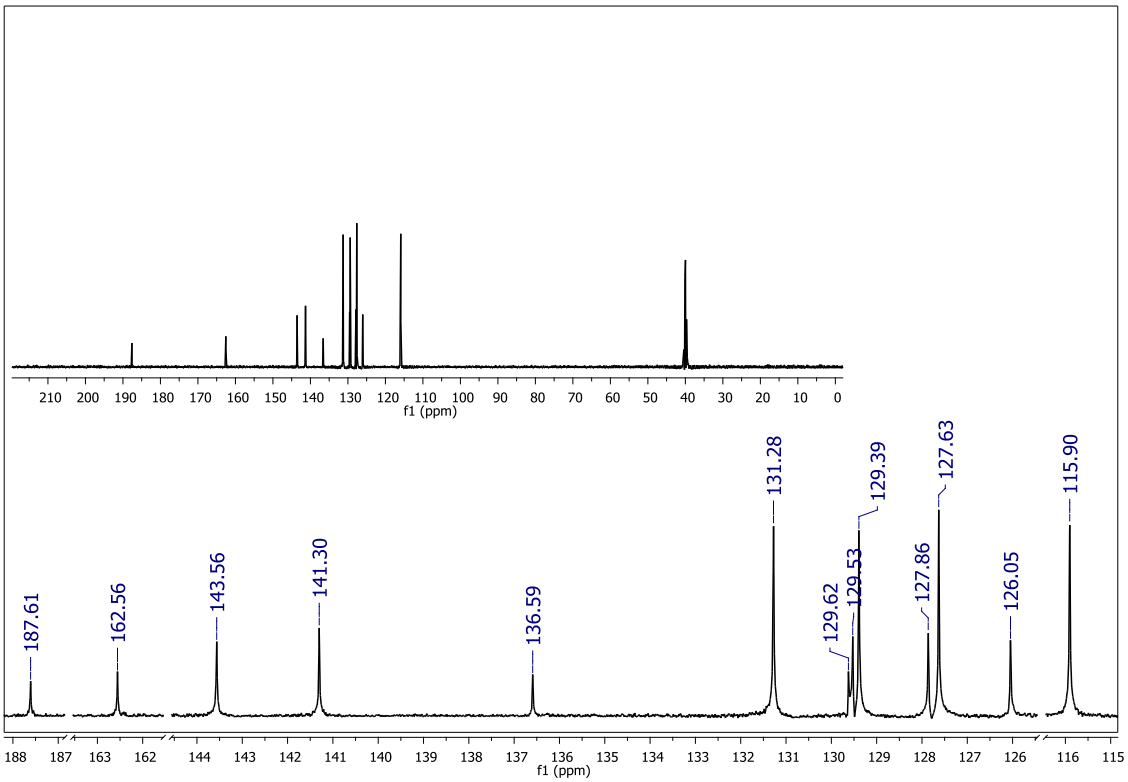

Figure S 21. ^{1}H NMR spectrum of compound **5b** (600 MHz, DMSO-d_6)

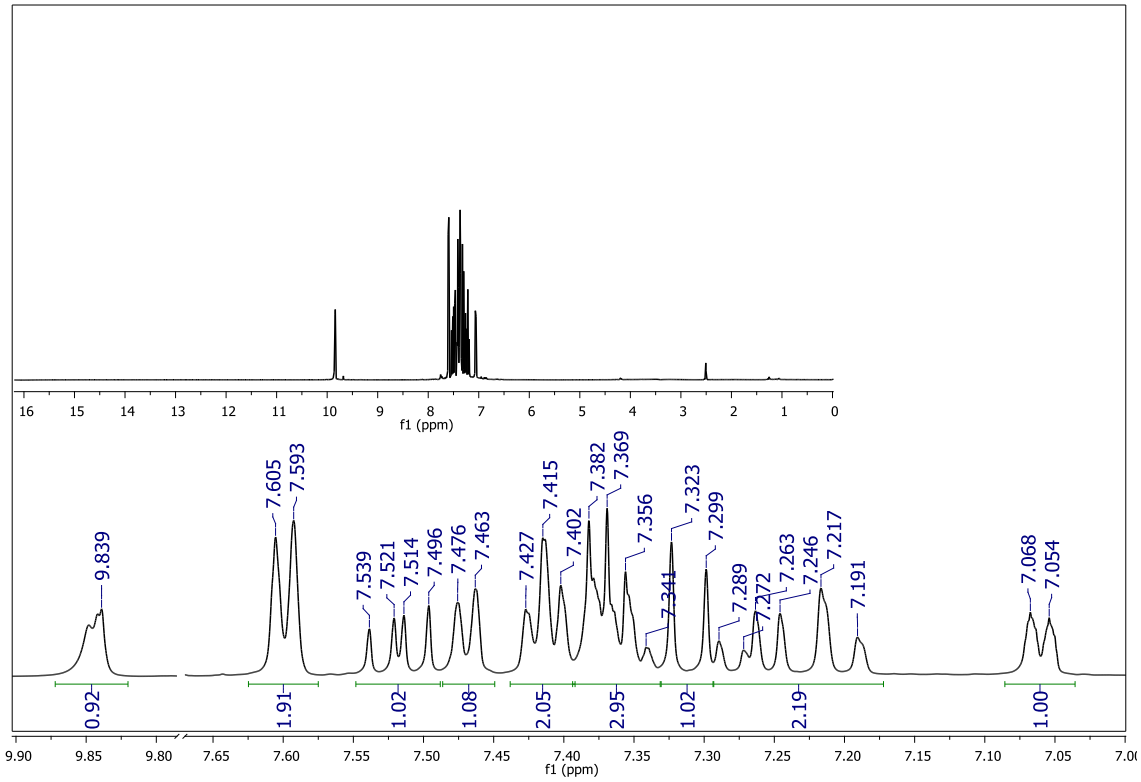

Figure S 22. ^{13}C NMR spectrum of compound **5b** (150 MHz, DMSO-d_6)

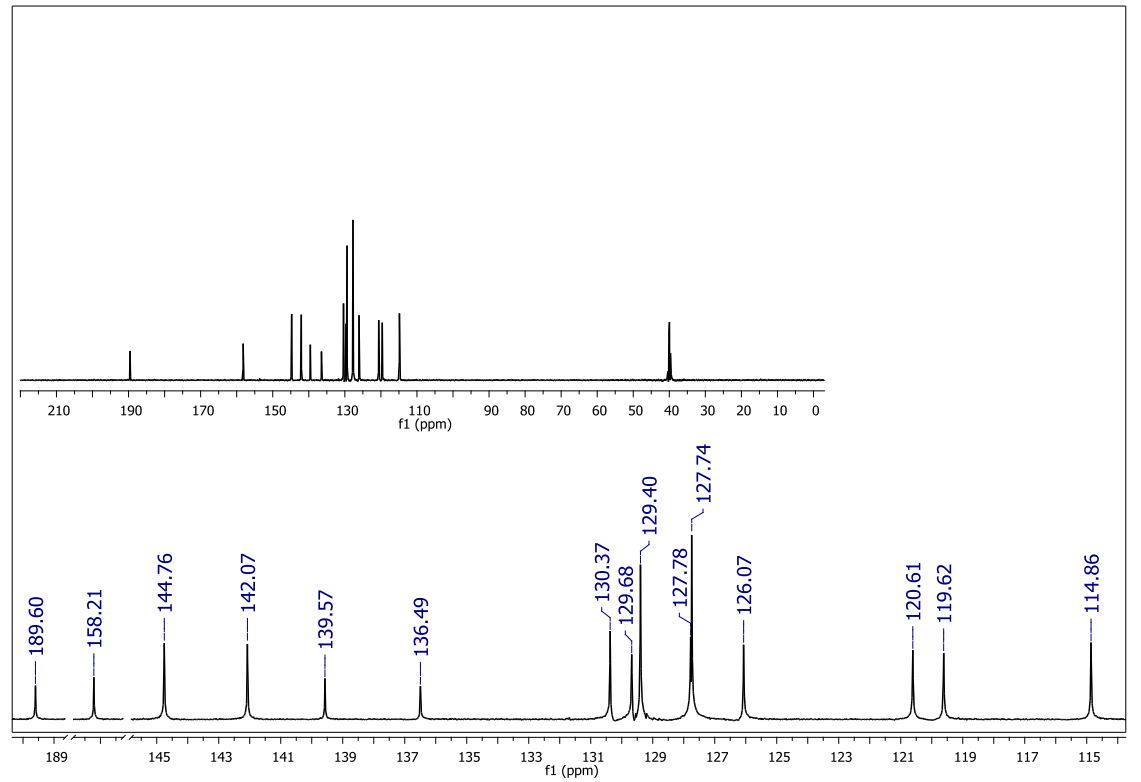

Figure S 23. ^{1}H NMR spectrum of compound **6b** (600 MHz, $CDCl_3$)

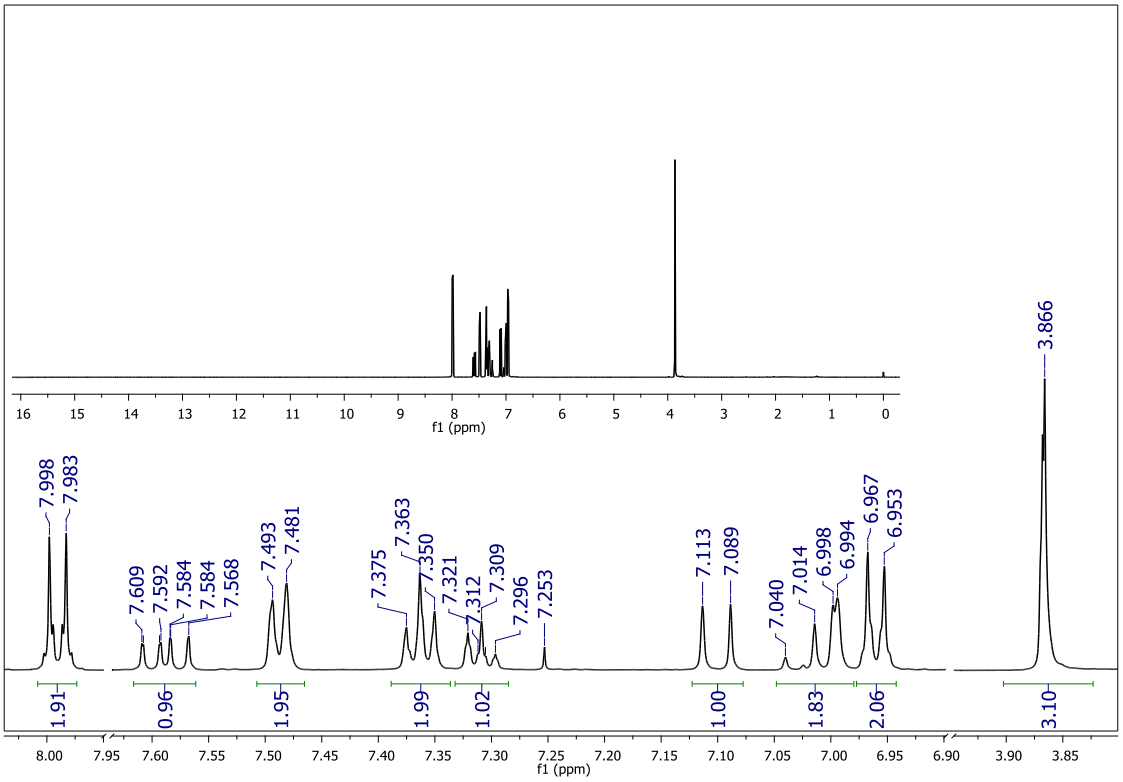

Figure S 24. ^{13}C NMR spectrum of compound **6b** (150 MHz, $CDCl_3$)

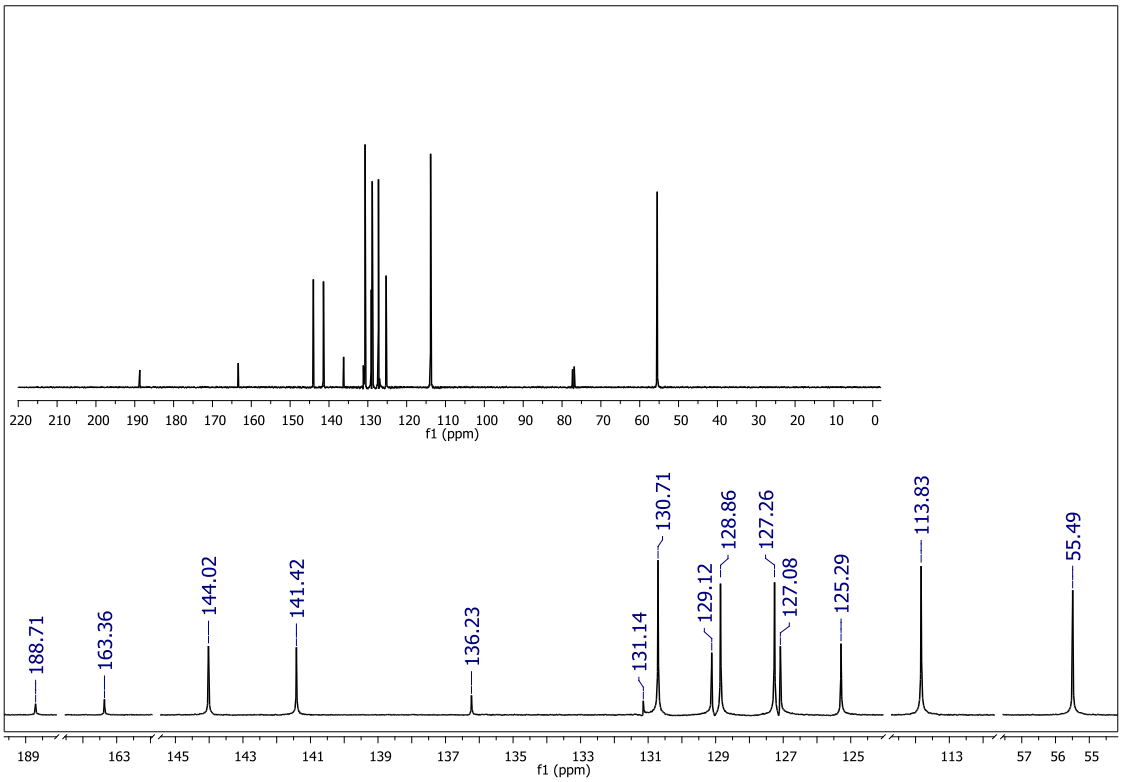

Capítulo III

6. Artigo Científico

Pro-apoptotic activity, inhibition of migration and invasion of 3'-hydroxychalcone (3HC) in human osteosarcoma cells are related with the induction of p53 and Hsp40 expression

Daiane Bertholin Anselmo [1], Letícia Ribeiro de Assis [1], Gabriel Silva [2], Viviane Seba [2], Ana Lúcia Fachin [2], Mozart Marins [2] and Luis Octavio Regasini [1,*]

[1] Laboratory of Antibiotics and Chemotherapeutics, Department of Chemistry and Environmental Sciences, Institute of Biosciences, Humanities and Exact Sciences, São Paulo State University (Unesp), São José do Rio Preto, SP 15054-000, Brazil; daiane_bertholin@hotmail.com (D.B.A); leticia-rda@hotmail.com (L.R.A.)

[2] Laboratory of Molecular Genetics and Bioinformatics, Biotecnology Unit, University of Ribeirão Preto (Unaerp), Ribeirão Preto, SP 14096-900, Brazil; biel-189@hotmail.com (G.S.); vivianeseba@gmail.com (V.S.); afachin@unaerp.br (A.L.F.)

***** Correspondence: luis.regasini@unesp.br (L.O.R.); mmarins@gmb.bio.br (M.M.); Tel.: +55-17-3221-2362 (L. O.R)

Abstract: Osteosarcoma (OS) is the most common and malignant bone cancer with high resistance to pharmacotherapy. In this study, we evaluated **3HC** (3'-hydroxychalcone) against human OS cells U2OS (p53 + / +) and Saos-2 (p53 - / -). Cell viability was measured by the MTT assay, with IC_{50} values of 22.4 μM and 45.0 μM, for U2OS and Saos-2, respectively, suggesting that the p53 protein may be its molecular target. Flow cytometric analysis indicated that this cell inhibition is related to the induction of death by apoptosis. The Western Blot assay demonstrated that **3HC** induced p53 and Hsp40 expression in a concentration-dependent manner in U2OS, this induction may contribute to p53 activity, important for apoptosis, since Hsp40 stabilizes the p53 protein conformation. Furthermore, **3HC** reduced migration, invasion and matrix metalloproteinase 2 (MMP-2) in U2OS of concentration-dependent manner, for wound healing assays, transwell and zymography, respectively. These results showed that **3HC** has anticancer activity, which may be associated with the expression

of genes involved in apoptosis, such as p53 and Hsp40, as well as its anti-migration, anti-invasion effect and reducing activity of MMP-2 in U2OS, suggesting that **3HC** represents an anticancer promise for the development of new chalcones for OS therapy.

Keywords: osteosarcoma; hydroxychalcone; p53; apoptosis; migration; invasion; matrix metalloproteinase 2

6.1. INTRODUCTION

Osteosarcoma (OS) is highly malignant and the most common bone cancer, which can develop anywhere in the bone structure. This cancer affects mainly children, adolescents and young adults, as well as, 60% of cases occur between 10 and 20 years-old and its incidence is higher in men than women (KANSARA et al., 2014). Current OS treatments include local surgery associated with cisplatin, doxorubicin, methotrexate and ifosfamide pharmacotherapy. Despite effective treatment, OS has a high predisposition for local invasion and metastasis. Consequently, this aggressiveness and invasiveness led to lack of treatment (JAFFE et al., 2013; INCA, 2019).

One of main therapeutic strategies for the OS treatment is the metastasis inhibition. However, due to drug resistance, the chances of success in treatment are low, which decreases the long-term survival rate to approximately 20–30%. Secondary neoplasia remains as the most important cause of OS death, mainly because the lung is the most common site and leads to death in one year (INCA, 2019; ANDERSON, 2016). Furthermore, side effects of chemotherapy include cardiotoxicity, nephrotoxicity, neurotoxicity and consequent secondary neoplasia, and these factors also affect desirable anti-cancer effects (ANDERSON, 2016). Thus, innovative antiproliferative drugs with reduced toxicity, anti-metastatic effects and more effective treatments to achieve the necessary target against this disease are needed.

The chalcones, flavonoids abundant in fruits, vegetables and plants (JANDIAL et al., 2014; MIRZAEI et al., 2016), have shown efficacy in the treatment of several diseases, such as: anti-diabetic, anti-inflammatory, antibacterial, antioxidants, antifungal, anti-*Leishmania*, antiproliferative, antimalarial, antiprotozoal and anti-HIV effects (MIRZAEI et al., 2016; SINGH et al., 2014). Some studies have shown its ability to inhibit OS cells mediated by

caspase-dependent apoptosis induction (SILVA et al., 2016), decrease migration, invasion, MMP-2 activity and regulate genes involved in epithelial-mesenchymal transition, as well as induce the p53 expression that may be related to anti-metastatic effects (SEBA et al., 2018).

In addition, several studies have reported that the structure of chalcone can be easily modified to enhance its biological action, such as by adding a wide variety of functional groups as aryls, halogens, hydroxyls, carboxylic groups, benzenes, etc (JANDIAL et al., 2014). In our previous work, we demonstrated that *trans*-chalcone inhibits the cell viability of OS cancer cells (U2OS). Thus, encouraged by our previous results, we investigated the anticancer effects and possible underlying molecular mechanisms in the effect of **3HC** on OS cells. This substance was selected based on its stability and higher activity against various tumor cells, presented in our previous results, in submission phase, in which we also reported that **3HC** (3'-hydroxychalcone - hybrid of curcumin and cinnamaldehyde) proved to be a stable compound under physiological conditions when compared to curcumin (antiproliferative agent) which was quickly degraded. In the present study, the results showed that **3HC** has activity against U2OS, which may be related to the expression of genes involved in apoptosis such as p53 and Hsp40. In addition, **3HC** also decreased cell migration and invasion accompanied by inhibition of MMP-2 in U2OS.

6.2. MATERIALS AND METHODS

6.2.1 Synthesis of 3'-Hydroxychalcone (**3HC**)

Reagent and solvents were purchased from Merck®. 3'-Hydroxychalcone (**3HC**) (Figure 1) was synthesized by Claisen-Schmidt aldol condensation reaction, according to protocol described by Marques and co-authors with minor modifications (MARQUES et al., 2019). Reaction was carried out at room temperature using 3.0 mmol of 3'-hydroxyacetophenone and 3.0 mmol of benzaldehyde, which were dissolved in ethanol (30 mL). Sodium hydroxide in ethanol (1.0 mol/L) was added as catalyst solution. Reagents conversion was checked by thin layer chromatography. Reaction medium was poured onto ice (from distilled and deionized water) and filtered. Crude product was purified over silica gel column with hexane and ethyl acetate (4:1) as mobile phase. Structure of **3HC** was confirmed by ^{1}H and ^{13}C Nuclear Magnetic Resonance (^{1}H and ^{13}C NMR) spectra analyses. Purity of

3HC was measured by High Performance Liquid Chromatography with Diode Array Detector (HPLC-DAD).

Figure 1. Structure of 3'-hydroxychalcone **(3HC)**

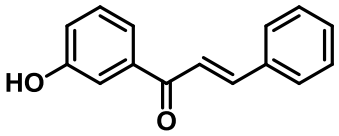

Source: author

6.2.2 Cell Culture

Human osteosarcoma cell lines U2OS (p53 wild) and Saos-2 (p53 null) and immortalized non-tumorigenic human keratinocyte cells (HaCaT - CLS 300493) were purchased from the Rio de Janeiro Cell Bank (BCRJ, Federal University of Rio de Janeiro, Rio de Janeiro, Brazil). U2OS and Saos-2 cells were grown in McCoy's 5A Medium (Sigma-Aldrich®) and HaCaT cells were grown in RPMI medium (Sigma-Aldrich®), supplemented with 10% fetal bovine serum (FBS), 100 U/mL penicillin, and 100 g/mL streptomycin (Sigma-Aldrich®). Cells were cultured at 37 °C under humidified atmosphere of 5% CO_2.

6.2.3 Cell Viability Assay

Cell viability was measured by the MTT [3-(4,5-dimethylthiazol-2-yl)-2,5-diphenyltetrazolium bromide] assay (Sigma-Aldrich®), using protocol described by Silva and co-authors (SILVA et al. 2018b) with minor modifications. This assay is based on the conversion from tetrazole-compound (yellow) to formazan crystals (purple), by the dehydrogenases of viable cells. Cells were seeded in 96-well plates at 1×10^4 cells/well. After overnight culture, cells were treated with 6, 11, 22, 45 and 89 µM/mL of **3HC** for 24 h, to obtain the IC_{50} value and use the concentrations needed for the next experiments. Curcumin was used as antiproliferative agent (6, 11, 22, 45 and 89 µM/mL) (MARQUES et al, 2019,

IQBAL et al., 2016; HSIEH et al., 2017) and doxorubicin (1, 2, 5, 9 and 18 µM/mL) (Sigma-Aldrich®) was used as reference antineoplastic drug. DMSO 0.1% was used as solvent for substances and vehicle control. After the treatment, the medium was replaced by fresh medium. 20 µL MTT of solution (5 mg/mL) was added to each well, and the plates were incubated for 3 h. Absorbance was measured spectrophotometrically at 550 nm by microplate reader (MultiSkan FC, Thermo Scientific, Waltham, MA, USA). Results were plotted as the percentage of cell viability inhibition (CVI) calculated as follows: CVI (%) = [1 - (absorbance of cells treated with compounds/absorbance of cells trated with DMSO 0.1%)] × 100. Data represent the average ± SD from three independent experiments combined. IC_{50} values were determined from non-linear regression using GraphPad Prism® (GraphPad Software, Inc., San Diego, CA, USA).

6.2.4 Apoptosis Assay

Apoptosis analysis was performed with double labeling (Annexin-V/propidium iodide), usingan FITC Annexin V Apoptosis Detection Kit I (BD Biosciences), according to the manufacturer's recommendations, with slight modifications. U2OS cells were cultured in 6-well plates (6.5×10^5 cells/well), then treated with IC_{50} concentration of **3HC** and curcumin (22.4 and 23.3 µM respectivelly) in a medium with 10% FBS for 24 h. After this treatment, adherent and floating cells were collected by centrifugation, washed with PBS, and resuspended in 300 µL of 1× binding buffer. Next, 5 µL of FITC Annexin V and 5 µL of propidium iodide were added and the cells were incubated at room temperature in the dark for 15 min. Finally, cells were analyzed using a BD FACS Calibur™ Flow Cytometer (BD Biosciences, San Jose, CA, USA). For the vehicle control 0.1% DMSO was used. Data represent the average ± SD from three independent experiments combined.

6.2.5 Wound-Healing Assay

A wound-healing assay was performed to analyze cell migration capacity according to the published protocols of literature (YUE et al., 2010) with minor modifications (SILVA et al., 2018b). Briefly, U2OS cells were grown in 24-wells plate until the cell monolayer reached

nearly 100% confluency, then a wound was created with a sterile 10 µL pipette tip. Floating cells were removed, followed by treatment with 5, 10, and 20 µM of **3HC** and curcumin for 24 h. The scratched areas were photographed in an optical microscope in time 0 and 24 h. The wound area was measured using ImageJ software (ImageJ2, National Institutes of Health, Bethesda, MD, USA). For the vehicle control 0.1% DMSO was used. Migration rates of **3HC** /curcumin group and DMSO group were calculated as follows: Migration rate (%) = [(wound area at 0 h - wound area at 24 h)/wound area at 0 h] ×100%. Data represent the average ± SD from three independent experiments combined.

6.2.6 Transwell Assay

A Transwell cell assay was used to analyze the effect of **3HC** on the invasion capacity of U2OS cells. The membrane of the Transwell plate with an 8 µm pore size (Corning, Corning, NY, USA) was pre-coated with 0.75 mm of Matrigel (Corning®) according to the manufacturer's instructions and then 2×10^5 cells resuspended in 200 µL serum-free medium were seeded into the upper chamber of plate. Into the lower chamber, 750 µL of complete medium (with 10% serum) containing the concentrations 5, 10, and 20 µM of **3HC** and curcumin was added. After treatment for 24 h, the cells that invaded and attached on the bottom side of the Transwell membrane were fixed with 3.7% of paraformaldehyde for 2 min, permeabilized with methanol 100%, and stained with Wright's Giemsa solution for 15 min at room temperature. The cells were destained with 100 µL of 33% acetic acid. The destaining solution was collected and the absorbance was measured at a wavelength of 490 nm by a microplate reader (MultiSkan FC). For the vehicle control 0.1% DMSO was used. The inhibition of invasion was calculated as follows: Inhibition (%) = [1 - (absorbance of treated group/absorbance of control group)] × 100. Data represent the average ± SD from three independent experiments (SILVA et al., 2018b).

6.2.7 Gelatin Zymography

Gelatin zymography was performed to quantify the matrix metalloproteinase-2 (MMP-2) activity. Briefly, U2OS cells were cultured in 6-well plates (5×10^5 cells/well) followed by

treatment with 5, 10 and 20 µM of **3HC** and curcumin for 24 h. After treatment, the supernatant (conditioned medium) for each sample was collected and then separated by 0.1% gelatin-7% SDS-PAGE electrophoresis. Next, the gels were washed in 2.5% Triton X-100 three times (30 min each) at room temperature and incubated in reaction buffer (10 mM $CaCl_2$, 40 mM Tris-HCl, and 0.01% NaN_3, pH 8.0) at 37 °C for 18 h. Gels were washed with distilled water, and stained with Coomassie brilliant blue R-250. After destaining steps, bands were digitally scanned, and the gelatinolytic activities were measured using ImageJ software (ImageJ2, National Institutes of Health, Bethesda, MD, USA). For the vehicle control 0.1% DMSO was used. Data represent the average ± SD from three independent experiments.

6.2.8 Western Blot

U2OS cells were cultured in 6-well plates (6.5×10^5 cells/well), followed by treatment with 5, 10, and 20 µM of **3HC** in serum-free medium for 24 h. Next, cells were harvested in RIPA buffer (Sigma-Aldrich®) supplemented with proteinase inhibitors and subjected to sonication (three times for 5 s each) and the cell lysate was centrifuged at 15.000 rpm for 15 min at 4 °C. The supernatant was collected, and the protein concentration was determined using the Pierce BCA Protein Assay Reagent (Thermo Scientific, Rockford, IL, USA). Amounts of total proteins (30 µg) were separated on 10% SDS-PAGE gel, and then transferred to AmershamTM ProtranTM 0.45-µm NC nitrocellulose membranes (GE Healthcare, Little Chalfont, UK). The membranes were blocked in Tris-buffered saline with Tween 20 (TBST) (25 mM Tris, 3mM KCI, 0.14 M NaCl, and 0.05% Tween 20), containing 5% nonfat milk, at room temperature for 1 h. Next, the membranes were incubated in TBST-5% nonfat milk, containing the primary p53, Hsp40/DNAJB1 and β-actin antibodies (1:1000) (Santa Cruz Biotechnology, Santa Cruz, CA) overnight at 4 °C. After washing with TBST, the membranes were incubated with horseradish peroxidase-conjugated secondary antibodies diluted in TBST-5% nonfat milk (1:10,000) for 1 h and washed several times. The proteins were detected by chemiluminescence, using the ECL Prime WB Detection Reagent (GE Healthcare) in an Image Quant LAS 500 luminescence analyzer (GE Healthcare). For the vehicle control 0.1% DMSO was used. The experiments were performed in three independent events.

6.2.9 Statistical Analisis

Statistical analysis was carried out using one-way ANOVA followed by Tukey test using the GraphPad Prism 7 (GraphPad Software, Inc., La Jolla, CA, USA). The results were considered statistically significant if $p< 0.05$, $p< 0.01$, $p< 0.001$ and $p< 0.0001$.

6.3. RESULTS AND DISCUSSION

6.3.1. **3HC** Inhibits Cell Viability of Osteosarcoma Cell Lines

We performed the MTT assay to determine the effect of **3HC** on cell viability of OS cell lines U2OS and Saos-2. Antiproliferative activity was expressed as IC_{50} values (concentration able to inhibit 50% of cell growth). Curcumin was used as antiproliferative agent (positive control) and doxorubicin was used as reference antineoplastic drug (Table 1).

Table 1. Antiproliferative activity of **3HC** against U2OS and Saos-2 cell lines expressed as IC_{5O} values (in µM[1])

Compounds	U2OS	Saos-2
3HC	22.4±1.3****	45.0±5.5****
curcumin	23.3±0.9****	35.6±2.8****
doxorubicin	4.0±1.3****	8.9±3.9****

[1] Mean value ± standard deviation from three independent experiments (IC_{50}= concentration able to inhibit 50% of cell growth). Values obtained by MTT assay after 24 h. U2OS = osteosarcoma (p53 wild); Saos-2 = osteosarcoma (p53 null).
**** p<0.0001 (treatment of U2OS vs. Saos-2).

Source: author

3HC reduced the viability of OS cell lines U2OS and Saos-2, with IC_{50} values of 22.4 ± 1.3 and 45.0 ± 5.5 µM, respectively. The higher activity of **3HC** against U2OS, with significant statistical difference (p<0.0001 vs. SAOS-2), indicates that the presence of p53

protein may be related to inhibition of cell. In addition, we suggest that the presence of Michael acceptor in structure could contribute to its action, because this moiety is very common in other compounds that exhibit antitumor activity (WANG et al., 2018). Interestingly, other study reported that cell growth was significantly suppressed by the treatment of 10 µM *trans*-chalcone with 24%, 58%, and 90% inhibition on day 1, 2 and 4, respectively, against U2OS cells (SILVA et al., 2016). Silva and co-authors described that after 24 h of treatment at the 10 µM concentration of 2'-hydroxy-5'-fluoride chalcone there was an inhibition of about 60% of U2OS cells (SILVA et al., 2018). On the other hand, 4'-amino-1'-naphthyl-chalcone and 4'-amino-4'-methyl-1'-naphthyl-chalcone showed a low capacity to inhibit the viability of OS cells (U2OS and Saos-2) (<30% inhibition) (SEBA et al., 2018).

Curcumin also showed higher activity against U2OS with IC_{50} values of 23.3 ± 0.9 and 35.6 ± 2.8 µM in U2OS and Saos-2 cells, respectively ($p<0.0001$), indicating that **3HC** and curcumin have similar effects against both cells, however curcumin has low bioavailability, limiting its use as a therapeutic agent (NELSON et al., 2017).

3HC showed moderate inhibition of cell viability of the OS cells when compared with doxorubicin which exhibited IC_{50} values of 4.0±1.3 and 8.9±3.9 µM, respectively ($p<0.0001$). Despite the lower activity, **3HC** is a promising substance based on the structure of natural products, since doxorubicin has several severe adverse effects including cardiotoxicity, nephrotoxicity, neurotoxicity, hepatotoxicity, affect the female reproductive system, causes skin problems, induction of secondary neoplasia and long-term may be related to atherosclerosis (PUGAZHENDHI et al., 2018). Finally, we evaluated the action of **3HC**, curcumin and doxorubicin against the immortalized non-tumor human keratinocyte cells (HaCaT), in which IC_{50} values were 23.0 ± 3.9, 7.6 ± 2.1 and 12.3 ± 2.1 µM respectively, showing that **3HC** less cytotoxic to HaCaT when compared to curcumin, however doxorubicin (a potent cytotoxic drug) showed a higher selectivity.

6.3.2. Inhibition of Cell Viability by **3HC** Results in Induction of Apoptosis

The main cell death pathways are apoptosis and necrosis (GRILO et al., 2019). However, apoptosis is an essential mechanism for the elimination of damaged, excess or

cancerous cells. Their deregulation often contributes to the development of cancer and resistance to therapy (KOFF et al., 2015).

In order to verify whether the reduction of U2OS cell viability was correlated to the induction of apoptosis, we performed Annexin V-FITC/PI double staining using flow cytometry. In conformity with the inhibition of cell viability, the **3HC** induced 30% of apoptosis in U2OS cells after 24 h of exposure to IC_{50} concentration **3HC**, with significant statistical difference ($p< 0.01$ vs. control) about five times more than the control, treated with DMSO (Figure 2). Cells treated with IC_{50} concentration of curcumin also induced apoptosis in 50% ($p< 0.001$ vs. control), in which there was a greater induction of apoptosis by curcumin than the **3HC** ($p< 0.01$ vs. curcumin). Furthermore, the number of necrotic cells was low, with values of 4% and 2% for **3HC** and curcumin, respectively. The data indicated that **3HC** has a cell viability reducing effect on OS cells mediated at least in part by apoptosis induction. We believe that 20% of cell death may have occurred due to other effects such as cell cycle arrest, because as some studies show, chalcones have other targets that also disrupt cell cycle progression and subsequent apoptotic signal (JANDIAL et al., 2014). These results were similar to other investigations, which after treatment with chalcones also showed induction of apoptosis in cervical cancer (HeLa) (MARKOVIC et al., 2015), breast cancer (MCF-7 and MDA-MB-231) (BORTOLOTTO et al., 2017; SANTOS et al., 2019), colorectal (HT-29) (MAI et al., 2014) hepatic (HepG2), lung (H460) (DONG et al., 2018) and OS (U2OS) cells (SILVA et al., 2016). Another study by Silva and co-authors reported that 2'-hydroxy-5'-fluoride chalcone showed higher apoptotic activity than *trans*-chalcone against U2OS cells (SILVA et al., 2018). On the other hand, 4'-amino-1'-naphthyl-chalcone and 4'-amino-4'-methyl-1'-naphthyl-chalcone did not induce apoptosis in OS cells (SEBA et al., 2018).

Figure 2. Analysis of apoptosis and necrosis induction in U2OS cells treated with DMSO (0.1%), **3HC** and curcumin at the IC_{50} concentrations (22.4 and 23.3 µM respectivelly) for 24 h.

The rate of apoptotic and necrotic cells was assessed by double staining flow cytometry assay with Annexin–FITC and PI. The data are expressed as mean values ± SD of three independent experiments. Different letters represent statistical differences ($p< 0.05$).

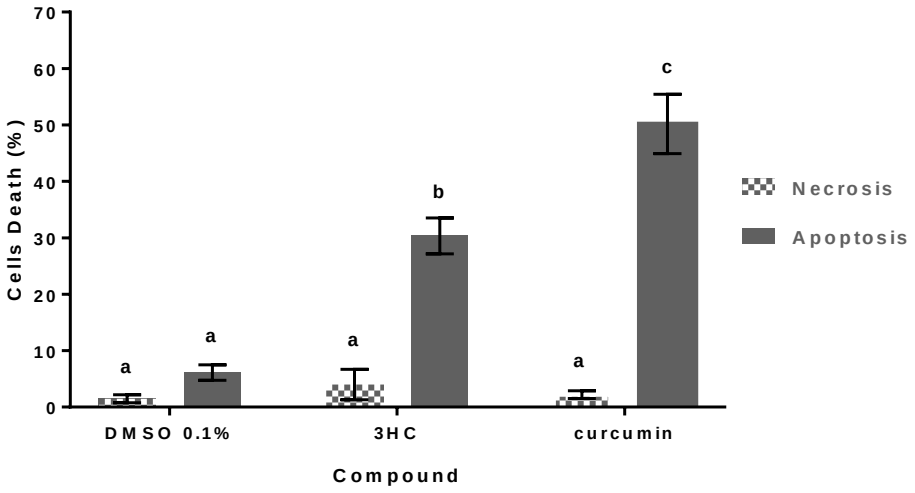

Source: author

6.3.3. **3HC** Decreases U2OS Cell Migration and Invasion

Metastasis is responsible for about 90% of cancer deaths. It is characterized by ability of cancer cells to migrate and invade tissues, causing the proliferation of cancer to other organs (SEYFRIED et al., 2013). These aspects are characteristic of tumor malignancy, mainly in the OS where the main causes of deaths are due to metastasis. In this way, inhibition of metastasis is one of main strategies of therapy of OS (ANDERSON et al., 2016), however one of great problems for success of its treatment is resistance to the drugs (LI et al., 2015). Thus, we evaluated the effect of **3HC** and curcumin on U2OS cell migration and

invasion using a wound-healing assay and a Transwell assay. U2OS cells were treated for 24 h with 5, 10 and 20 µM of **3HC** and curcumin. The choice of concentrations was performed according to data reported in literature, to verify the difference in the result by concentration-response with to the rounded value of the IC_{50} (SILVA et al., 2018b; LIMA et al., 2018). The wound-healing assay showed that **3HC** significantly inhibited ($p< 0.0001$ vs. control) wound closure in a concentration-dependent manner, with inhibition of 53% and 64% at 10 and 20 µM, respectively (Figure 3 a-b). Curcumin also inhibited migration in a concentration-dependent manner, of 31% and 51% at 10 and 20 µM, respectively. This data show with **3HC** exhibited higher potency of inhibition than curcumin, presenting significant difference in the concentration of 10 µM ($p< 0.05$ vs. curcumin). To evaluate the effect of **3HC** and curcumin on cell invasive capacity, we used Transwell coated with Matrigel, as shown in Figure 3 c-d; a number of U2OS cells that had invaded the Matrigel was significantly decreased (43%) by **3HC** at 20 µM ($p< 0.0001$ vs. control). Curcumin also showed similar results to **3HC** in inhibition the invasion of U2OS cells (showing no significant differences at any of the concentrations $p> 0.05$). These results suggest that **3HC** possesses an anti-migratory and anti-invasive effect in U2OS cells. Interestingly, others investigations have shown that chalcones suppressed migration and invasion of tumor cells, such as lung (H460) and liver (HepG2) (DONG et al., 2018). Studies by Seba and co-authors with OS tumor cells (U2OS) showed that 4'-amino-1'-naphthyl-chalcone and 4'-amino-4'-methyl-1'-naphthyl-chalcone markedly decreased the migration and invasion of the U2OS cells by more than 70% (SEBA et al., 2018).

Figure 3. 3HC inhibited cell migration and invasion in U2OS cells.

(**a-b**) The effect of **3HC** and curcumin on U2OS cell migration was evaluated by a wound healing assay. U2OS cells were scratched and treated with 5, 10, and 20 µM of **3HC** and curcumin for 0 and 24 h. The migration was observed under a phase-contrast microscope at a magnification of 40×. Migration inhibition (%) after treatment with **3HC** and curcumin was calculated and quantitative results are illustrated in the graphs; (**c-d**) For the invasion assay, the Transwell membrane was pre-coated with Matrigel, following which the cells were plated and treated as described above. Invasion Inhibition (%) was calculated and quantitative results are illustrated in the graphs. In all experiments, the data represent the mean ± SD of three independent experiments. Different letters represent statistical differences ($p< 0.05$).

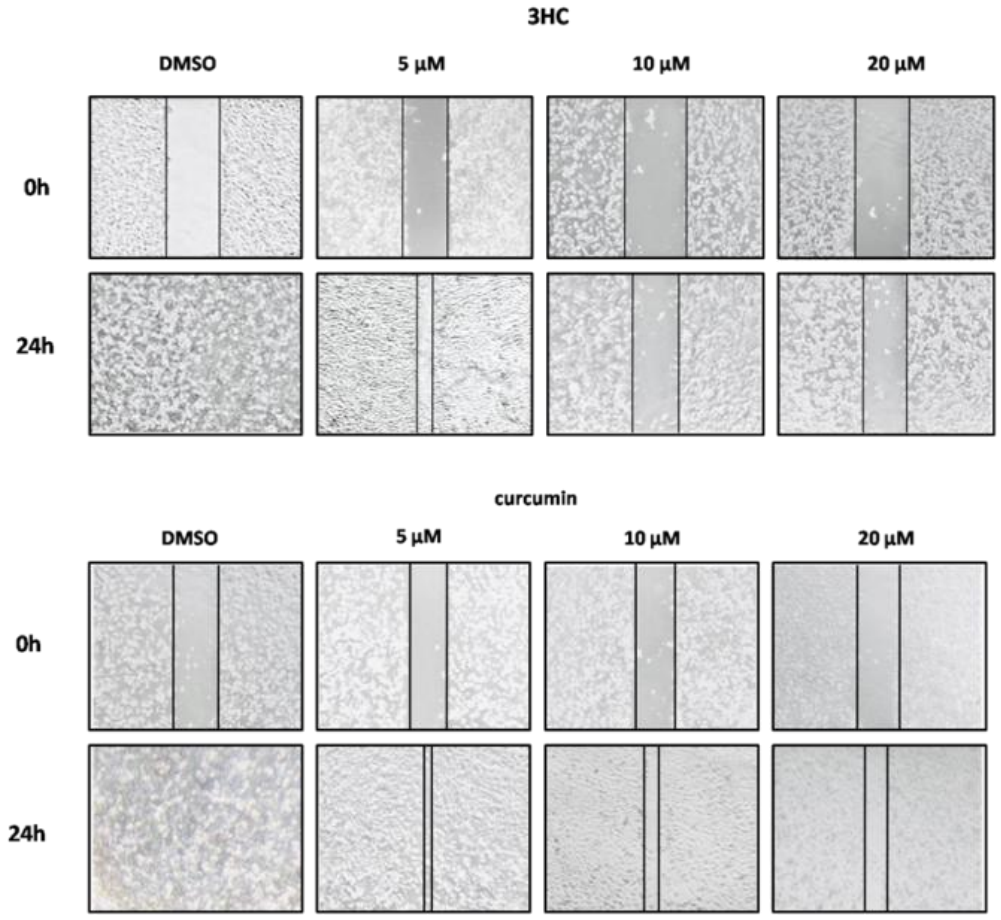
3HC
DMSO
5 µM
10 µM
20 µM
0h
24h
curcumin
DMSO
5 µM
10 µM
20 µM
0h
24h

(a)

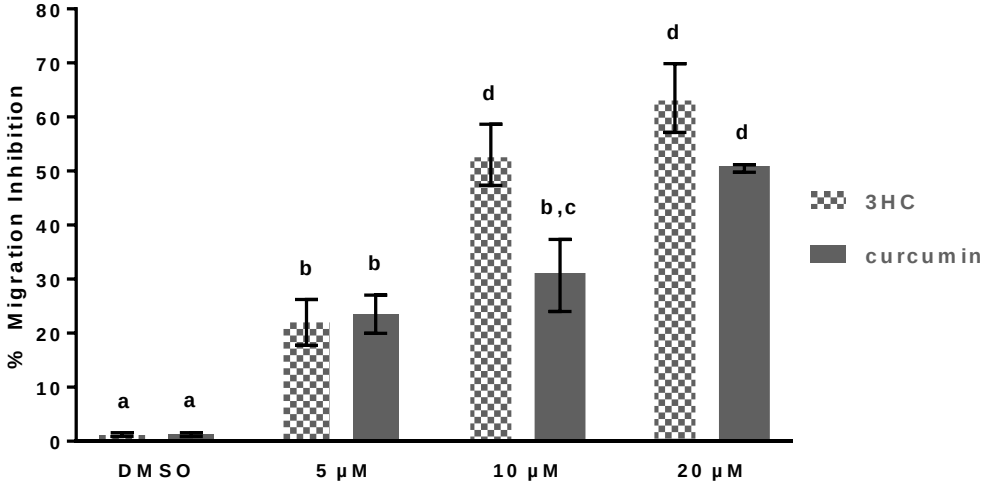
% Migration Inhibition
80
70
60
50
40
30
20
10
0
a
a
b
b
d
b,c
d
d
DMSO
5 µM
10 µM
20 µM
3HC
curcumin

(b)

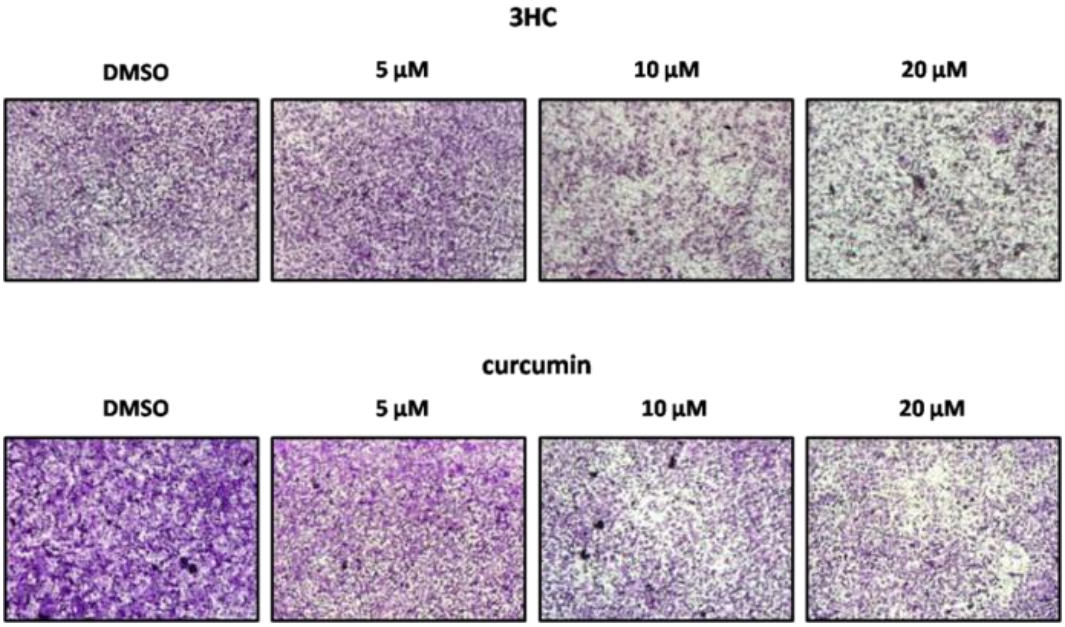
3HC
DMSO
5 µM
10 µM
20 µM
curcumin
DMSO
5 µM
10 µM
20 µM

(c)

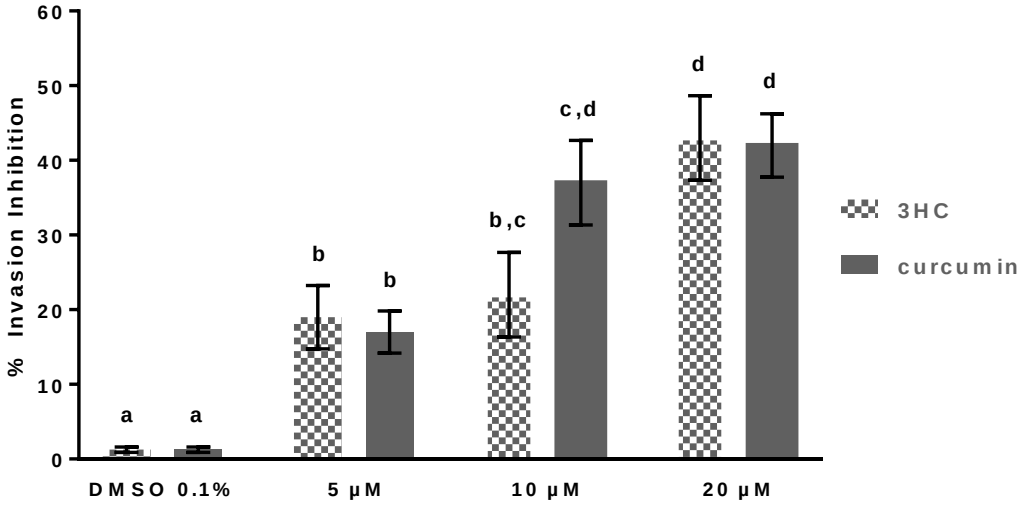
% Invasion Inhibition
60
50
40
30
20
10
0
a
a
b
b
b,c
c,d
d
d
DMSO 0.1%
5 µM
10 µM
20 µM
3HC
curcumin

(d)

Source: author

6.3.4. **3HC** Reduces Activity of MMP-2 in U2OS Cell

MMP-2 is one of main matrix metalloproteinases (MMPs), its over expression is involved in the process of tumor cell migration, invasion and metastasis by degrading the extracellular matrix (PITTAYAPRUEK et al., 2016). Several studies have reported the involvement of MMP-2 in the migration and invasion of OS cells (BJORNLAND et al., 2005; JIN et al., 2013; LEI et al., 2015), associated with lung metastasis and lower overall survival of these patients (LI et al., 2014). Based on this, we examined by gelatin zymography analysis whether the reduction of migration and invasion were accompanied by a decrease in the activity of metalloproteinase 2. U2OS cells were treated for 24 h with 5, 10 and 20 μM of **3HC** and curcumin, and then the activity of MMP-2 was assessed. There was a reduction in the MMP-2 collagenase activity in **3HC**-treated U2OS cells compared to control cells, in a concentration-dependent manner with a significant ($p < 0.0001$ vs. control) remarkable effect at 20 μM (fold—9.5) (Figure 4 a-b). Curcumin also reduced MMP-2 activity in a concentration-dependent manner, fold—6.1 compared to the control in 20 μM. However, **3HC** exhibited higher potency in reducing MMP-2 than curcumin at a concentration of 10 μM ($p < 0.05$ vs. curcumin), but at concentration 20 μM there was no significant difference ($p > 0.05$ vs. curcumin). These results together with those previously investigated indicate that anti-migration and anti-invasion effect of **3HC** is confirmed, at least in part, by reduction of MMP-2 secretion. This relationship was also observed in other study in which they evaluated the effect of the 4'-amino-1'-naphthyl-chalcone and 4'-amino-4'-methyl-1'-naphthyl-chalcone in OS cell (U2OS). In addition, they showed that these chalcones decreased the activities of MMP-2 by gelatin zymography and significantly reduced mRNA expression of MMP-2 (SEBA et al., 2018). Silva and co-authors also showed that the MMP-2 transcript was downregulated after *trans*-chalcone treatment in OS cells (U2OS) (SILVA et al., 2016).

Figure 4. 3HC decrease activity of MMP-2 in U2OS cells.

(**a-b**) U2OS cells were treated with **3HC** and curcumin (5, 10 and 20 µM) for 24 h and then the activity of secreted MMP-2 was measured by gelatin zymography assay. A demonstrative gel and quantitative results (graphic) are presented. In all experiments, the data represent the mean ± SD of three independent experiments. Different letters represent statistical differences ($p < 0.05$).

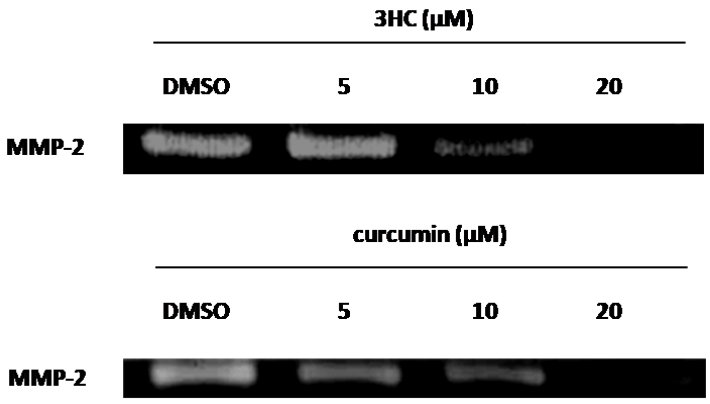

(a)

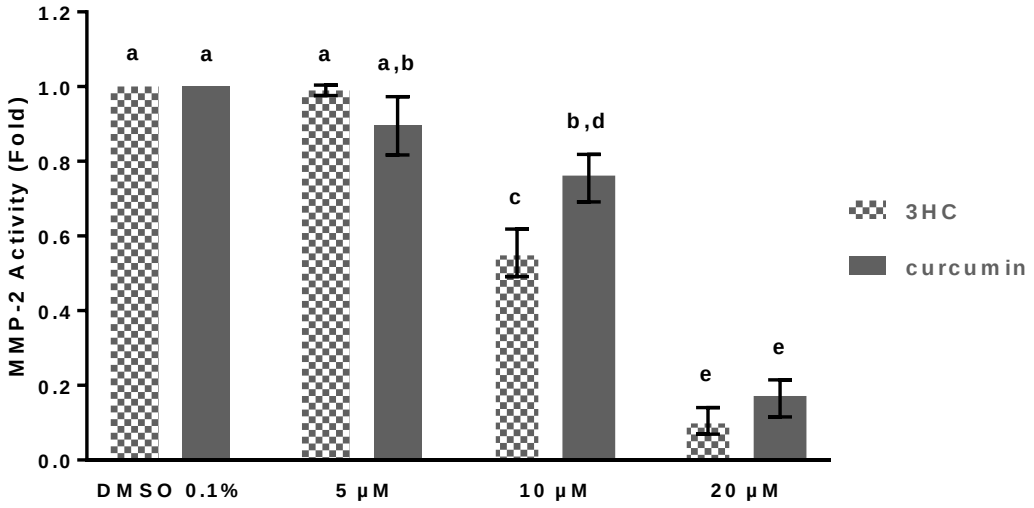

(b)

Source: author

6.3.5. **3HC** Increases p53 and DNAJB1/Hsp40 Protein Levels in U2OS Cell

The p53 protein regulates several biological functions such as DNA damage repair, controls proliferation, migration, invasion and causes induction of apoptosis. Thus, p53 expression is essential due to their antitumor properties (NIAZI et al., 2018; YAMADA et al., 2019). It is already established that the inactivation of p53 has a great relation with OS and consequent lung metastasis (LIU et al., 2000; LIU et al., 2017). It was also identified that Hsp40 binds to p53 regulating their conformation and stability (HIRAKI et al., 2015; SILVA et al., 2018). To further investigate the underlying molecular mechanisms of **3HC**-mediated anticancer activities, the expression level of p53 and DNAJB1/Hsp40 proteins were examined in U2OS cells treated with **3HC**, using Western blotting analysis. The p53 and DNAJB1/Hsp40 proteins were expressed following **3HC** treatment, in which p53 was higher expressed in a concentration dependent manner with a significant ($p < 0.0001$ vs. control) (Figure 5 a-b). Others investigations also reported p53 expression in OS (U2OS), lung (A549) oral (FaDu), colorectal (HCT-116) and breast (MCF-7) cancer cell lines after treatment with chalcones (SILVA et al., 2016; IFTIKHAR et al., 2017; SEBA et al., 2018; SANTOS et al., 2019). Furthermore, these results indicating the possible participation of Hsp40 in p53 stabilization, which consequently contributes to its activity, which is very important for the mechanisms of induction of apoptosis. Studies performed by Silva and co-authors showed that after treatment of U2OS with the *trans*-chalcone, the Hsp40 and p53 proteins were also highly expressed, however, the silencing of Hsp40 partially blocked p53 upregulation induced by *trans*-chalcone, suggesting that Hsp40 contributed to p53 stability. Curiously this same study showed that 4'-hydroxy chalcone was also able to induce DNAJB1/Hsp40 protein. In addition, the authors also reported that chalcones with other substituents (2'-hydroxy-5'-fluoride chalcone, 4'-amine-4'-fluoride chalcone, 4'-amino-4'-chlorine chalcone and 6'-amino-4'-methyl chalcone) also induced p53 expression (SILVA et al., 2018). Thus, **3HC**-mediated p53 expression may also be correlated with inhibition of cell viability, induction of apoptosis, reduction of migration, and invasion of U2OS cells, as presented by results of this study.

Figure 5. 3HC increases the expression of p53, and DNAJB1 proteins in U2OS cells.

(**a-b**) The cells were grown in 6-well plates and then were incubated with **3HC** at the indicated concentrations for 24 h. After treatment, cell lysates (30 µg of total protein) were obtained and examined by Western blot analysis. A demonstrative gel (a) and quantitative results (b) are presented. In all experiments, the data represent the mean ± SD of three independent experiments. Different letters represent statistical differences ($p < 0.05$).

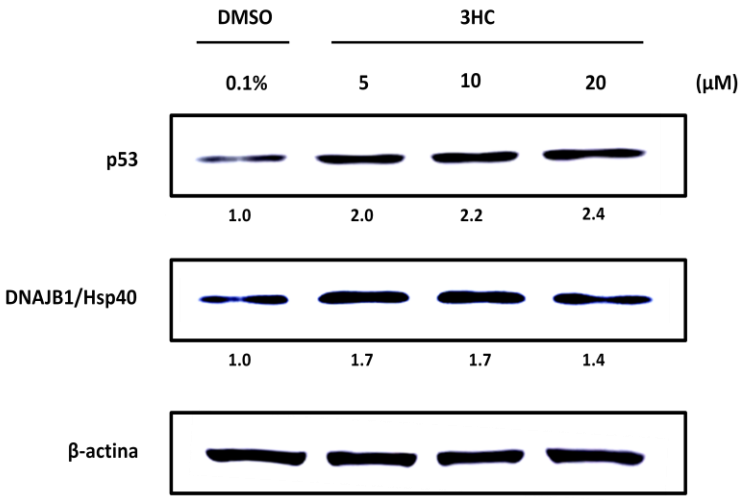

(a)

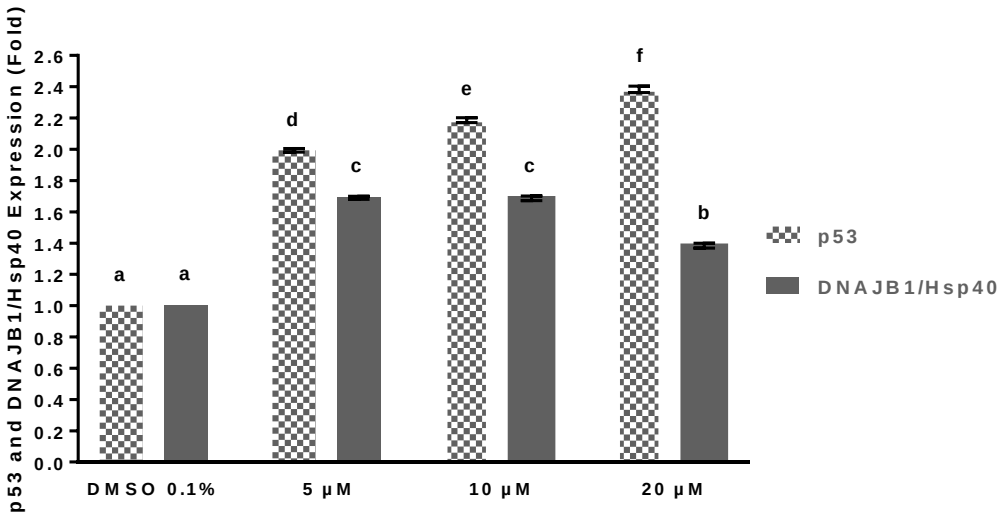

(b)

Source: author

6.4. CONCLUSIONS

In conclusion, we evaluated effects of **3HC** as part of continuous search for antitumor compounds based on chalcones structure. **3HC** was found to be an important hit with activity against OS cells, in which, its mode of action may be associated with the higher expression of apoptosis-involved genes such as p53 and Hsp40, which is an important target for the development of novel anticancer agents. Furthermore, **3HC** showed anti-migration, anti-invasion effect and reduced activity of matrix metalloproteinase 2 in U2OS. In addition to all these activities presented, **3HC** is very interesting for future *in vivo* trials, as **3HC** is a stable substance under physiological conditions, unlike curcumin. Altogether, our results corroborate the potential of chalconic skeleton as a privileged framework for the discovery of new chalcones for OS therapy.

6.5. ACKNOWLEDGEMENTS

The authors thank UNESP (São Paulo State University - São José do Rio Preto Campus; UNAERP (University of Ribeirão Preto) and USP (University of São Paulo - Ribeirão Preto Campus) for all support and infrastructure.

This research was funded by Coordination for Improvement of Higher Education Personnel (CAPES, Coordenação de Aperfeiçoamento de Pessoal de Nível Superior, Finance Code 001); Brazilian Council for Scientific and Technological Development (CNPq, Conselho Nacional de Desenvolvimento Científico e Tecnológico, Grants #471129/2013-5, 306251/2016-7 and 429322/2018-6); São Paulo Research Foundation (FAPESP, Fundação de Amparo à Pesquisa do Estado de São Paulo, Grants # 2014/18330-0 and 2018/15083-2). D.B.A. was funded by CAPES (finance code 001). All authors thank Center of Biomolecular Innovation (FAPESP Grant # 2009/53989-4), National Institute of Science and Technology – Biodiversity and Natural Products INCT-BioNat (Grants FAPESP # 2014/50926-0 and CNPq # 465637/2014-0).

6.6. REFERENCES

Anderson, M.E. Update on survival in osteosarcoma. *Orthop. Clin. North Am.* **2016**, *47*, 283-292. [doi: 10.1016/j.ocl.2015.08.022]

Bjornland, K.; Flatmark, K.; Pettersen, S.; Aaasen, A.O.; Fodstad, O.; Maelandsmo, G.M. Matrix metalloproteinases participate in osteosarcoma invasion. *J. Surg. Res*. **2005**, *127*, 151–156. [doi: 10.1016/j.jss.2004.12.016]

Bortolotto, L.F.B.; Barbosa, F.R.; Silva, G.; Bitencourt, T.A.; Beleboni, R.O.; Baek, S.J.; Marins, M.; Fachin, A.L. Cytotoxicity of *trans*-chalcone and licochalcone A against breast cancer cells is due to apoptosis induction and cell cycle arrest. Biomed. Pharmacother. **2017**, *85*, 425–433. [doi: 10.1016/j.biopha.2016.11.047]

Dong, N.; Liu, X.; Zhao, T.; Wang, L.; Li, H.; Zhang, S.; Li, X.; Bai, X.; Zhang, Y.; Yang, B. Apoptosis-inducing effects and growth inhibitory of a novel chalcone, in human hepatic cancer cells and lung cancer cells. *Biomed. Pharmacother*. **2018**, *105*, 195-203. [doi: 10.1016/j.biopha.2018.05.126]

Grilo, A.; Mantalaris, A. Apoptosis: A mammalian cell bioprocessing perspective. *Biotechnol. Adv*. **2019**, *37*, 459-475. [doi: 10.1016/j.biotechadv.2019.02.012]

Hiraki, M.; Hwang, S.; Cao, S.; Ramadhar, T.R.; Byun, S.; Yoon, K.W.; Lee, J.H.; Chu, K.; Gurkar, A.U.; Kolev, V.; Zhang, J.; Namba, T.; Murphy, M.E.; Newman, D.J.; Mandinova, A.; Clardy, J.; Lee, S.W. Small-molecule reactivation of mutant p53 to wild-type-like p53 through the p53-Hsp40 regulatory axis. *Chem. Biol*. **2015**, *22*, 1206–1216. [doi: 10.1016/j.chembiol.2015.07.016]

Hsieh, M.; Chang, L.; Hung, H.; Lin, H.; Shih, M.; Tsai, C.; Kuo, S.; Lee, K. New bis (hydroxymethyl) alkanoate curcuminoid derivatives exhibit activity against triple-negative breast cancer *in vitro* and *in vivo*. *Eur. J. Med. Chem*. **2017**, *131*, 141–151. [doi: 10.1016/j.ejmech.2017.03.006]

Iftikhar, S., Khan, S., Bilal, A., Manzoor, S., Abdullah, M., Emwas, A.H., Sioud, S.; Gao, X.; Chotana, G.A.; Faisal, A.; Saleem, R.S.Z. Synthesis and evaluation of modified chalcone based p53 stabilizing agents. *Bioorg. Med. Chem. Lett*. **2017**, *27*, 4101-4106. [doi: 10.1016/j.bmcl.2017.07.042]

INCA - Instituto Nacional de Câncer José Alencar Gomes da Silva. Tipos de câncer - Osteossarcoma - versão para profissionais de saúde. Available online: https://www.inca.gov.br/tipos-de-cancer/cancer-infantojuvenil/osteossarcoma/profissional-de-saude (accessed on 27 December 2019).

Iqbal, B.; Ghildiyal, A.; Sahabjada; Singh, S.; Arshad, M.; Mahdi, A.A.; Tiwari, S. Antiproliferative and apoptotic effect of curcumin and TRAIL (TNF related apoptosis inducing ligand) in chronic myeloid leukaemic cells. *J. Clin. Diagn. Res*. **2016**, *10*, XC01-XC05. [doi: 10.7860/JCDR/2016/18507.7579]

Jaffe, N.; Puri, A.; Gelderblom, H. Osteosarcoma: evolution of treatment paradigms. *Sarcoma* **2013**, *2013*, 1-7. [doi.org/10.1155/2013/203531]

Jandial, D.D.; Blair, C.A.; Zhang, S.; Krill, L.S.; Zhang, Y.; Zi, X. Molecular targeted approaches to cancer therapy and prevention using chalcones. *Curr. Cancer Drug Targets* **2014**, *14*, 181–200. [doi: 10.2174/1568009614666140122160515]

Jin, J.; Cai, L.; Liu, Z.M.; Zhou, X.S. miRNA-218 inhibits osteosarcoma cell migration and invasion bydown-regulating of TIAM1, MMP2 and MMP9. *Asian Pac. J. Cancer Prev*. **2013**, *14*, 3681–3684. [doi: 10.7314/apjcp.2013.14.6.3681]

Kansara, M.; Teng, M.W.; Smyth, M.J.; Thomas, D.M. Translational biology of osteosarcoma. *Nat. Rev. Cancer* **2014**, *14*, 722-735. [doi: 10.1038/nrc3838]

Koff, J.L.; Ramachandiran, S.; Bernal-Mizrachi, L. A time to kill: targeting apoptosis in cancer. *Int. J. Mol. Sci*. **2015**, *16*, 2942-2955. [doi: 10.3390/ijms16022942]

Lei, P.; He, H.; Hu, Y.; Liao, Z. Small interfering RNA-induced silencing of galectin-3 inhibits the malignantphenotypes of osteosarcoma *in vitro*. *Mol. Med. Rep*. **2015**, *12*, 6316–6322. [doi: 10.3892/mmr.2015.4165]

Li, H.; Zhang, K.; Liu, L.H.; Ouyang, Y.; Bu, J.; Guo, H.B.; Xiao, T. A systematic review of matrix metalloproteinase 9 as a biomarker of survival in patients with osteosarcoma. *Tumour Biol.* **2014**, *35*, 5487–5491. [doi: 10.1007/s13277-014-1717-3]

Li, S.; Sun,W.; Wang, H.; Zuo, D.; Hua, Y.; Cai, Z. Research progress on the multidrug resistance mechanismsof osteosarcoma chemotherapy and reversal. *Tumor Biol*. **2015**, *36*, 1329–1338. [doi: 10.1007/s13277-015-3181-0]

Lima, F.T.; Seba, V.; Silva, G.; Torrezan, G.S.; Polaquini, C.R.; Pinhanelli, V.C.; Baek, S.J.; Fachin, A.L.; Regasini, L.O.; Marins, M. The curcumin analog CH-5 exerts anticancer effects in human osteosarcoma cells via modulation of transcription factors p53/sp1. *Int. J. Mol. Sci*. **2018**, *19*, e1909. [doi: 10.3390/ijms19071909]

Liu, G.; McDonnell, T.J.; Luna, R.M.O.; Kapoor, M.; Mims, B.; El-Naggar, A.K.; Lozano, G. High metastatic potential in mice inheriting a targeted p53 missense mutation. *Proc. Natl. Acad. Sci. USA* **2000**, *97*,4174–4179. [doi: 10.1073/pnas.97.8.4174]

Liu, D.D.; Kang, Y. Ets2 anchors the prometastatic function of mutant p53 in osteosarcoma. *Genes Dev*. **2017**, *31*, 1823–1824. [doi: 10.1101/gad.307439.117]

Mai, C.W.; Yaeghoobi, M.; Abd-Rahman, N.; Kang, Y.B.; Pichika, M.R. Chalcones with electron-withdrawing and electron-donating substituents: anticancer activity against TRAIL resistant cancer cells, structure–activity relationship analysis and regulation of apoptotic proteins. *Eur. J. Med. Chem.* **2014**, *77*, 378-387. [doi: 10.1016/j.ejmech.2014.03.002]

Markovic, V.; Debeljak, N.; Stanojkovic, T.; Kolundzija, B.; Sladic, D.; Vujcic, M.; Janovic, B.; Tanic, N.; Perovic, M.; Tesic, V.; Antic, J.; Joksovic, M.D. Anthraquinone–chalcone hybrids: synthesis, preliminary antiproliferative evaluation and DNA-interaction studies. *Eur. J. Med. Chem.* **2015**, *89*, 401-410. [doi: 10.1016/j.ejmech.2014.10.055]

Marques, B.C.; Santos, M.B.; Anselmo, D.B.; Monteiro, D.A.; Gomes, E.; Saiki, M.F.C.; Rahal, P.; Rosalen, P.L.; Sardi, J.C.O.; Regasini, L.O. Methoxychalcones: effect of methoxyl group toward antifungal, antibacterial and antiproliferative activities. *Med. Chem.* **2019**, 15, 1. [doi: 10.2174/1573406415666190724145158]

Mirzaei, H.; Emami, S. Recent advances of cytotoxic chalconoids targeting tubulin polymerization: Synthesis and biological activity. *Eur. J. Med. Chem*. **2016**, *121*, 610–639. [doi: 10.1016/j.ejmech.2016.05.067]

Nelson, K. M.; Dahlin, J. L.; Bisson, J.; Graham, J.; Pauli, G.F.; Walters, M.A. The essential medicinal chemistry of curcumin: miniperspective. *J. Med. Chem.* **2017**, *60*, 1620-1637. [doi: 10.1021/acs.jmedchem.6b00975]

Niazi, S.; Purohit, M.; Niazi, J.H. Role of p53 circuitry in tumorigenesis: A brief review. *Eur. J. Med. Chem*. **2018**, *158*, 7-24. [doi: 10.1016/j.ejmech.2018.08.099]

Pittayapruek, P.; Meephansan, J.; Prapapan, O.; Komine, M.; Ohtsuki, M. Role of matrix metalloproteinases in photoaging and photocarcinogenesis. *Int. J. Mol. Sci*. **2016**, *17*, 868. [doi: 10.3390/ijms17060868]

Pugazhendhi, A.; Edison, T.N.J.I.; Velmurugan, B.K.; Jacob, J.A.; Karuppusamy, I. Toxicity of Doxorubicin (Dox) to different experimental organ systems. *Life sciences* **2018**, *200*, 26-30. [doi: 10.1016/j.lfs.2018.03.023]

Santos, M.B.; Anselmo, D.B.; Oliveira, J.G.; Jardim-Perassi, B.V.; Monteiro, D.A.; Silva, G.; Gomes, E.; Fachin, A.L.; Marins, M.; Zuccari, D.A.P.C.; Regasini, L.O. Antiproliferative activity and p53 upregulation effects of chalcones on human breast cancer cells. *J. Enzyme Inhib. Med. Chem*. **2019**, *34*, 1093–1099. [doi: 10.1080/14756366.2019.1615485]

Seba, V.; Silva, G.; Santos, M.B.; Baek, S.J.; França, S.C.; Fachin, A.L.; Regasini, L.O.; Marins, M. Chalcone derivatives 4'-amino-1-naphthyl-chalcone (D14) and 4'-amino-4-methyl-1-naphthyl-chalcone (D15) suppress migration and invasion of osteosarcoma cells mediated by p53 regulating EMT-related genes. *Int. J. Mol. Sci*. **2018**, *19*, 2838. [doi: 10.3390/ijms19092838]

Seyfried, T.N.; Huysentruyt, L.C. On the origin of cancer metastasis. *Crit. Rev. Oncog*. **2013**, *18*, 43-73. [doi: 10.1615/critrevoncog.v18.i1-2.40]

Silva, G.; Marins, M.; Fachin, A.L.; Lee, S.; Baek, S.J. Anti-cancer activity of *trans*-chalcone in osteosarcoma: involvement of sp1 and p53. *Mol. Carcinog.* **2016**, *55*, 1438–1448. [doi: 10.1002/mc.22386]

Silva, G.; Marins, M.; Chaichanasak, N.; Yoon, Y.; Fachin, A.L.; Pinhanelli, V.C.; Regasini, L.O.; Santos, M.B.; Ayusso, G.M.; Marques, B.C.; Wu, W.W.; Phue, J.; Shen, R.; Baek, S.J. *Trans*-chalcone increases p53 activity via DNAJB1/HSP40 induction and CRM1 inhibition. *PLoS ONE* **2018**, *13*, e0202263. [doi: doi.org/10.1371/journal.pone.0202263]

Silva, G.; Lima, F.T.; Seba, V.; Lourenço, A.L. M.; Lucas, T.G.; Andrade, B.V.; Torrezan, G.S.; Polaquini, C.R.; Garcia, M.E.; Couto, L.B.; Bestetti, R.B.; França, S.C.; Fachin, A.L.; Regasini, L.O.; Marins, M. Curcumin analog CH-5 suppresses the proliferation, migration, and invasion of the human gastric cancer cell line HGC-27. *Molecules* **2018b**, *23*, e279. [doi: 10.3390/molecules23020279]

Singh, P.; Anand, A.; Kumar, V. Recent developments in biological activities of chalcones: A mini review. *Eur. J. Med. Chem*. **2014**, *85*, 758–777. [doi: 10.1016/j.ejmech.2014.08.033]

Wang, J.; Yun, D.; Yao, J.; Fu, W.; Huang, F.; Chen, L.; Wei, T.; Yu, C.; Xu, H.; Zhou, X.; Huang, Y.; Wu, J.; Qiu, P.; Li, W. Design, synthesis and QSAR study of novel isatin analogues inspired Michael acceptor as potential anticancer compounds. *Eur. J. Med. Chem.* **2018**, *144*, 493-503. [doi: 10.1016/j.ejmech.2017.12.043]

Yamada, K.; Yoshida, K. Mechanical insights into the regulation of programmed cell death by p53 via mitochondria. *Biochim. Biophys. Acta Mol. Cell Res*. **2019**, *1866*, 839-848. [doi: 10.1016/j.bbamcr.2019.02.009]

Yue, P.Y.; Leung, E.P.; Mak, N.K.; Wong, R.N. A simplified method for quantifying cell migration/wound healing in 96-well plates. *J. Biomol. Screen*. **2010**, *15*, 427-33. [doi: 10.1177/1087057110361772]

Zhang, M.; Zhang, X. Association of MMP-2 expression and prognosis in osteosarcoma patients. *Int. J. Clin. Exp. Pathol*. **2015**, *8*, 14965–14970. [doi not available]

Capítulo IV

7. Conclusões

Capítulo II

Os híbridos de curcumina-cinamaldeído da série I foram agentes antiproliferativos mais potentes que a série II;

Os dados indicaram que uma ligação dupla carbono-carbono foi mais relevante para a atividade antiproliferativa do que duas ligações duplas carbono-carbono;

De modo geral, os híbridos foram mais potentes que o cinamaldeído;

Híbridos contendo grupos hidroxilados foram mais ativos que os metoxilados;

O híbrido **5a** apresentou a maior potência em inibir a proliferação celular de todas as células avaliadas de câncer feminino com exceção da linhagem MCF-7, com valores de IC_{50} variando de 2.7 a 36.5 μM;

5a demonstrou maior potência que a curcumina contra as células CaSki, SiHa, C33 e A431, além de ter exibido um maior IS (8.5) que a curcumina (0.7);

5a inibiu a formação de colônias da célula (A431) em que apresentou maior atividade (IC_{50} = 2.7 μM);

5a demonstrou ser uma substância estável sob condições fisiológicas, ao contrário da curcumina e cinamaldeído;

Uma breve investigação *in silico* corroborou as propriedades farmacocinéticas e *drug-likeness* de **5a**;

Capítulo III

Nas linhagens de osteossarcoma, **3HC (5a)** foi mais potente contra a linhagem U2OS (IC_{50} = 22.4 μM) quando comparado a SAOS-2 (IC_{50} = 45.0 μM), sugerindo que a proteína p53 pode ser o seu alvo molecular;

O efeito antiproliferativo de **3HC** foi mediado pela indução de apoptose;

3HC reduziu a migração, invasão celular e atividade da metaloproteinase MMP-2;

3HC induziu a expressão de p53 e DNAJB1 (Hsp40), essa indução pode contribuir na atividade de p53, importante para a apoptose, visto que Hsp40 estabiliza a conformação da proteína p53;

Estes dados destacam a importância da hibridação molecular e da presença de grupos hidroxilados para potencializar a ação em alvos moleculares antitumorais, na qual corroboram o potencial da curcumina e cinamaldeído como iniciais protótipos privilegiados para o desenvolvimento de novos híbridos com atividade pró-apoptóticas e inibição da migração e invasão.

Apêndice A – Artigos Publicados

International Journal of
Molecular Sciences

MDPI

Article

Design of Antibacterial Agents: Alkyl Dihydroxybenzoates against *Xanthomonas citri* subsp. *citri*

Ana Carolina Nazaré [1,*], Carlos Roberto Polaquini [1], Lúcia Bonci Cavalca [2,3], Daiane Bertholin Anselmo [1], Marilia de Freitas Calmon Saiki [4], Diego Alves Monteiro [4], Aleksandra Zielinska [3], Paula Rahal [4], Eleni Gomes [4], Dirk-Jan Scheffers [3], Henrique Ferreira [2] and Luis Octavio Regasini [1,*]

1 Department of Chemistry and Environmental Sciences, Institute of Biosciences, Humanities and Exact Sciences, São Paulo State University, São José do Rio Preto, SP 15054-000, Brazil; carlos_polaquini@hotmail.com (C.R.P.); daiane_bertholin@hotmail.com (D.B.A.)
2 Department of Biochemistry and Microbiology, Biosciences Institute, São Paulo State University, Rio Claro, SP 13506-900, Brazil; l.bonci@hotmail.com (L.B.C.); henrique.ferreira@unesp.br (H.F.)
3 Department of Molecular Microbiology, Groningen Biomolecular Sciences and Biotechnology Institute, University of Groningen, 9747 AG Groningen, The Netherlands; a.u.zielinska@rug.nl (A.Z.); d.j.scheffers@rug.nl (D.-J.S.)
4 Department of Biology, Institute of Biosciences, Humanities and Exact Sciences, São Paulo State University, IBILCE, São José do Rio Preto, SP 15054-000, Brazil; macal131@gmail.com (M.d.F.C.S.); diego8monteiro@hotmail.com (D.A.M.); prahal@ibilce.unesp.br (P.R.); eleni@ibilce.unesp.br (E.G.)
* Correspondence: acarolnazare@gmail.com (A.C.N.); luis.regasini@unesp.br (L.O.R.); Tel.: +55-17-3221-2362 (L.O.R.)

Received: 24 August 2018; Accepted: 1 October 2018; Published: 6 October 2018

Abstract: *Xanthomonas citri* subsp. *citri* (Xcc) causes citrus canker, affecting sweet orange-producing areas around the world. The current chemical treatment available for this disease is based on cupric compounds. For this reason, the objective of this study was to design antibacterial agents. In order to do this, we analyzed the anti-Xcc activity of 36 alkyl dihydroxybenzoates and we found 14 active compounds. Among them, three esters with the lowest minimum inhibitory concentration values were selected; compounds **4** (52 μM), **16** (80 μM) and **28** (88 μM). Our study demonstrated that alkyl dihydroxybenzoates cause a delay in the exponential phase. The permeability capacity of alkyl dihydroxybenzoates in a quarter of MIC was compared to nisin (positive control). Compound **28** was the most effective (93.8), compared to compound **16** (41.3) and compound **4** (13.9) by percentage values. Finally, all three compounds showed inhibition of FtsZ GTPase activity, and promoted changes in protofilaments, leading to depolymerization, which prevents bacterial cell division. In conclusion, heptyl dihydroxybenzoates (compounds **4**, **16** and **28**) are promising anti-Xcc agents which may serve as an alternative for the control of citrus canker.

Keywords: citrus canker; antimicrobial; plant disease; membrane disruption; phenolic acids

1. Introduction

Citrus canker is caused by *Xanthomonas citri* subsp. *citri* (Xcc), which is responsible for a severe form of the disease (Asian citrus canker) [1–3]. Typical symptoms of this plant disease are brownish eruptive lesions on their aerial parts, which may be surrounded by chlorotic halos. Bacteria infect leaves, stems, and fruit, which leads to defoliation, twig dieback and early fruit drop. As a consequence, the disease brings significant economic losses to the citrus sector [3–6].

JOURNAL OF ENZYME INHIBITION AND MEDICINAL CHEMISTRY
2019, VOL. 34, NO. 1, 1093–1099
https://doi.org/10.1080/14756366.2019.1615485

Taylor & Francis
Taylor & Francis Group

SHORT COMMUNICATION

OPEN ACCESS Check for updates

Antiproliferative activity and p53 upregulation effects of chalcones on human breast cancer cells

Mariana Bastos dos Santos[a], Daiane Bertholin Anselmo[a], Jéssica Gisleine de Oliveira[b], Bruna V. Jardim-Perassi[b], Diego Alves Monteiro[c], Gabriel Silva[d], Eleni Gomes[c], Ana Lucia Fachin[d], Mozart Marins[d], Débora Aparecida Pires de Campos Zuccari[b] and Luis Octavio Regasini[a]

[a]Department of Chemistry and Environmental Chemistry, Institute of Biosciences, Humanities and Exact Sciences (IBILCE), São Paulo State University (UNESP), São Paulo, Brazil; [b]Department of Molecular Biology, Medicine College of São José do Rio Preto (FAMERP), São Paulo, Brazil; [c]Department of Biology, Institute of Biosciences, Humanities and Exact Sciences (IBILCE), São Paulo State University (UNESP), São Paulo, Brazil; [d]Biotechnology Unit, University of Ribeirão Preto (UNAERP), São Paulo, Brazil

ABSTRACT

Chalcones are valuable structures for drug discovery due to their broad bioactivity spectrum. In this study, we evaluated 20 synthetic chalcones against estrogen-receptor-positive breast cancer cells (MCF-7 line) and triple-negative breast cancer (TNBC) cells (MDA-MB-231 line). Antiproliferative screening by MTT assay resulted in two most active compounds: 2-fluoro-4′-aminochalcone (**11**) and 3-pyridyl-4′-aminochalcone (**17**). Their IC_{50} values ranged from 13.2 to 34.7 μM against both cell lines. Selected chalcones are weak basic compounds and maintained their antiproliferative activity under acidosis conditions (pH 6.7), indicating their resistance to ion-trapping effect. The mode of breast cancer cells death was investigated and chalcones **11** and **17** were able to induce apoptosis rather than necrosis in both lines. Antiproliferative target investigations with MCF-7 cells suggested **11** and **17** upregulated p53 protein expression and did not affect Sp1 protein expression. Future studies on chalcones **11** and **17** can define their *in vivo* therapeutic potential.

ARTICLE HISTORY
Received 21 March 2019
Accepted 28 April 2019

KEYWORDS
Chalcones; cancer; p53; antiproliferative; apoptosis

Introduction

Breast cancer is the most common type of cancer that affects women around the world, corresponding to 25% of cases. It is also the main cause of cancer death among women[1–3]. Its classification is based on the presence of cellular receptors: (i) Hormone-Receptor (HR), with Estrogen (ER) and/or Progesterone-Receptors (PR); (ii) Human Epidermal Growth Factor-2 receptor (HER2); and (iii) Triple-Negative Breast Cancer (TNBC), which does not express ER, PR, or HER2 receptors[4–6]. Chemotherapy choices for breast cancer are made according to its classification aiming to reach specific targets. ER-positive cancer treatments include ER modulators, such as tamoxifen or aromatase inhibitors. HER2-positive cancer is treated with monoclonal antibodies, such as trastuzumab, which is administered alongside tyrosine-kinase inhibitors[7–9]. TNBC cancer treatment is focused on cytotoxic agents, such as taxanes or doxorubicin. This cancer has poor response to chemotherapy, particularly at metastatic sites, with survival rates below 2 years. Altogether, TNBC cancer has been considered the most severe and difficult to treat due to a lack of targeted therapy[10–12].

Chalcones are valuable structures for drug discovery due to their broad bioactivity spectrum, as well as their versatile and simple synthesis. Their structures, bearing two benzene rings (A and B), are linked by an enone bridge. They have demonstrated antiproliferative activity against cancer cells, including breast cancer[13–15]. Mai et al. described chalcone was effective against ER-positive breast cancer cells (MCF-7 line) targeting 20 apoptotic markers[16]. Iftikhar et al. reported that chalcone bearing chlorine at position 2 was effective against breast cancer cells (CAL-51 line) and induced accumulation of p53 protein[17]. Silva and coauthors described unsubstituted chalcone increased p53 protein activity in osteosarcoma cells (U2OS line) through the induction of heat shock protein DNAJB1[18].

In our ongoing search for anticancer compounds with structures based on chalcone framework, we evaluated the antiproliferative activity of 20 chalcones against ER-positive cells (MCF-7 line) and TNBC (MDA-MB-231 line). The two most active chalcones (**11** and **17**) were selected to antiproliferative evaluation under acidosis conditions (pH 6.7) and pro-apoptotic activity in MCF-7 and MDA-MB-231 lines. In addition, we investigated tumour molecular targets of **11** and **17** in MCF-7 line, which were able to upregulate p53 protein expression.

Materials and methods

Chemical procedure for synthesis of chalcones 1–20

Reagents and solvents were purchased from Merck® (Kenilworth, NJ). Series of 20 chalcones was synthesised by Claisen–Schmidt aldol condensation reaction, according to protocol described by

CONTACT Luis Octavio Regasini luis.regasini@unesp.br Department of Chemistry and Environmental Chemistry, Institute of Biosciences, Humanities and Exact Sciences (IBILCE), São Paulo State University (UNESP), São José do Rio Preto, São Paulo, Brazil

Supplemental data for this article can be accessed here.

Methoxychalcones: Effect of Methoxyl Group toward Antifungal, Antibacterial and Antiproliferative Activities.

Marques BC[1], Santos MB[1], Anselmo DB[1], Monteiro DA[2], Gomes E[2], Saiki MFC[2], Rahal P[2], Rosalen PL[3], Sardi JCO[3], Regasini LO[1]

Author information

Medicinal Chemistry (Shariqah (United Arab Emirates)), 23 Jul 2019,
DOI: 10.2174/1573406415666190724145158 PMID: 31339075

Abstract

BACKGROUND:Chalcones substituted by methoxyl groups have presented a broad spectrum of bioactivities, including antifungal, antibacterial and antiproliferative effects. However, a clear and unambiguous investigation about the relevance of this substituent on the chalcone framework has not been described. OBJECTIVE:The purpose of this work is to assess the antibacterial, antifungal and antiproliferative activities of two series of seventeen synthesized regioisomeric methoxychalcones. Series I and II were constituted by chalcones substituted by methoxyl groups on rings A (5-12) and B (13-21), respectively. In addition, the library of methoxychalcones was submitted to in silico drug-likeness and pharmacokinetics properties predictions. METHODS:Methoxychalcones were synthesized and their structures were confirmed by NMR spectral data analyses. Evaluations of antimicrobial activity were performed against five species of Candida, two Gram-negative and five Gram-positive species. For antiproliferative activity, methoxychalcones were evaluated against four human tumorigenic cell lines, as well as human non-tumorigenic keratinocytes. Drug-likeness and pharmacokinetics properties were predict using Molinspiration and PreADMET toolkits. RESULTS:In general, chalcones of series I are the most potent antifungal, antibacterial and antiproliferative agents. 2',4',5'-Trimethoxychalcone (11) demonstrated potent antifungal activity against Candida krusei (MIC = 3.9 µg/mL), eight times more potent than fluconazole (reference antifungal drug). 3'-Methoxychalcone (6) displayed anti-Pseudomonas activity (MIC = 7.8 µg/mL). 2',5'-Dimethoxychalcone (9) displayed potent antiproliferative effect against C-33A (skin), A-431 (skin) and MCF-7 (breast), with IC50 values ranging from 7.7 to 9.2 µM. Its potency was superior to curcumin (reference antiproliferative compound), which exhibited IC50 values ranging from 10.4 to 19.0 µM. CONCLUSION:Our studies corroborated the relevance of methoxychalcones as antifungal, antibacterial and antiproliferative agents. In addition, we elucidated influence of the position and number of methoxyl groups toward bioactivity. In silico predictions indicated good drug-likeness and pharmacokinetics properties to library of methoxychalcones.